Thyroid hormone action in the central nervous system and peripheral tissues

Ph.D. Thesis

Petra Tímea Mohácsik

Semmelweis University
János Szentágothai Ph.D. School of Neuroscience

Institute of Experimental Medicine
Hungarian Academy of Sciences

Tutor: Balázs Gereben D.V.M., Ph.D., D.Sc.

Opponents: István Ábrahám M.D., Ph.D., D.Sc
Orsolya Dohán M.D., Ph.D.

Chairman of committee: Alán Alpár M.D., Ph.D., D.Sc.
Members of committee: Veronika Jancsik Ph.D.
Zita Puskár Ph.D.

Budapest
2016

1. Table of contents

2. Abbreviations

3’ FR - 3’ flanking region

5’ FR – 5’ flanking region

ABC - Avidin-biotin-peroxidase complex

AMPK - AMP activated protein kinase

ARC - Arcuate nucleus

ATA – American Thyroid Association

BAT - Brown adipose tissue

BBB - Blood-brain barrier

BSA - Bovine serum albumin

BT - Biotinylated tyramide

BW – Bodyweight

cAMP – Cyclic adenosine monophosphate

cDNA – complementary DNA

ChP – Choroid plexus

CMV – Cytomegalovirus

CNS - Central nervous system

CRE - cAMP-response-element

CREB - cAMP-response-element binding protein

CRH - Corticotropin-releasing hormone

D1 - Type 1 deiodinase

D2 - Type 2 deiodinase

D3 - Type 3 deiodinase

DAB - Diaminobenzidine

DCV – Dense core vesicle

DMEM - Dulbecco's Modified Eagle's Medium

DMN - Dorsomedial nucleus

DTT - DL-dithiothreitol

DR – Direct repeats

EDTA - Ethylenediaminetetraacetic acid

EEC – Expression enhancer casette

EGTA - Ethylene glycol tetraacetic acid

ER – Endoplasmic reticulum

FBS –Fetal Bovine Serum

FFA – Free fatty acids

FISH – Fluorescence *in situ* hybridization

GAPDH – Glyceraldehyde-3-phosphate dehydrogenase

GHRH - Growth hormone-releasing hormone

GnRH - Gonadotropin-releasing hormone

gw – gestational week

HPLC – High pressure liquid chromatography

HPT axis - Hypothalamus-pituitary-thyroid axis

HT - Hypothalamus

iBAT - Interscapular brown adipose tissue

i.p. - Intraperitoneal

IR - Immunoreactive

IRD – Inner ring deiodination

KO - Knock out

LAT - L-type amino acid transporter

LPS – Bacterial lipopolysaccharide

Luc – Firefly Luciferase

MBH – Mediobasal hypothalamus

MCT family – Monocarboxylate transporter family

MCT8 - Monocarboxylate transporter type 8

MCT10 - Monocarboxylate transporter type 10

ME - Median eminence

MPOA – Medial preoptic area

NE – Norepinephrine

NFκB - Nuclear factor-kappa B

NiDAB – Nickel-Diaminobenzidine

NHS - Normal horse serum

NST- Non-shivering thermogenesis

NTIS – Non-thyroidal illness syndrome

OATP - Organic anion transporting polypeptide

OATP1C1 - Organic anion transporting polypeptide 1c1

ORD – Outer ring deiodination

PB – Phosphate buffer

PBS - Phosphate buffered saline

PCR – Polymerase chain reaction

PFA - Paraformaldehyde

PKA – Protein kinase A

POA – Preoptic area

PVN - Paraventricular nucleus

PTU – 6-n-propyl-2-thiouracil

RLU – Relative light unit

ROI – Region of interest

RT – Room temperature

RTH – Resistance to thyroid hormone syndrome

rT3 - Reverse T3, 3,3',5' triiodothyronine

RXR - Retinoid X receptor

SCN - Suprachiasmatic nucleus

SNS – Sympathetic nervous system

SST - Somatostatin

STORM – Stochastic Optical Reconstruction Microscopy

T2 - Diiodothyronine

T3 - 3,5,3' triiodothyronine

T4 - Thyroxine

TH, THs - Thyroid hormone, thyroid hormones

THAI-Mouse – Thyroid hormone action indicator mouse

THAIC – Thyroid hormone action indicator construct

TK promoter – Thymidine kinase promoter

TR, TRs - Thyroid hormone receptor, thyroid hormone receptors

TRα - Thyroid hormone receptor alpha

TRα1 - Thyroid hormone receptor alpha type 1

TRα2 - Thyroid hormone receptor alpha type 2

TRβ - Thyroid hormone receptor beta

TRβ1 - Thyroid hormone receptor beta type 1

TRβ2 - Thyroid hormone receptor beta type 2

TRE - Thyroid hormone response element

TRH - Thyrotropin-releasing hormone

TSH - Thyroid stimulating hormone

TSHβ - Thyroid stimulating hormone beta subunit

UCP-1 - Uncoupling protein-1

VMH – Ventromedial hypothalamus

WT - Wild type

Abbreviations used only once were explained in the text.

3. Introduction

3.1 Thyroid hormones

Thyroid hormones (TH) are crucial regulators of many fundamental biological processes e.g. metabolism (Lechan and Fekete, 2006), neuronal development (Bernal et al., 2003; Williams, 2008), reproduction (Dawson, 1993; Nakao et al., 2008), stress (Baumgartner et al., 1998; Araki et al., 2003), and growth (Giustina and Wehrenberg, 1995). It has been well established, that untreated congenital hypothyroidism has devastating consequences on newborns represented by growth retardation and impaired neuronal development manifested in mental retardation, loss of hearing, speech and coordination problems and low muscle tone. Millions of people are suffering from TH deficiencies around the word and require TH supplementation to correct hypothyroidism and get rid of fatigue and mental dysfunctions while in contrast, need medications to lower TH levels and normalize cardiac function and neurological symptoms caused by hyperthyroidism. The high prevalence and high impact of TH-related symptoms on medical conditions and life quality and the essential role played by TH in the proper function of the brain and various organ systems calls for intense investigations addressing the regulation of TH economy.

The human thyroid gland produces mainly thyroxin (T4) and in a lesser extent triiodothyronine (T3) (Larsen et al., 1998). Both molecules are derived from the amino acid tyrosine and contain an inner tyrosyl ring and an outer phenolic ring linker via an ester bond, covalently bound to iodine molecules. To exert it's biological effect the T4 prohormone needs to be activated to T3 that can bind the thyroid hormone receptor (TR). TH are stable molecules, T4 and T3 half-life in humans are ~ 1 week and 1 day, respectively, while in rats is 11, and 4 hours, respectively. TH are hydrophobic molecules and their vast majority (~99%) is bound to carrier proteins in the blood. The daily TH production is tightly controlled by the hypothalamus-pituitary-thyroid (HPT) axis keeping serum T3 levels in the physiological range via negative feedback regulation at the different levels of the HPT axis. Stability of serum TH levels is important but TH action occurs predominantly at the tissue level and the HPT axis itself is not capable to achieve tissue-specific and tightly regulated TH availability. Thus tissue/cell-type specific regulation of TH levels are achieved by a complex regulatory system that allows to customize TH availability in a cell-type specific manner. This

system involves the transport of TH by various TH transporters, the activation and inactivation by deiodinase enzyme family and the regulation of TH action by TH receptors and it's co-regulators **(Figure 1)**. This tissue-specific system is functionally interlinked with the HPT axis in the hypothalamus.

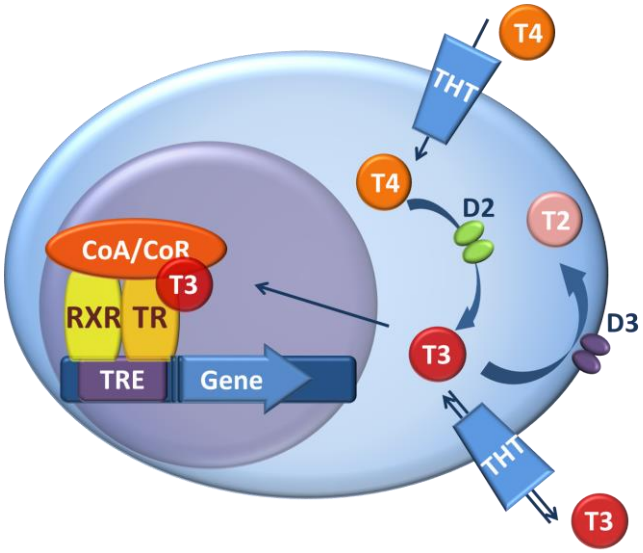

Figure 1. TH action and its regulation by TH transporters and deiodinases. T3 ligands the TR/RXR(Retinoid X receptor) heterodimer binding to a thyroid hormone response element (TRE) in the regulatory region of TH responsive genes. The ability of TR/RXR receptor to affect gene transcription is modulated by co-activators/co-repressors (CoA/CoR) and factors regulating intracellular TH availability; TH transporters (THT) and deiodinases. As the first step in the regulation of TH action, type 2 deiodinase (D2) activates T4 by converting it to T3. Type 3 deiodinase (D3) catalyzes the inactivating pathway by degrading T3 and converting T4 to the transcriptionally inactive reverse T3. The expression of the two main deiodinases, D2 and D3, varies according to cell-type.

3.2 Structure and function of the HPT axis

The hypothalamus is the integrator of hormonal and sensory information reflecting the internal and external environment and regulates homeostasis by responding to changing conditions. The hypothalamus represents the center of the endocrine brain and works as the central regulator of neuroendocrine systems. Consequently, it controls growth, metabolism, reproduction, stress response, water balance, and contraction of smooth muscle cells during delivery and nursing (Reichlin, 1967). The hypothalamus is

bordered from anterior-posterior direction by the stria terminalis and the region located posterior to the corpus mamillare while the thalamus and the ventral surface of the brain represent its dorsal and ventral borders, respectively (Flament-Durand, 1980). Central regulators of different endocrine axes are located in specific regions of the hypothalamus. Parvocellular neurosecretory neurons, like thyrotropin releasing hormone (TRH) or corticotrophin releasing hormone (CRH) expressing neurons are located in the paraventricular nucleus (PVN)(Lennard et al., 1993; Merchenthaler and Liposits, 1994; Fekete et al., 2000) while gonadotropin releasing hormone (GnRH) expressing neurons are in the medial preoptic area (MPOA) (Merchenthaler et al., 1980; Rance et al., 1994) and GnRH and growth hormone releasing hormone (GHRH) neurons are restricted to arcuate nucleus (ARC) (Sawchenko et al., 1985). Despite the distinct location of the neuronal cell bodies, axons of all hypophysiotropic neurons expand to external zone of median eminence (ME) where they terminate in close proximity of fenestrated portal capillaries of the anterior pituitary (Wiegand and Price, 1980; Merchenthaler et al., 1984) **(Figure 2)**. Their peptide hormones are secreted to the ME and travels via the fenestrated capillaries in blood to target cells of the anterior pituitary to evoke the release of pituitary hormones to the circulation (Sawyer, 1978). Magnocellular neurons like angiotensin-vasopressin, and oxytocin neurons are located in PVN and supraoptic nucleus and send their axons directly to the posterior pituitary via the ME and release neuropeptides in peripheral blood (Vandesande and Dierickx, 1975).

The ME belongs to the circumventricular organs by sharing a unique feature of these brain regions to be located outside of the blood brain barrier (BBB) (Ganong, 2000). This way numerous blood derived factors can gain access to the dense network of axon terminals of the ME. Therefore this region allows hypophysiotropic TRH neurons to get into direct contact with serum TH levels. TRH expressing neurons can be also found outside the hypothalamus (e.g. in the thalamus, brain stem or the spinal cord) but hypophysiotropic TRH neurons, the central regulators of HPT axis (Fekete and Lechan, 2014), are confined to the medial parvocellular and periventricular subdivision of PVN in rat (Merchenthaler and Liposits, 1994; Fekete et al., 2000). TRH axon terminals expand to the external zone of the ME in the mediobasal hypothalamus (MBH) where they secrete the TRH peptide into fenestrated, portal capillaries that reaches the

thyrotropes and evokes thyroid stimulating hormone (TSH) release into peripheral blood to allow TSH-induced stimulation of follicular cells of the thyroid gland. TH regulate their own production by negative feedback both at the level of the pituitary and the hypothalamus (Segerson et al., 1987; Dahl et al., 1994). The reference level of serum TH-s in blood are set by set point formation during development and as a consequence the axis is programmed to keep circulation T3 levels in the desired range **(Figure 2)**.

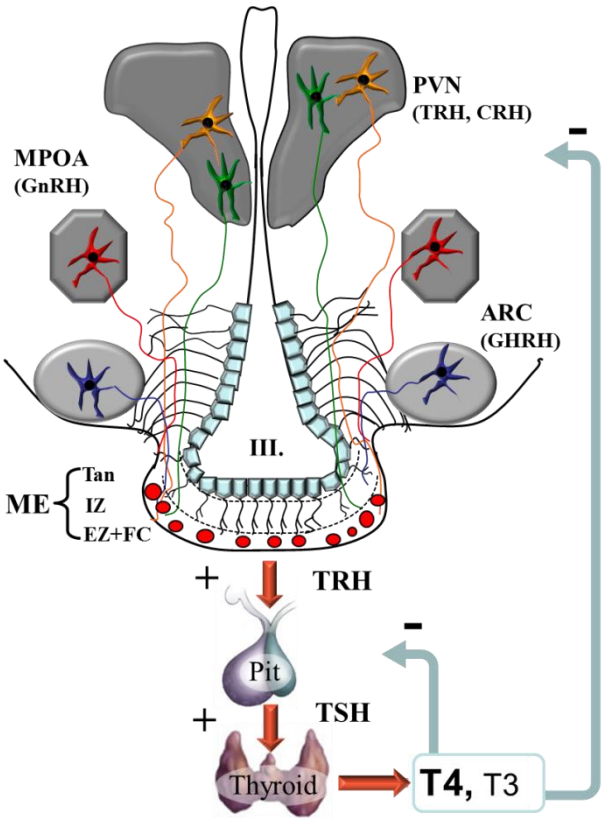

Figure 2. The hypothalamo-pituitary-thyroid axis regulation and localization of hypophysiotropic parvocellular neurons in the hypothalamus. Hypophysiotropic parvocellular neurons are restricted to distinct regions of hypothalamus while all neurons send their axons to the external zone (EZ) of median eminence (ME), where neuropeptides are secreted from axon terminals into fenestrated portal capillaries (FC). Neuropeptides reach the anterior pituitary and evoke the release of the appropriate hormones into the peripheral blood. TRH cells, the main regulators of HPT axis are located in paraventricular nucleus (PVN) and evoke TSH release from pituitary thyrotropes followed by the induction of TH secretion from the thyroid gland. TH regulate their own production by negative feedback both at the level of the hypothalamus and the pituitary. Tanycytes (Tan) are specialized glial cells lining the

floor and wall of the third ventricle (III.) This cell-type forms the exclusive type 2 deiodinase (D2) expressing cellular compartment in the hypothalamus and represents the main source of T3 in this region. IZ: internal zone; MPOA: medial preoptic area; ARC: arcuate nucleus.

The pituitary responds within minutes to altered plasma TH and regulate TSH secretion. Minor increase in TH levels inhibits TRH action on thyrotropes and decreases TSH secretion (Snyder and Utiger, 1972) and in contrary, a modest decrease in TH levels is sufficient to sensitize the anterior pituitary to TRH (Vagenakis et al.). Both T3 and T4 can directly inhibit TSH synthesis (Weiss et al., 1997). TH feedback on TRH neurons works via nuclear TR-mediated transcriptional actions that makes this pathway more time consuming compared to non-transcriptional events. Negative feedback control on TRH neurons is mediated by nuclear thyroid hormone receptor beta 2 (TRβ2) (Abel et al., 2001) and results in decreased proTRH mRNA levels. In hypothyroid mice TH supplementation requires ~5 hours to normalize TRH expression in PVN (Sugrue et al., 2010). In the first step TH-s have to gain access to brain across BBB, and needs to be transported via specific TH transporters. T4 is the TH form that preferentially transported into the brain thus local activation to T3 is especially important, to exert TH action at specific brain regions. In the brain, D2 is the dominant activating enzyme which is mostly expressed in glial compartment and which serves as a T3 source for neurons (Crantz et al., 1982; Guadano-Ferraz et al., 1997). It is well known that D2-mediated T3 conversion is essential in feedback regulation of hypophysiotropic TRH neurons (Gereben et al., 2008; Fonseca et al., 2013). In contrast to D2, D3 is involved in the inactivation of T3 in the neuronal compartment (Tu et al., 1999; Verhoelst et al., 2002). Therefore, in addition to the peripheral TH levels, the hypothalamic activity of deiodinase enzymes determines the local level of T3 that regulates the hypophysiotropic TRH neurons in the hypothalamus. In the hypothalamus, the main T3 generating, D2 expressing cells are tanycytes, the specialized glial cells, lining the floor and wall of the third ventricle (Tu et al., 1997; Guadano-Ferraz et al., 1999; Gereben et al., 2004). While the cell bodies of TRH neurons are located in some distance to tanycytes (Wiegand and Price, 1980), the axon terminals and tanycyte processes are in close proximity in the ME, representing a locus where tanycyte derived T3 can act on TRH

neurons **(Figure 2)**. This is supported by studies in astrocyte-specific D2 knock out (KO) mice demonstrating that preserved tanycytal D2 activity is sufficient to maintain normal T4 dependent negative feedback and unchanged TH economy (Fonseca et al., 2013).

3.3 Development of hypothalamic TH-mediated negative feedback

The timing and mechanism of hypothalamic set point formation is poorly understood. Studies in human fetuses and infants are limited by ethical considerations while rodents provide a poor model for these studies due to the different developmental kinetics of the HPT axis. Pituitary development starts early in humans, at gestational week (gw) 4 with the formation of Rathke pouch from the oral ectoderm, which will form later the anterior pituitary. In mouse this event occurs at embryonic day (E)9 during midgestation and results in fully differentiated thyrothrop cells only few days before birth at E17 (Japon et al., 1994). In humans, the anterior pituitary is fully differentiated at gw16, however biologically active TSH is released after gw17 (Pope et al., 2006). The neural lobe, and the infundibulum develops from neural tube ectoderm. The rodent hypothalamus is formed before E16 and the differentiation of nuclei occurs between E19 and day 10 of postnatal life (Szentágothai, 1968; Hyyppä, 1969). Compared to the slow hypothalamic development of rodents, human newborns have a well-developed hypothalamic axis at birth. Hypothalamic nuclei start to differentiate and compartmentalize during gw15-17, the ME is also evolved at gw18 and all nuclei, including the parvocellular subdivision of PVN, reach adult-like structure at gw24-33 (Koutcherov et al., 2002). In the last trimester of gestation all anatomical structures are present for the matured and functional regulation of the HPT axis in the human fetus.

In rodents, serum T4 levels start to increase exponentially at E18-22 several days prior to birth, which phenomenon occurs in human fetus much earlier, at the beginning of the third trimester. TRH is expressed in the rat hypothalamic PVN from E16 (Burgunder and Taylor, 1989), but TH inhibits the hypophysiotropic TRH expression only from day 7 after birth (P7) in this species (Taylor et al., 1990). In humans the HPT axis is largely maturated at gw28-34. Fetal pituitary is already sensitive to TRH in gw25 and responds with elevated TSH when mother is injected with TRH (ROTI et al., 1983). In preterm (gw28) hypo/hyperthyroid infant, the pituitary can respond with elevated or decreased serum TSH (Fisher and Klein, 1981). However, in E18 rat thyroid function is largely

dependent on pituitary TSH secretion and negative feedback on thyrotropes but is not affected by the HT (Jost et al., 1974). It can be concluded that the kinetics of HPT axis development is strikingly different in rodents and humans that make rodent a poor models for these studies.

However, in contrast to the relatively low developmental state reached by rats and mice at the time of prenatal-postnatal transition, chickens have a well-developed HPT axis at hatching (Debonne et al., 2008). Similarly to mammals, a time gap between the onset of HPT function and TH-mediated negative feedback can be also observed during the ontogeny of the chicken embryo. This is supported by the observation that the chicken anterior pituitary starts promoting thyroidal secretion already at E10 (Thommes et al., 1984) followed by the increase of T4 and T3 levels in the serum and brain tissue (Prati et al., 1992; Grommen et al., 2008). However, despite the increasing TH levels, the thyroid stimulating hormone beta subunit (TSHβ) mRNA level increases until E19 (Gregory et al., 1998) indicating the lack of negative feedback before this developmental stage. Hypothalamic TRH peptide level also increases continuously during chicken development although no data are available specifically on the level of TRH in the hypophysiotropic neurons (Geris et al., 1998). Despite the non-mammalian nature of the chickens models the mentioned arguments make chicken a useful model for studies aimed to better understand the development of the human HPT axis(De Groef et al., 2008).

3.4 Regulation of tissue thyroid hormone levels

While serum TH levels are generally kept stable, tissue-specific TH availability can be largely independent from serum levels due to the function of a complex regulatory mechanism which is represented in many tissues and is characteristic for a given tissue/cell-type. Members of this machinery are the TH transporters, the TH activating/inactivating deiodinase enzymes and TH receptors along with their co-regulators.

3.4.1 Cellular thyroid hormone uptake is mediated by thyroid hormone transporters

TH need to enter the cell to exert their biological effects. It was earlier speculated that TH as an apolar molecule penetrates the cells by diffusion (Hillier, 1970) and forms a gradient from the plasma membrane to the nucleus. However, it has become clear that TH uptake is mediated by active transport through different TH transporters. Monocarboxylate transporter 8 (MCT8) is a member of the MCT family and is the best characterized TH transporter. The MCT8 gene is located on the X chromosome the protein involves 12 transmembrane domains and forms homodimers in the lipid layer of the plasma membrane. It is expressed in different species in various tissues like liver, heart, thyroid, brown adipose tissue and brain (Visser, 2007). MCT8 is the predominant neuronal T3 transporter (Dumitrescu et al., 2004; Friesema et al., 2004) but it can also transport T4 (Friesema et al., 2003). MCT8 is widely expressed in the brain, including choroid plexus (Chp), amygdala, hippocampus, hypothalamus, different cortical areas and in the microvessels of anterior pituitary (Müller and Heuer, 2014). Mutations and the resulting impaired function of MCT8 is manifested in severe phsychomotoric retardation, delayed myelinilation, axial hypotonia, muscle hypoplasia and as a consequence poor head control and almost completely absent of speech in infants (Schwartz and Stevenson, 2007). TH homeostasis is highly affected, and patients have markedly low T4 and high T3 levels in serum, but normal TSH. This deficiency was identified as the genetic background of the previously described Allan-Herndon-Dudley syndrome (AHDS) (Schwartz et al., 2005).The MCT8 KO mice have the same endocrine phenotype, however they lack neuronal abnormalities (Trajkovic et al., 2007). MCT10 is another member of MCT family, and has a 49% identity to MCT8. It also contains 12 transmembrane domains, and transports T3 preferably according to *in vitro* experiments in COS-1 cells. (Friesema et al., 2008) MCT10 is ubiquitously expressed but available information on physiological function is limited (Ramadan et al., 2006).

Transporters of organic anion transporting polypeptide (OATP) family have affinity for a broad range of ligands, but one member, the organic anion transporting polypeptide 1c1 (OATP1c1) prefers mostly iodothyronines (T4, T3, reverse T3 (rT3)) making this protein a potent TH transporter. Its affinity for T3 is 6-fold lower than that for T4. OATP1c1 has been reported to be expressed at the BBB, mostly in endothelial cells of

rodent brain capillaries, astrocytes (Schnell et al., 2015), and also at brain-cerebrospinal fluid barrier, in ChP, and Leydig cells of the testicle (Sugiyama et al., 2003; Tohyama et al., 2004).

In the MBH glial derived tanycytes also express both MCT8 (Alkemade et al., 2005) and OATP1c1 (Roberts et al., 2008) representing a focal TH metabolizing locus, where T4 can be accumulated, converted to T3 by D2, and released to the surrounding region. Lack of neurological phenotype of MCT8 KO mice predicted that beyond MCT8 other TH transporter(s) also contribute significantly to the TH homeostasis of the mouse brain. Indeed, it has been demonstrated that the deletion of both MCT8 and OATP1c1 are required to severely impact TH homeostasis in the mouse brain (Mayerl et al., 2014).

L-type amino acid transporters (LAT-s) were also identified as TH transporters. Due to wide ligand binding affinity LAT1 and LAT2 are transporting large neutral amino acids like tryptophane, and leucine , and facilitate TH transport in mouse and human (Ritchie et al., 1999; Friesema et al., 2001; Zevenbergen et al., 2015). *In vitro* experiments on *Xenopus laevis* oocytes revealed, that large excess of amino acids or high dose iodothyronines inhibited LAT-1 transporter-mediated uptake conversely in a concentration dependent manner (Friesema et al., 2001).

3.4.2 Regulation of thyroid hormone metabolism by the deiodinase enzyme family

TH metabolism is regulated by members of the selenodeiodinase enzyme family. Biochemically the activation of T4 can be catalyzed both by type 1 and type 2 deiodinase enzymes by removing one iodine from the 5' phenolic ring of the T4 molecule. While D2 removes iodine exclusively from the outer ring (outer ring deiodination (ORD)), D1 can also perform inner ring deiodination (IRD) that converts T4 to rT3. Importantly, under *in vivo* euthyroid conditions TH activation is catalyzed almost exclusively by D2 since due to the low substrate affinity D1 cannot generate T3 only in hyperthyroidism when T3 is elevated (Maia et al., 2005). Furthermore, both T4 and T3 can be inactivated by D3 by IRD **(Figure 3A)** (Bianco et al., 2002).

Only 20% of human daily T3 production is related to the intrathyroidal deiodination while the rest is produced in extrathyroidal tissues by D2-mediated T3 generation.

Compared to humans, the contribution of the rodent thyroid gland to T3 production is higher, since in rodents ~40% of daily T3 is born in the gland (Bianco et al., 2002; Bianco et al., 2014). Still, even in these species D2 mediated T3 generation is highly significant. Thus D2-mediated TH activation is a critical process to meet the T3 demand of the body.

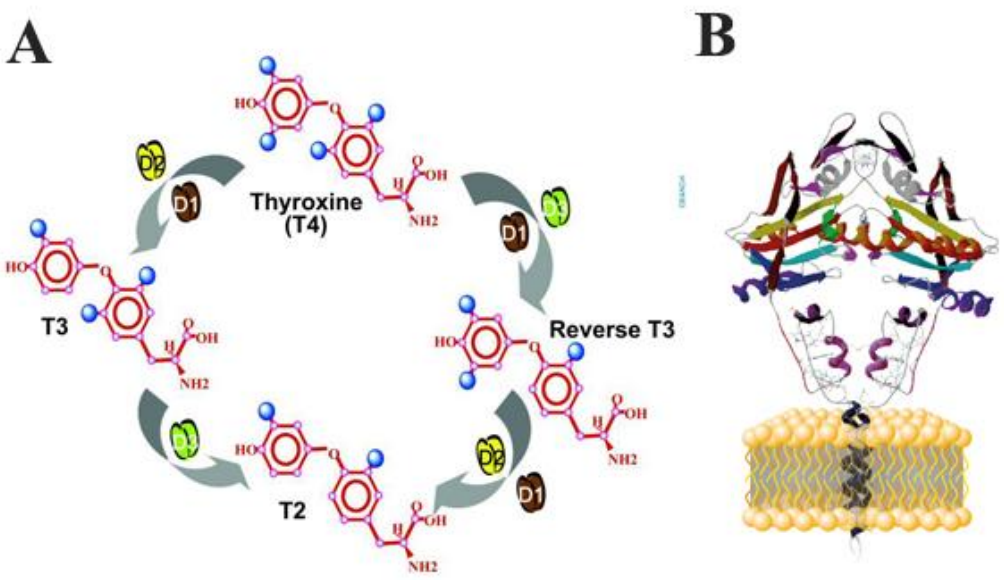

Figure 3. Schematic representation of deiodinase-mediated TH metabolism and deiodinase protein structure (A) Type 2 deiodinase (D2) and type 1 deiodinase (D1) can activate T4 to T3 by removing one iodine from outer ring, while D1 can also deiodinate the inner ring and convert T4 to reverse T3 (rT3). Type 3 deiodinase (D3) inactivates TH-s and produces rT3 or diiodothyronine (T2). (B) Deiodinases are one transmembrane domain containing proteins that are anchored to a membrane bilayer and need to form homodimers to achieve catalytic activity.
A (Gereben et al., 2008); B *http://deiodinase.org/wp-content/uploads/2015/10/Deiodinase-Structure1.jpg*

3.4.2.1 Structure and subcellular localization of deiodinase enzymes

Iodothyronine converting enzymes are responsible for regulation of active TH levels in the serum and locally in tissues. Deiodinases are selenoproteins and contain

selenocysteine, a rare amino acid, in their active center. Selenocysteine is encoded by an in-frame UGA that normally serves as a stop codon. However, in selenoproteins UGA is subjected to read through and dictates the incorporation of the rare amino acid selenocysteine. The underlying complex co-translational machinery consists of a *cis*-acting mRNA stem-loop structure located in the 3' untranslated region of the selenoprotein encoding mRNA called as the selenocysteine insertion sequence (SECIS) along with several *trans*-acting factors e.g. the the SECIS binding protein-2 (SBP-2) and a specific elongation factor, EFsec. Insertion of selenocysteine is a low efficiency process that results in a low translation rate of selenoproteins that also limits the production of deiodinases. However, importantly selenocysteine increases substrate affinity of D2 to T4 with three orders of magnitude compared to cysteine along with its effect to decrease translational activity by several hundred fold (Steinsapir et al., 2000). When the selenocysteine residue of D1 was

mutated to cysteine, an ~ 400-fold higher amount of D1 could be produced (Berry et al., 1992) but this mutated protein had decreased deiodination capacity (Berry et al., 1991; Bianco et al., 2002). Thus the presence of selenocysteine in selenoproteins allows that a low amount of deiodinase enzyme can perform the oxido-reductive deiodination in a highly effective manner. This scenario clearly represent a massive biological advantage due to the highly controllable nature allowed by the low amount of deiodinase enzymes.

D2 is targeted to the endoplasmic reticulum (ER) (Maciel et al., 1979; Baqui et al., 2000), while D1 and D3 are located in the plasma membrane (Baqui et al., 2000; Baqui et al., 2003). Due to this specific location deiodinases have a distinct role in regulation of TH availability at the cellular level. ER resident D2 produces T3 in the cytoplasm in close vicinity of the cell nucleus making D2 the main source of nuclear T3, while D1-mediated conversion on the cytoplasm membrane rapidly equilibrates with plasma pool, and has minor contribution to intranuclear T3 availability (Silva and Larsen, 1978).

Deiodinase enzymes contain a single transmembrane domain, and a ~15 amino acid long active center, that is relatively well conserved among the three enzymes. Deiodinase enzymes form homodimers and this process is a prerequisite of allowing the globular domains to reach the conformation required by the active center for efficient deiodination (Curcio-Morelli et al., 2003a) **(Figure 3B)**. One functional D1 subunit has

50% activity of native homodimer(Leonard et al., 2001), while D2 lost 90% of its activity if no homodimers are formed (Leonard et al., 2005). A highly conserved amino acid sequence in the C-terminal portion of the globular domains is responsible for homodimer binding, and mutation or deletion of this domain results in decreased enzyme activity (Leonard et al., 2005; Simpson et al., 2006). Fluorescence resonance energy transfer (FRET) studies in HEK-293 cells transiently overexpressing truncated D2 lacking transmembrane domain, revealed that this domain plays also an important role in homodimerization (Sagar et al., 2007). Both domains contribute to formation of dimers, however it has been shown, that binding site in the globular domain is sufficient to form catalytically active enzyme if the dimerizing partner has an intact transmembrane domain (Leonard et al., 2001; Sagar et al., 2007). Heterodimerization was also detected among deiodinases in a lesser extent, but biological significance of this phenomenon needs to be elucidated (Sagar et al., 2008).

3.4.2.2 Tissue distribution of deiodinases

In humans D1 enzyme is expressed in liver, kidney, pituitary and thyroid but it is absent from the central nervous system (CNS)(St Germain and Galton, 1997; Kester et al., 2004). In the rat D1 is also expressed in CNS, placenta, and intestine (Bates et al., 1999). Due to its highly T3 sensitive promoter, D1 can rapidly react to elevating serum T3 levels, while the contribution of D1 to extra thyroidal T3 production is not dominant in euthyroid humans (LoPresti et al., 1989).

D2 is widely expressed in the human CNS, pituitary, thyroid, heart, skeletal muscle, placenta, however in rats D2 is expressed also in brown adipose tissue (BAT), but is absent form heart, skeletal muscle and thyroid (Croteau et al., 1996). D2 is expressed in embryonic and newborn mouse liver with a peak expression at P1 that is followed by a rapid decline during development (Fonseca et al., 2015). While D2 is absent from the adult rat and human liver, it is expressed in this organ of chickens (Gereben et al., 1999). Both in the rodent and chicken hypothalamus D2 is predominantly expressed in tanycytes (Gereben et al., 2004).

D3 is expressed in human CNS (Kallo et al., 2012), fetal liver (Richard et al., 1998), and it is the predominant deiodinase in placenta (Huang et al., 2003). This protects the fetus from high maternal TH levels. More is known about D3 distribution in rat and mouse tissues. D3 is expressed widely in adult rat CNS (Tu et al., 1999), skin (Huang et al.,

1985) and placenta (Galton et al., 1999), and D3 has been found in skeletal muscle, intestine and liver of newborn rats (Bates et al., 1999).

3.4.2.3 Enzymatic properties

Selenocysteine is essential in catalysis of deiodination in all three enzymes (see 3.4.2.1 "Structure and subcellular localization of deiodinase enzymes"). Deiodinases have distinct enzymatic properties and kinetics. D1 was identified as the only deiodinase sensitive to 6-n-propyl-2-thiouracil (PTU) (Oppenheimer et al., 1972), an anti-thyroid drug used in hyperthyroid patients to inhibit TH synthesis in thyroid. D1 can catalyze both IRD and ORD, compared to exclusive ORD capacity of D2 an IRD deiodination of D3 (Fekkes et al., 1982) **(Figure 3.)** D1 enzyme activity follows ping-pong kinetics, between two substrates: iodothyronine and endogenous thiol cofactor (Visser et al., 1976).

According to *in vitro* measurements D2 has three orders of magnitude lower Michaelis-Menten constant (K_M) for T4, than D1. In addition, compared to T4, rT3 is just a slightly worse substrate of D2. D2 catalyzes deiodination with sequential kinetics, which means that binding of both the iodothyronine and the thiol cofactor are required for catalysis (Visser et al., 1982). In contrast to D1, D2 is insensitive to PTU. Not only D2, but D1 and D3 can be inhibited by iopanoic acid (Wu et al., 2005), and amiodarone (Rosene et al., 2010).

D3 is an obligate inner ring deiodinase and catalyzes the T3 to rT3 and T3 to T2 conversion, producing transcriptionally inactive hormones. It plays a crucial role in prevention of tissues from toxic levels of T3. D3 is insensitive to PTU, and follows sequential kinetics like D2 (Kaplan et al., 1983).

3.4.2.4 Complex regulation of D2-mediated TH activation

D2 activity is tightly regulated by different transcriptional and post-translational mechanism, to fine tune T3 availability rapidly and effectively by altered activation capacity. Human and rat *Dio2* gene has been shown to be positively regulated in promoter studies by nuclear factor-kappa B (NfκB), a second messenger molecule, involved in bacterial lipopolysaccharide (LPS) and cytokine signalling (Fekete et al., 2004). Computer analysis and promoter studies in cell culture revealed that the *Dio2* gene promoter contains functional cyclic-AMP-response elements (CRE) which make

this gene cyclic adenosine monophosphate (cAMP) responsive in human, rat and mouse tissues (Bartha et al., 2000; Canettieri et al., 2000; Song et al., 2000). Norepinephrine induced cAMP signalling trans-activates D2 transcription, that is essential in non-shivering thermogenesis in cold stressed interscapular BAT (iBAT). Nkx2.1, a homeodomain containing transcription factor has regulatory effect on the expression of D2 in the human thyroid while the DIO2 promoter contains two functional Nkx2.1 binding sites none of them is presented in the case of rat, resulting in lack of induction in promoter studies (Gereben et al., 2001).

The T3-mediated transcriptional suppression of D2 is well known, but the mechanism of the action remains to be clarified. A negative thyroid hormone response element (TRE) is predicted in the promoter but it has not been identified (Kim et al., 1998). At the post-translational level, D2 activity is regulated by its substrates T4 and rT3. D2 protein is degraded rapidly (activity half-life decreases under 1h) by ubiquitination-mediated selective proteolysis in the presence of T4 (Gereben et al., 2000). Importantly, the von Hippel-Lindau protein-interacting deubiquitinating enzyme-1 (VDU-1 also called as USP33) serves as deubiquitinase of D2 (Curcio-Morelli et al., 2003b) and makes the process reversible by removing ubiquitin.

3.4.3 Compartmentalization of TH activation and inactivation in the CNS

TH activation and inactivation is highly compartmentalized in the CNS. Astrocytes and tanycytes of the neuroglial compartment are the predominant source of T3 present in the brain while TR in neurons represents a major target of TH (Mohácsik et al., 2011). Astrocytes, distributed throughout the brain, and tanycytes, lining the floor and the wall of the third ventricle, take up T4 and convert it to T3 via D2. Neurons cannot generate T3 but they can take it up from glial cells with MCT8 transporter, and they can further regulate intracellular TH levels by inactivating deiodinase, D3 **(Figure 4)**. Direct evidence of neuroglia derived T3 - neuron interaction could be obtained in a two-dimensional H4-SK-N-AS glioma-neuron cell system where physiological amount of T4 in the D2 expressing glial compartment modulated TH-sensitive gene expression in the neuronal cell layer (Freitas et al., 2010).

Glial cells are not only source of T3 but also represent a target of this hormone (Mohácsik et al., 2011). TH affects the differentiation and maturation of different glial

subtypes including astrocytes, oligodendrocytes, and microglia (Almazan et al., 1985; Lima et al., 2001; Trentin, 2006). Impaired maturation of oligodendrocytes in hypothyroidism results in decreased number of, myelin producing oligodendrocyte cell bodies in the main white matter tracts (Schoonover et al., 2004) and along with delayed expression of myelin encoding genes, the myelination of axons are insufficient (Berbel et al., 1994; Ibarrola and Rodríguez-Peńa, 1997). Astrocytes secrete epidermal growth factor (EGF), basic fibroblast growth factor (bFGF), and nerve growth factor (NGF), in a T3-dependent manner regulating extracellular matrix formation(Trentin et al., 2003), neuronal migration (Martinez and Gomes, 2002), and neurite growth (Lindsay, 1979; Alvarez-Dolado et al., 1994; Hashimoto et al., 1994).

D3 protects neurons from T3 excess. The absence of this enzyme results in uncontrolled TH action that can trigger serious damage in TH sensitive tissues, especially in developing animal. Studies in (Hernandez et al., 2006) mice revealed, that D3 is essential in formation of negative feedback in the HPT axis. General D3 KO mice suffer from thyrotoxicosis during embryonic and neonatal life, at the time period when HPT axis set points are set, and this results in the development of central hypothyroidism in adulthood. From age P15 peripheral tissues are also hypothyroid, animals are smaller than wild type mice, and suffer from low fertility (Hernandez et al., 2006).

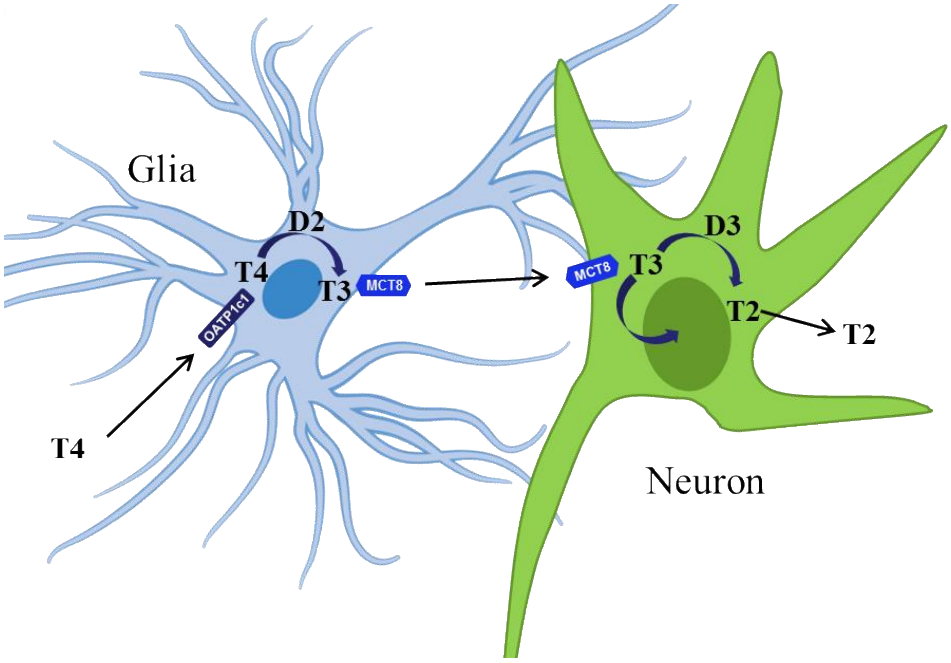

Figure 4. Compartmentalization of TH activation and inactivation in the CNS. Glial cells are the main source of activated TH in the CNS by taking up T4 by organic anion transporting polypeptide 1c1 (OATP1c1) transporter and converting it to T3 via type 2 deiodinase (D2). Neurons depend on glia released T3 that gets into neurons via monocarboxylate transporter 8 (MCT8). T3 impacts neuronal gene expression and metabolism and can be inactivated by type 3 deiodinase (D3). (Depiction of the glial cell was obtained from *https://commons.wikimedia.org/wiki/File:Diagram_of_an_astrocyte_-_a_type_of_glial_cell_CRUK_029.svg* was subjected to modifications.)

3.4.4 TR-s regulate transcription of TH targeted genes

TR represents a prerequisite of TH action. TR is a ligand-induced transcription factor and belongs to the nuclear receptor superfamily.TRα and TRβ are encoded by two separate genes. TRα has 4 isoforms that differ in the length and amino acid sequence of their C-terminals. Only the primary transcript, TRα1 is capable to bind T3, and initiate transcriptional activation. TRα2 is an alternative splice variant of the TRα1, while two other forms the TRdα1 and TRdα2 are alternative transcripts of TRα gene transcribed from an intronic internal promoter (Chassande et al., 1997). TRβ1 and 2 differ in length and amino acid composition of N terminus and are transcribed from TRβ gene using

two different promoters and alternative splicing. The TRβ3 isoform is reported only in rats (Williams, 2000). The ligand binding and DNA binding domain of the four transcriptionally active isoforms is highly conserved and later recognizes the TRE in the promoter region of target genes. All isoforms form heterodimers with retinoid X receptors (RXR). The α/RXR heterodimers are currently hold responsible for TH action (Brent, 2012). TR homodimers also exist but their role remains to be better understood. TRα1 and β1 are universal receptors and are reported in all studied issue. However, TRα1 is dominant in heart, intestine and brain, while TRβ1 expression is more pronounced in kidney, liver, and skeletal muscle. TRβ2 is essential in negative feedback regulation of HPT axis, and in correct development of retina, and inner ear (Forrest et al., 1996a).

Mutations in TR have several consequences. The Resistance to thyroid hormone (RTH) syndrome is caused by mutations/deletions of TRβ gene (Refetoff et al., 1993). The unfunctional receptor dramatically lowers the effect of T3 on TRβ dominant tissues, resulting in growth and mental retardation, retinal degeneration, impaired hearing, and HPT axis regulation hallmarked by elevated serum free TH and TSH levels (Forrest et al., 1996c; Ferrara et al., 2012). Mutation in TRα gene results in growth retardation, gastrointestinal abnormalities; however the HPT axis is minimally affected. Patients have normal serum TH levels and TSH, but TRα dominant tissues are resistant to TH action (Bochukova et al., 2012) (Moran et al., 2014). There are several TRβ knock-out and knock-in mouse models available to investigate the RTH syndrome showing a similar phenotype found in human patients (Forrest et al., 1996b).

3.4.5 Regulation of tissue-specific TH action

Cellular transport is the first rate limiting step in TH action followed by deiodinase-mediated customization of T3 availability in the cell prior to TR binding, that induces conformational changes allowing co-activators/repressors to associate with the receptor **(Figure 1**). TH responsive genes can be regulated by TH either in a positive or negative manner. A complex combination of different promoter elements, DNA methylation pattern, co-action of TR isoforms, TR homo/heterodimerization and activity of co-activators and co-repressors can determine whether T3 will upregulate or downregulate transcription of TH responsive target gene. In the promoter of a gene positively

regulated by TH, TRE-s should be present that are unique consensus sequences serving as a binding site for heterodimeric TR. The most widely characterized TRE-s consist of two hexamer half sites, called direct repeats (DR), separated by 4 base pairs (DR+4) (Harbers et al., 1996) that can bind both TRα and TRβ. However, other TRE-s are also know, e.g. ones with different orientation and spacing of half-sites, like inverted repeat 0 (IR0), in rat growth hormone promoter (Brent et al., 1989), and everted repeat 6 (ER6), in rat and mouse myelin basic protein promoter (Farsetti et al., 1997). Still in the absence of T3 TR/RXR heterodimers are bound to TRE and recruit repressor molecules like N-CoR, that form a complex with histone deacetylases and change chromatin structure to suppress transcriptional activity (Darimont et al., 1998; Astapova et al., 2008). In case the receptor is liganded by T3, co-repressor complex dissociates and chromatin structure changes in a way that AF-2 activator domain of TR-s get available for nuclear receptor coactivator-1 (SRC-1), and transcription activity increases (Darimont et al., 1998; Alonso et al., 2009). Hepatic D1 mRNA is highly sensitive to T3, and shows a more robust increase to T3, than other well characterized TH sensitive genes in liver like Spot-14 and α-glicerophosphate dehidrogenase (Zavacki et al., 2005). The human *DIO1* gene promoter has been found to be the most responsive to T3 (Toyoda et al., 1995). Promoter of human *DIO1* gene contains two functional TRE-s, but canonical TRE-s in rat and mice *Dio1* 5' FR has not been identified until now. T3 effect on rat and mouse D1 mRNA is transcriptional and cannot be blocked by cycloheximide indicating no need for intermediate protein synthesis (Maia et al., 1995; Kim et al., 1998). There are also genes which are negatively regulated by T3. These are proteins e.g. involved in negative feedback regulation of HPT axis, like TRH (Lezoualc'h et al., 1992; Abel et al., 2001), TSHβ (Weiss et al., 1997), and D2 (Kim et al., 1998). TRβ is critical in negative trans-repression of these genes, and DNA binding is essential in negative regulation (Shibusawa et al., 2003), but the mechanism of this action is still under extensive characterization. Negative TREs are heterogenous and poorly understood.

3.5 Regulation of the HPT axis under pathophysiological conditions

Humoral and neuronal inputs to TRH neurons can overwrite normal feedback regulation in specific conditions and challenges like fasting, cold exposure, infection. The non-

thyroidal illness syndrome (NTIS) is a striking example of altered regulation of the HPT axis and occurs typically in critically ill patients. It is characterized by falling serum TSH and TH levels that is not followed by the upregulation of the HPT axis (Fekete et al., 2004; Gereben et al., 2008; Boelen et al., 2011). Although severe NTIS is strongly related to high mortality rate, it is still debated whether it should be considered as a metabolic adaptation or calls for therapeutic intervention (De Groot, 2015; Gereben Balázs, 2016).

A frequently used model of NTIS in rodents is the systemic inflammation induced by LPS (bacterial lipopolysaccharide) injection. After LPS administration circulating TH levels are falling but both TRH and TSH are decreased (Fekete et al., 2004; Fekete et al., 2005a) Importantly, in this model D2 is upregulated in hypothalamic tanycytes supposedly with the involvement of NfκB-mediated signalling pathways (Fekete et al., 2004; Zeold et al., 2006a). Previous studies in mice demonstrated, that LPS induced a~50% decrease in TRH expression in the PVN of wild type C57BL/6 mice while it did not occur in D2-KO animals (Freitas et al., 2010) indicating that D2 plays an important role in this process. Unilateral transection of ascending brain stem did not inhibit LPS induced fall in TRH expression, indicating that these inputs are not involved in this phenomenon (Fekete et al., 2005b). Dissection of altered regulation of TH action in NTIS would be required to better understand the nature and potential treatment of this syndrome.

3.6 The role of TH in iBAT-mediated non-shivering thermogenesis

The iBAT plays an instrumental role in energy dissipation via non-shivering thermogenesis (NST) (Lowell and Spiegelman, 2000) both in rodents and in human newborns (Hull, 1977; Cannon and Nedergaard, 2004). Recent imaging techniques also allowed to establish the presence of functional BAT islands in different regions of the body of human adults (Nedergaard et al., 2007; Virtanen et al., 2009), that put this tissue into the frontline of obesity research. The activation of this tissue in cold is crucial for heat generation in cold. The process is regulated by the central and peripheral sympathetic nervous system (SNS). Cold sensitive receptors at the periphery send signal to ventromedial hypothalamus (VMH), through the preoptic area (POA), and activate sympathetic afferent fibers to the BAT (Streckfuß et al., 2005).

Brown adipocytes have abundant mitochondria supply and express uncoupling protein-1 (UCP-1) or thermogenin. This protein is located in the inner mitochondrial membrane (Aquila et al., 1985) and uncouples the respiratory chain that results in the promotion of heat production instead of making ATP. The mechanism of NST has been intensively studied. Cold induced hypothalamic response facilitates norepinephrine (NE) release from sympathetic nerve endings (Schonbaum et al., 1963) that evokes cAMP response through β3-adrenergic receptors in brown adipocytes (Rubio et al., 1995). cAMP signalling increases UCP-1 and D2 expression rapidly and the increased T3 generation further accelerates cAMP production and UCP-1 transcription (Bianco et al., 1988). Free fatty acids (FFA) are released from lipid stores due to active lipases phosphorylated by protein kinase A (PKA), to serve as a substrate for the uncoupling (Fedorenko et al., 2012). UCP-1 uncouples the mitochondrial respiratory chain, by dissipating the proton gradient between the two mitochondrial membranes and facilitates FFA oxidation and heat production instead of making ATP **(Figure 5)**.

TH-s have a key role in this process (Lowell and Spiegelman, 2000). Hypothyroid rats cannot maintain normal body temperature and die several hours after acute cold exposure (Bianco and Silva, 1987). T3 is responsible for sufficient lipogenesis (Christoffolete et al., 2004), and adequate thermogenesis (de Jesus et al., 2001) during cold exposure. Local T3 excess saturates TRs rapidly and TRβ1 induces UCP-1 transcription while TRα1 mediates the thermogenic response (Martinez de Mena et al., 2010; Ribeiro et al., 2010). D2 has been shown to be a crucial component of BAT induced thermogenesis (Silva and Larsen, 1983; de Jesus et al., 2001). T3 also affects the central regulation of thermogenic response, and energy consumption. T3 evoked decreased AMP activated protein kinase (AMPK) phosphorylation and modulated lipid metabolism selectively in VMH of rats, resulting in elevated sympathetic activation, increased amount of thermogenic markers in the BAT and lower body weight (Lopez et al., 2010).

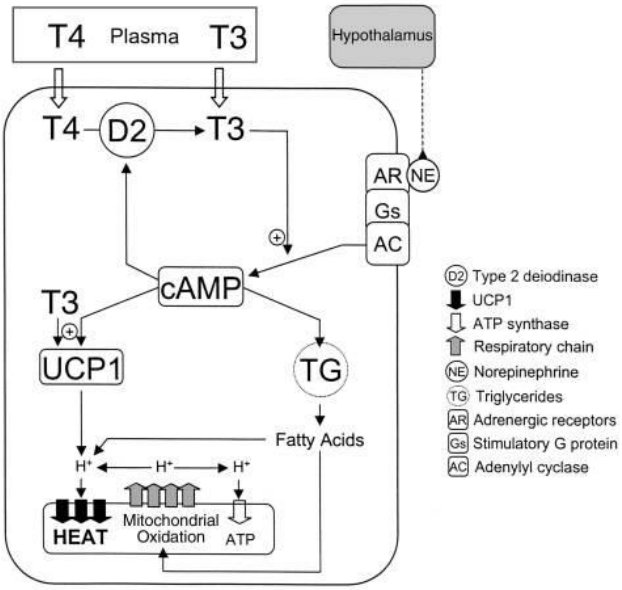

Figure 5. Cold induced sympathetic activation of iBAT is regulated by the hypothalamus and local mechanisms. Norepinephrine (NE) released from sympathetic nerve terminals in interscapular brown adipose tissue (iBAT) acts on β3-adrenergic receptors and increases uncoupling protein-1 (UCP-1) and type 2 deiodinase (D2) expression via cAMP signalling, furthermore facilitates the release of triglycerides from cell stores. D2-mediated T3 production accelerates cAMP response and UCP-1 expression. UCP-1 uncouples the mitochondrial respiratory chain and produces heat instead of ATP using fatty acids as a substrate.(de Jesus et al., 2001)

4. Aims

Our studies were performed to better understand the regulation of tissue-specific TH action. Specifically, we aimed to

1. study how onset of negative feedback regulation of the HPT axis occurs
   - determine the period of the onset of TH-mediated negative feedback in the developing chicken hypothalamus
   - identify underlying mechanisms governing set point formation of the HPT axis

2. study the regulation of thyroid hormone availability in hypothalamic neuroendocrine axes
   - address TH inactivation in parvocellular neurosecretory neurons of rats
   - investigate how regulation of TH availability in neurosecretory neurons responds to challenges in a model of non-thyroidal illness syndrome

3. generate a novel transgenic mouse model allowing the detection of tissue-specific thyroid hormone action in live animals and tissue samples
   - characterize the Thyroid hormone action indicator mouse model
   - study the hypothalamic pathogenesis of the non-thyroid illness syndrome and interscapular BAT regulation using this model

5. Materials and methods

5.1 Experimental animals

All animal experiments were conducted in compliance with the European Communities Council Directive (2010/63/EU) and (Decree 86/609/EEC) and approved by the Animal Care and Use Committee of the Institute of Experimental Medicine (Hungarian Academy of Sciences, Budapest). Experiments on chicken embryos and posthatch chickens were also conducted in accordance with legal requirements of Ethical Committee for animal experiments of the KU Leuven (Leuven, Belgium).

5.1.1 Chicken

White Leghorn chicken embryos and posthatch chickens were obtained from Ceva-Phylaxia (Budapest, Hungary) and Wyverkens (Halle, Belgium). The incubation was started at E0. Posthatch chickens were kept in a room with a 14L/10D photoperiod and water and food available *ad libitum*.

5.1.2 Rat and Mouse

Adult, male Wistar rats (N=20, b.w. 220–250 g, Toxi-Coop Ltd., Budapest) and Thyroid Hormone Action Indicator (THAI) mice (FVB/Ant background; new transgenic mouse line) were kept under standard laboratory conditions with food and water *ad libitum*.

5.1.3 Human tissue sample

For testing antibody specificity with Western blot, fresh-frozen hypothalamic samples were obtained from the Human Brain Tissue Bank, Semmelweis University from Prof. Miklós Palkovits.

5.1.4 Generation of transgenic THAI-Mouse by transposon-mediated technology

To generate transgenic founders, the pronucleus of fertilized FVB/Ant (FVB.129P2-Pde6b+ Tyrc-ch/AntJ) (Errijgers et al., 2007) oocytes was injected with a mixture containing the plasmid harbouring the targeting transposon cassette **(Figure 20)** (1

ng/µl) along with *in vitro* transcribed mRNA encoding the Sleeping Beauty transposase (Mates, 2011) (5 ng/µl). Four females were identified as founders using TaqMan assay on tail DNA with a luciferase probe and crossed with wild/type FVB/Ant (FVB.129P2-Pde6b+ Tyrc-ch/AntJ) male mice followed with inbred coupling of F1 generation. Indirect evidence obtained with luciferase TaqMan polymerase chain reaction (PCR) on different lines and generations suggest that a single copy of the transgenic cassette was inserted into the genome of all lines. Pronuclear injection, breeding and genotyping was made by Ferenc Erdélyi and Gábor Szabó, Medical Gene Technology Unit, Institute of Experimental Medicine, Budapest, Hungary.

5.1.4.1 Determination of copy number of transgenic THAI-Mouse lines

Copy number of the transgenic cassette was determined with fluorescence *in situ* hybridization (FISH). FISH was carried out on lymphocytes, isolated from spleen under aseptic conditions. Chromosomal preparations were performed according to standard techniques using 0.067 M KCl followed by fixation in methanol/acetic acid. We labelled an 1045bp fragment of the dCpG Luciferase coding sequence (nt 599-1644) with digoxigenin using Dig-Nick translation mix (Roche, Germany) and precipitated with mouse COT-1 DNA (Invitrogen) according to the manufacturer's instructions. Precipitated probe was dissolved in hybridization buffer. FISH was performed on methanol/acetic acid-fixed cells suspensions. Slides/DNA preparation and hybridization were carried out according to standard techniques. Hybridized sections were incubated overnight at room temperature with anti-digoxigenin-POD (1:100) antibody (Roche, Germany) in 1% BSA solution. Signal was biotin:tyramide (1:1000) amplified for 10 min in 0.05M Tris-HCl buffer pH 7.6 containing 0.003% H_2O_2). The deposited reaction product was detected with Fluorescein-(DTAF)-streptavidin antibody (Jackson Immunoresearch, USA). The analysis was done in at least 100 interphase nuclei and in a few metaphases if present on the hybridization area. FISH was performed by Irén Haltrich and Zsuzsa Tóth; 2nd Department of Pediatrics, Faculty of Medicine, Semmelweis University, Budapest, Hungary

5.1.4.2 Insertion site mapping in #4 THAI-Mouse with Splinkerette PCR

Splinkerette PCR was performed, as described (Potter and Luo, 2010). In brief, genomic DNA was digested with BstYI restriction enzyme. A universal splinkerette oligonucleotide was used to amplify the region between the 5' end of the cassette and the first BstYI site. The cassette-specific oligonucleotide was specific for the multiple cloning site of the PT/2BH vector located 3' to the 5' inverted terminal repeat (ITR) sequence. Nested PCR was performed to reamplify the PCR product followed by sequencing.

5.2 Recombinant DNA technology

The recombinant DNA constructs, e.g. the thyroid hormone action indicator construct (THAIC), chicken deiodinase promoter constructs and vectors containing inserts to generate RNA probes for *in situ* hybridization were prepared with standard techniques. DNA fragments were amplified with Taq or Vent polymerase driven PCR and cloned to plasmid vectors by ligating the overhanging restriction sites cleaved by various restriction enzymes with T4 ligase. The newly prepared recombinant DNA was transformed to bacteria, and the correct clone was amplified in bacterial culture in the presence of antibiotics (Gereben et al., 1999; Zeold et al., 2006a).

5.3 Animal treatments and sample collection

5.3.1 TH administration to chicken embryos and posthatch chickens, to study the formation of negative feedback on TRH neurons.

Animals were injected intravenously with either 1μg T4, 200 ng T3 or vehicle (saline with 5mM NaOH) as control 8h before sampling at stage E19 and P2. The applied 5:1 ratio of injected T4 and T3 mirrored the average ratio of T4:T3 present in the yolk (Prati et al., 1992; Van Herck et al., 2013). Injections were performed in embryos into a chorioallantoic blood vessel just beneath the egg shell or into the leg vein in hatched animals. Animals were euthanized by decapitation. Brains were removed quickly from the skull, immediately frozen in isopentane at -35 °C, covered with powdered dry ice and stored at -80 ºC until further use to *in situ* hybridization.

Pituitaries were removed at the same time and snap frozen on dry ice, and subsequently used for Taqman qPCR. Injection was performed by Pieter Vancamp and Veerle M. Darras, Department of Biology, Division of Animal Physiology and Neurobiology, KU Leuven, Belgium.

5.3.2 T3 administration to adult male rats, and ME microdissection for in vitro D3 activity measurement

Adult male Wistar rats were injected *i.p.* with 50 µg/of T3/100 g body weight (N=9) or vehicle (N=9) every second days in 8 days. After decapitation the ME was dissected under a Zeiss Semi DV4 stereomicroscope (Carl Zeiss GMBH, Hamburg, Germany) and immediately frozen on dry ice. Three ME samples were pooled from nine, while five cortex samples were collected from five animals.

5.3.3 Modulation of serum TH level in THAI-Mouse to study TH responsiveness of different tissues

The F2 generation was screened for tissue luciferase activity. To characterize basal and TH-induced luciferase activity of peripheral tissues and brain regions, 60-70 day old males were injected *i.p.* with 5µg/day/mouse of L-T4 or vehicle control for 3 days or 1 µg/g bw of L-T3 for one day. Hypothyroid mice were generated by adding 0.1% sodium perchlorate and 0.5% methimazole in drinking water for 3 weeks combined with low iodine diet. After decapitation tissues were removed, snap frozen on dry ice and stored at -80°C for luciferase activity measurement.

5.3.4 LPS treatment and microdissection of hypothalamic subdivisions of THAI-Mice

70 day-old male THAI line #23 mice were treated *i.p.* with LPS (150 µg/animal; E. coli 0127:B8, Sigma) and decapitated 6, 8 and 10h after injection. Brains were removed from skull, snap frozen in -25°C isopentane, and 1 mm coronal sections were prepared with blades in a pre-cooled mouse brain cast. Brain areas (ARC + ME and PVN) were microdissected with punch needle from frozen sections placed on pre-cooled glass

slides (Palkovits, 1986). Punch samples from two animals were pooled, and subsequently were assayed with real-time quantitative PCR after RNA isolation.

5.3.5 LPS treatment on Wistar rats and sample preparation for double-labelling immunohistochemistry for D3 and parvocellular releasing hormones

200g male Wistar rats were treated *i.p.* with LPS (250 µg/ 100g bw; E. coli 0127:B8, Sigma) for 12 hours, and brains were transcardially fixed with 4% paraformaldehyde (PFA) (for detection of GnRH, CRH, GHRH and somatostatin) or 4% acrolein/2% PFA (for detection of TRH).

5.3.6 Sympathetic denervation of iBAT and cold stress in THAI-Mice

iBAT was unilaterally denervated with surgical transection of its sympathetic nerves (Pulinilkunnil et al., 2011). Cold stress was applied three days after surgery. During cold stress, single housed animals were kept under standard light conditions at 4°C; water and food were available *ad libitum*. Control animals were kept at room temperature (22°C) under same conditions. After decapitation, samples from the iBAT were collected on dry ice and stored at -80°C for NE measurement, deiodination assay (see 5.8.3) and Taqman analysis.

5.3.7 GC24-treatment: Testing selectivity of GC24, a TRβ-specific compound in THAI-Mice

70-day old, male THAI #4 mice were made hypothyroid by adding 0.1% sodium perchlorate and 0.5% methimazole to the drinking water and feeding animals with iodine-deficient diet (Research Diets Inc., New Brunswik, NJ) for three weeks to inhibit endogenous TH production. Hypothyroid mice were treated with a single, *i.p.* injection of 1.53 nM/g bw GC24 (a kind gift of Dr. Tom Scanlan), (equimolar to 1 µg/g BW T3), or dimethyl sulfoxide as vehicle 24 h before tissue sampling. After decapitation, liver (TRβ-dominant tissue) and heart (TRα-dominant tissue) were removed and snap frozen on dry ice.

5.4 Immunohistochemistry, and in situ hybridization on embryonic and posthatch chicken brain

5.4.1 In situ hybridization and cRNA probe labelling

5.4.1.1 Preparation of S35 labelled cRNA probes for in situ hybridization

Chicken D2 cRNA probe was generated as previously described (Gereben et al., 2004). Chicken D3 cRNA probe was generated from the pCI-neo plasmid containing the 1366 bp fragment of chicken D3 complementary DNA (cDNA) (Van der Geyten et al., 1997). After EcoRI digestion, T3 RNA polymerase (Promega Corp., Madison, WI) was used to transcribe cRNA antisense probe in the presence of [S^{35}]-labelled UTP. Sense probe was generated after XbaI digestion with T7 polymerase. An 860 bp long fragment of chicken Nkx2.1 mRNA corresponding to bases 40-899 of GeneBank# NM_204616.1 was amplified on E7 chicken embryo cDNA with Taq polymerase using the following oligos: sense, CATACGACTCCTTTCTCAGTGT; and antisense, GTCTGATGGCTCTGATGCTGT and was cloned into pGemT vector (Promega). Antisense probe generation was carried out with SP6 RNA polymerase after ApaI digestion, whereas NotI digestion and T7 polymerase was used for the sense probe. We generated a 600 bp-long chicken proTRH probe by amplifying a chicken brain cDNA with Taq polymerase using the following oligos: sense, ATTAAACATGCCTCTGCCACA; antisense, AAACAATTACTTTCTCATTCCTCTG followed by cloning into a pGemT vector (Promega). The cloned region was identical to the one described earlier (Vandenborne et al., 2005). Antisense probe generation was carried out with SP6 RNA polymerase after NcoI digestion, whereas NotI digestion and T7 polymerase was used for the sense probe. Radio-labelled riboprobes were purified with Quick spin columns for radio-labelled RNA purification (Roche Applied Science, Mannheim, Germany) following the manufacturer's instructions.

5.4.1.2 In situ hybridization

Serial 12 μm thick coronal sections were cut from native brains on a cryostat (Leica Microsystems GmbH, Wetzlar, Germany), mounted on gelatine coated slides, air dried at 42ºC overnight and stored at -80°C. After thawing, the sections were fixed with 4%

PFA (in 0.1M phosphate buffer (PB) pH 7.4) for 10 minutes and the *in situ* hybridization was carried out as previously described (Fekete et al., 2007). The hypothalamic sections referred to as "anterior" represent the region located posterior to the optic chiasm and anterior to the inferior hypothalamic nucleus while the "posterior" sections originate from the region of the inferior hypothalamic nucleus. Autoradiograms were developed after 6-weeks exposure at 4 ºC in the case of D2 hybridization and after 3 weeks when Nkx2.1 expression was examined. Slides hybridized for D3 mRNA were developed after 4 days exposure and after 2 days for proTRH hybridization. The specificity of hybridization was confirmed using sense probes that resulted in the complete absence of hybridization signal in the brain. The sections were counterstained with 0.005% Cresyl violet dissolved in 70% alcohol and coverslipped with DPX mounting medium (Alvarez-Buylla et al., 1990). The Cresyl violet staining was visualized under epifluorescent illumination using a rhodamine filter set. Images of the *in situ* hybridization signals were taken by AxioImager M1 microscope equipped with an MR5 digital camera (Zeiss) using darkfield illumination. Densitometric analysis of Nkx2.1 *in situ* hybridization signal was performed with ImageJ software on E13 and P2 sections of the same plane, measuring mean silver grain density over α and β tanycytes (in the wall and the floor of the third ventricle, respectively).

5.4.2 Pretreatment for light microscopic immunohistochemistry

After sectioning on freezing microtome (Leica Microsystems GmbH, Wetzlar, Germany) sections were stored in cryoprotective solution (30% ethylene glycol; 25% glycerol; 0.05 M PB) and stored at -20°C. First, the sections were washed out of cryoprotective with phosphate buffered saline (PBS), and incubated in a mixture of 0.5% H_2O_2 and 0.5% Triton X-100 in PBS for 15 minutes to increase antibody penetration and reduce endogenous peroxidase activity. To reduce nonspecific antibody binding, the sections were treated with 2% normal horse serum in PBS for 20 minutes. Sections were first incubated in primary antisera (conditions indicated in **Table 1**) then were reacted with biotinylated donkey anti-rabbit IgG (1:500; Jackson ImmunoResearch, West Grove, PA) at room temperature for 2 hours, and incubated with avidin-biotin complex (ABC, 1:1,000; Vector, Burlingame, CA) for 1 hour. To detect the peroxidase signal we used nickel-diaminobenzidine (NiDAB) developer

consisting of 0.05% diaminobenzidine, 0.15% nickel ammonium sulfate, and 0.005% H_2O_2 in 0.05 M Tris buffer (pH 7.6). The resulting reaction product was silver-gold-intensified using the Gallyas method (Liposits et al., 1984; Kallo et al., 2001). The immunostained sections were mounted onto glass slides from polyvinyl alcohol (Elvanol, Sigma, Budapest, Hungary), dried and coverslipped with DPX mounting medium (Fluka, Buchs, Switzerland).

Table 1: Preparation of sections and staining conditions for light microscopic immunohistochemistry; FM: freezing microtome, RT: Room temperature, PFA: paraformaldehyde

Experiment	Fixation	Sectioning	Pretreatment	Primary antibody	Secundary antibody	Detection method
E18, and P2 hypothalamic chicken D3	immersion PFA 4%, 8h RT	20 µm, FM	for light microscopy	rabbit anti-chicken D3 polyclonal 1:24000, 48h, 4oC,	biotinylated donkey anti-rabbit IgG 1:500, 2h, RT	peroxidase based, NiDAB chromogene
hypothalamic rat D3	transcardiac perfusion 4% PFA	25 µm, FM	for light microscopy	rabbit anti-rat D3 polyclonal 0.5-1 ug/ml, 48h, 4oC NBP1-05767B, Novus Biologicals	biotinylated donkey anti-rabbit IgG 1:500, 2h, RT	peroxidase based, NiDAB chromogene

5.4.3 Pretreatment for immunofluorescent double and triple-labelling

Immunofluorescent colocalization experiments were carried out on tissue sections fixed with 4% PFA (for detection of GnRH, CRH, GHRH and somatostatin) or 4% acrolein/2% PFA (for detection of TRH). Sections were cut on freezing microtome (Leica Microsystems GmbH, Wetzlar, Germany), and stored in cryoprotective solution (30% ethylene glycol; 25% glycerol; 0.05 M PB), at -20^{o}C, until use. Acrolein was inactivated with 1% sodium borohydride (30 min). All sections were pre-treated with H_2O_2 combined with Triton X-100 (0.5% each in 0.1 M PBS, 20 min), followed by normal horse serum (2% in 0.1 M PBS) for 10 min.

5.4.4 Immunofluorescent double-labelling for D3, and parvocellular releasing- or release inhibiting hormones in control and LPS treated rat hypothalamus

Pretreated sections were incubated in rabbit anti-D3 antiserum (2 µg/ml, 48 h), which was detected with biotinylated-donkey anti-rabbit IgG (1:500, 2 h) and Alexa-488-conjugated streptavidine (1:400, 12 h). Then, one of the following primary antibodies (48 h, 4°C) were used: guinea pig anti-GnRH (#1018, 1:5,000) (Hrabovszky et al., 2011); sheep anti-TRH (#08W2, 1:1,500) (Wittmann et al., 2009); guinea pig anti-CRH (#T-5007, Bachem, 1:3,000); sheep anti-GHRH (#19–4, 1:30,000, kindly donated by Dr. I. Merchenthaler Baltimore, MD, USA) (Hrabovszky et al., 2005); rat anti-somatostatin (#354; Chemicon, 1:50). These primary antibodies were reacted (12 h, 4°C) with appropriate Cy3-conjugated secondary IgG raised in donkeys (1:500, Jackson ImmunoResearch Laboratories, Inc.).

5.4.5 Immunofluorescent triple-labelling for D3, MCT8, and parvocellular releasing- or release inhibiting hormones

Sections were pretreated identically as described above were incubated in rabbit anti-MCT8 antiserum (1:1000, 48 h, kind gift of Dr. TJ Visser Rotterdam, The Netherlands), and detected with Alexa 555-conjugated anti-rabbit IgG (1:500, 2 h). Then, one of the following primary antibodies (48 h, 4°C) were used: guinea pig anti-GnRH (#1018, 1:5,000) (Hrabovszky et al., 2011); sheep anti-TRH (#08W2, 1:1,500) (Wittmann et al., 2009); guinea pig anti-CRH (#T-5007, Bachem, 1:3,000); sheep anti-GHRH (#19–4, 1:30,000, kindly donated by Dr. I Merchenthaler Baltimore, MD, USA) (Hrabovszky et al., 2005); rat anti-somatostatin (#354; Chemicon, 1:50). (Liposits et al., 1984)These primary antibodies were reacted (2 h) with appropriate FITC-conjugated secondary IgG that were raised in donkeys (1:50, Jackson ImmunoResearch Laboratories, Inc.). Double-labelled sections were incubated in biotinylated rabbit anti-D3 antiserum (2 µg/ml, 48 h), followed by treatment in ABC (1:1000, 2 h). The sections were then subjected to tyramide amplification according to the manufacturer's instructions (NEN, Boston, MA). To further amplify the reaction product, the ABC treatment and the

tyramide amplification were repeated. Finally the sections were incubated in Cy5-conjugated streptavidin (1:250).

5.5 Subcellular localization of D3 with Superresolution microscopy (N-STORM)

Coronal 10 µm-thick sections through the anteroposterior extent of the ME of rats perfused with 4% PFA in PBS (150 ml) were cut on a freezing microtome. The sections were pretreated for light microscopic immunocytochemistry as described above (See V.5.4.2). The pretreated sections were incubated in one of the following antisera for 3 days at 4°C: rabbit anti-D3 serum (4 µg/ml), guinea pig anti-GnRH (#1018, 1:4,000,000) (Hrabovszky et al., 2011), mouse monoclonal anti-Rab3a IgG clone 42.2 (1:2000; Synaptic Systems). After washing in PBS, the sections were immersed overnight at 4°C in 1:50 dilution of donkey anti rabbit, guinea pig or mouse IgG (Jackson Laboratories), respectively, doubly conjugated with Cy3 (GE Healthcare) and Alexa 647 (Invitrogen). The Cy3/IgG ratio of the conjugated IgG was between 2 and 3, while the Alexa 647/IgG ratio was between 0.6 and 0.8. After washing in PBS, the sections were mounted on glass coverslip and air dried. Just before imaging the coverslipes holding the slides were mounted on glass slide using the following imaging medium: DPBS, 1 M mercaptoethylamine (MEA), 50% glucose solution in water, and the GLOX system (10 mg of glucose oxidase plus 25 µl of catalase and 100 µl of DPBS) in 80:10:10:1 volume ratio (Dani et al., 2010). Axon varicosities located in the external zone of the ME were imaged using a Nikon N-STORM super-resolution microscope system (Nikon Instruments Ltd.) based on Nikon inverted Ti-E microscope equipped with perfect-focusing system (PFS) and the Nikon 100x NA 1.49 oil TIRF objective. A 561 nm wavelength laser (Sapphire 561-100-CW, Coherent) was used for excitation of the activator dye (Cy3) while a 647 nm wavelength laser (MPB Communications Inc, Montreal, Canada) was applied for excitation and bleaching of the reporter dye (Alexa647). The 2D images were acquired with an Andor Ixon DU-897 EMCCD camera (AndorTechnology, Belfast, Northern Ireland) using 30 ms exposition, one activation frame followed by three frames of imaging for 4000 cycles. The image trajectories were analysed by the N-STORM 2 module of the NIS-Elements followed by exporting as a high resolution bitmap (1.4 nm/pixel).

Using the NIKON NIS software, the diameter of at least 500 immunoreactive clusters from each staining was measured.

5.6 Confocal imaging in double and triple-labelling studies and quantification of colocalization of D3 with the different hypophysiotropic peptides

Confocal images of double and triple-labelled sections were taken from the external zone of the ME using 60 X oil immersion objective, scanned by a Radiance 2100 confocal microscope (Bio-Rad Laboratories, Hemel Hempstead, UK). Deconvolution of 150 nm thick optical slices was performed using Xming (public domain at http://sourceforge.net/projects/xming/) software. The fluorochromes were detected with laser lines and filters summarized in **Table 2**. Pinhole sizes were set to obtain optical slices less than 0.7 μm thick.

Colocalization of D3 with the different peptides was counted in the axon varicosities in the external zone. For each double-labelling combination, brain sections from three animals were used. One randomly selected microscopic field (2600 μm2 each) from the external zone of ME of each animal was analysed. Every field was divided into 100 equal parts to facilitate the counting of the double-labelled axon varicosities and the percentage of D3 occurrence in immunostained varicosities was determined.

Table 2. Filter sets used for confocal imaging of colocalization of type 3 deiodinase (D3) or monocarboxylate transporter 8 (MCT8) with hypophysiotropic peptides, and imaging triple labelling for D3, MCT8, and hypophysiotropic peptides

Staining	Target	Fluorochrome	Laser lines [nm]	Dichroic/ Emission filters [nm]
Double labeling for D3 and hypophysiotropic peptides	**D3**	Alexa 488	488	560/500-530
	GnRH, TRH, CRH, GHRH, somatostatine	Cy3	543	560-625
Triple labeling for D3, MCT8 and hypophysiotropic peptide	**D3**	Cy5	637	660-long pass
	MCT8	Cy3	543	650/565-625
	GnRH, TRH, CRH, GHRH, somatostatine	FITC	488	560/500-530

5.7 Specificity of antibodies

Specificity of the antisera against the hypophysiotropic hormones was earlier described (Hrabovszky et al., 2005; Wittmann et al., 2009; Hrabovszky et al., 2011). The employed secondary antibodies were designed for multiple labelling and pre-absorbed by the producer with immunoglobulins of several species, including those in which the current non-corresponding primary antibodies were raised. Omission of any of the primary antisera from the triple-labelling immunofluorescence did not influence the pattern of the other two immunoreaction signals.

5.7.1 Determination of staining specificity of D3 antiserum by preabsorption

The specificity of the D3 antiserum in the rat brain was described elsewhere (19). To further determine the specificity of the antiserum in the examined region, the D3 antiserum was preabsorbed with the immunizing peptide (10 μg/ml) that resulted in loss of immunoreaction product in the MBH **(Figure 13A inset)**.

5.7.2 Determination of D3 antiserum specificity by Western blot

The specificity of the antiserum was also demonstrated by western blot showing bands of expected size for rat and human D3 **(Figure 12)** western blot was performed using standard methodologies as described earlier (Zeold et al., 2006b). Adult, male, Wistar rats were decapitated and the hypothalamus immediately frozen. A fresh-frozen human hypothalamic sample was obtained from the Human Brain Tissue Bank, Semmelweis University. Fifty micrograms of rat and human hypothalamic protein sonicate was resolved by 10% SDS PAGE, and the D3 band identified using rabbit anti-D3 antibody (NBP1-05767, Novus, 0.5 ug/ul) and visualized using the BM Chemiluminescence Western Blotting Kit (Roche Diagnostics Co., Indianapolis, IN, USA).

5.8 Deiodination assay

5.8.1 Measurement of D2 activity

Enzyme activity measurement is based on the determination of the amount of free I^{125} removed by D2 from the outer ring of I^{125} labelled T4, *in vitro*, in tissue lysates. (27)

Fresh-frozen tissue samples were homogenized with sonication in PE buffer (0.1M potassium phosphate, 1 mM ethylenediaminetetraacetic acid (EDTA), pH 6.9) containing 0.25M sucrose and 10 mM DL-dithiothreitol (DTT). Free I^{125} from spontaneous deiodination of I^{125} labelled T4 is removed on Sephadex LH20 silica column on the day of measurement. Purified T4-I^{125} and cold T4 serves as substrate for D2. To detect only D2-mediated T4 conversion assay mix contains 1mM PTU, and 1μM T3 to selectively inhibit D1 and D3 activity, according to the ATA guide (Bianco et al., 2014). Assay background was determined using the tissue of the proper experiment, assayed under the same conditions except that a D2 saturating concentration (100 nM) of unlabelled T4 was applied. Assays were run on 37^{o}C, and all samples were measured in duplicate. Assay conditions for different experiments are presented in **Table 3**.

5.8.2 Measuring D2 activity in chicken hypothalamic samples

Hypothalamus (without MBH region) and MBH tissue samples were collected from E15, E18 and P2 chicks and immediately frozen on dry ice. D2 activity was determined with some modification of the previously described protocol (Gereben et al., 1999). Assay was run under the same conditions described above, and in **Table 3**. To increase signal to background ratio in MBH samples, we decreased the amount of unlabelled T4 in assay mix to 0.1 nM and incubated the samples for 3 hours on 37 ^{o}C. The reaction also contained 1mM PTU and 1 μM T3 to block D1 and D3 according to the ATA guide (Bianco et al., 2014).

5.8.3 Measuring D2 activity in intact and denervated iBAT tissue in THAI-Mice exposed to cold stress

D2 activity was determined by *in vitro* enzyme activity measurement, from tissue lysates of intact and denervated iBAT samples. The tissue preparation was the same as described above and assay conditions are summarized in **Table 3**.

Table 3. Deiodination assay conditions for D2; MBH: Mediobasal hypothalamus, HT-MB: hypothalamic block lacking MBH; iBAT: interscapular brown adipose tissue; PTU: 6-n-propyl-2-thiouracil; DTT: DL-dithiothreitol

Deiodinase assay conditions	T4 substrate	protein (µg)	assay time (min)	assay mixture
E15, E18, P2 chicken MBH and HT-MBH samples	0.1nM	100	180	20mM DTT, PTU, 1µM T3
Intact and denervated iBAT samples	1nM	100	120	10mM DTT, PTU, 100nM

5.8.4 Measurement of D3 activity

D3 catalytic activity was determined by *in vitro* enzyme activity assay combined with HPLC method. The samples were sonicated in 0.1 M phosphate, 1 mM EDTA at pH 6.9 with 10 mM DTT and 0.25 M sucrose, and subjected to D3 assay as previously described (Richard et al., 1998; Simonides et al., 2008). D3 enzyme activity in tissue samples was assayed by Rafael Arrojo e Drigo and Antoni C. Bianco, at University of Miami Miller School of Medicine, Miami, USA.

5.9 Detection of luciferase activity in vitro and in vivo

5.9.1 In vitro luciferase activity measurement

Tissue samples were milled to powder in liquid nitrogen and sonicated in luciferase lysis buffer (100 mM KH_2PO_4, 4 mM ethylene glycol tetraacetic acid (EGTA), 4 mM EDTA pH 7.8) freshly prepared with 0.7mM phenylmethylsulfonyl fluoride and 0.1mM DTT. Brain tissue was lysed in one step, with brief sonication in lysis buffer. After a 10 min centrifugation at 14.000 g at 4°C, supernatant was removed for luciferase activity measurement. Assay on tissue samples or Thyroid Hormone Action Indicator Construct (THAIC)-HEK293T cells was performed with Luciferase assay system reagent (Promega) on a Luminoskan Ascent (Thermo Electron Corp. Labsystems, Vantaa, Finland) luminometer. Detected RLU was normalized to protein content of the sample.

5.9.2 Detection and quantification of luciferase activity in live animals

In vivo imaging of iBAT of T3 treated and cold-stressed animals was performed 24 h after 1 µg /g bw *i.p.* T3 injection or after 24 h exposure to 4°C. Live imaging was obtained in ketamine-xylazine (ketamine 50 µg/g, xylazine 10 µg/g bw, *i.p.*) anaesthetized mice whose fur over the iBAT and abdominal organs had been removed with depilatory cream. D-luciferin (Gold Biotechnology) was dissolved in PBS and *i.p.* injected (150 and 750 µg/g bw for the T3 treated and cold-stressed animals, respectively) 15 min before *in vivo* imaging. Emitted light was detected with an IVIS Lumina II In vivo Imaging System (PerkinElmer Waltham, MA, USA) and quantitated in all animals using a region of interest (ROI) of identical size and shape. Data are reported as emitted photon/second. T3 treated or cold-stressed animals were studied using identical imaging parameters (binning and exposure time) as their corresponding controls in both dorsal and ventral positions.

5.10 Studies in cell cultures

5.10.1 Determination of chicken Dio2 promoter responsiveness to Nkx2.1 in U87 glioma cell line

5.10.1.1 Cell culture, and transfection

U87 human glioma cells were maintained under standard conditions in Dulbecco's Modified Eagle's Medium (DMEM) supplemented with 10% fetal bovine serum (FBS) and were transfected using the calcium-phosphate precipitation method as described (Gereben et al., 2001) using a slight modification. Briefly, transfection was carried out in a 24-well plate (Corning) using 1600 ng/well total DNA. 20.000 cells were seeded in each well one day before transfection, and the cells were harvested 48 hours later.

5.10.1.2 Promoter studies

pGL3-cDIO2(-3586/-1) and pGL3-hDIO2(-6860/+7) luciferase reporter constructs were previously generated by inserting ~3.6kb of chicken and ~6.8kb of human 5' FR of *DIO2* promoter into pGL3 basic vector (Fekete et al., 2004; Christoffolete et al., 2010). The pGL3-cDIO2(-588/-1) construct was generated with Vent PCR using pGL3-cDIO2(-3586/-1) as a template and confirmed by sequencing. A chicken *Dio3* 5' FR containing plasmid was obtained by genome walking of the region upstream of the D3

coding sequence. The pGL3-cD3(-623/-1) construct was subsequently generated by amplification of 623 bp of the 5' FR and cloning the fragment into the pGL3-basic vector. Each well of a 24 well plate was transfected with 1600 ng total DNA, containing 400 ng pGL3-basic based firefly luciferase reporter vector construct (with promoter or empty control), 200ng of Nkx2.1 expressing (or CDM8 control) vector, 1ng phRL-hβactin(-213+932) *Renilla* luciferase construct (Doleschall et al., 2007) as internal control, made up with pUC19 carrier DNA. The rat Nkx2.1 expressing vector was kindly provided by Dr. R. Di Lauro (Guazzi et al., 1990). To determine promoter activities, Dual-Luciferase Reporter Assay System (Promega) was used as previously described (Zeold et al., 2006a). The luciferase activities of at least four independent transfections were measured in duplicate using a Luminoskan Ascent Luminometer Ascent (Thermo Electron Corp. Labsystems, Vantaa, Finland). Firefly luciferase activity was normalized to *Renilla* luciferase activity.

5.10.2 Generation of the THAIC-HEK293T cell line

HEK293T cells were cultured in DMEM+10% FBS and transfected with the THAIC targeting construct **(Figure 20)** along with the pcGlobinSB100 transposase encoding vector (Mates et al., 2009) (provided by Zsuzsanna Izsvák and Lajos Mátes) to allow Sleeping Beauty recombinase assisted genomic integration. Clone selection was performed in the presence of 150 μg/ml zeocin. Clones were cultured for 24 h in charcoal stripped FBS (Egri and Gereben, 2014) followed by the induction with 100 nM T3 for 24h in the presence of transiently coexpressed mouse TRα. Cells were lysed in passive lysis buffer of the Dual-Luciferase assay system (Promega) before luciferase assay.

5.11 Taqman real-time quantitative PCR

All Taqman PCR reactions were performed in a standardized way: Total RNA was isolated from snap frozen tissue samples, with RNeasy Lipid Tissue Mini kit (Quiagen) according to manufacturer's instructions. 0.25 or 1 μg (for hypothalamic punch samples, or iBAT and chicken pituitary, respectively) total RNA was reverse transcribed with High-Capacity cDNA Reverse Transcription Kit (Thermo Fisher Scientific). cDNA

concentration was determined with the Qubit ssDNA assay kit. 10ng cDNA was used in each Taqman reaction. mRNA expression of target genes was detected with Taqman Gene expression probe sets using Taqman Fast Universal PCR Mastermix (Thermo Fisher Scientific) and compared to housekeeping gene expression. Reactions were assayed on Viia 7 Real-time PCR instrument (Applied Biosystems). Expression of the GAPDH housekeeping gene was also analysed under all challenge conditions applied: LPS challenge in THAI-Mouse model did not evoke significant changes in GAPDH expression as analysed by one-way ANOVA in four different time points after LPS injection. Cold stress had no effect on GAPDH expression either in intact or in denervated iBAT lobes.

Sympathetic denervation, however, consistently down-regulated GAPDH expression by 2-fold, thus, this was taken into account when calculating results of the denervation experiments by dividing fold changes of Luc/GAPDH and D2/GAPDH rations by 2. In chicken pituitary samples GAPDH expression did not changed, neither to T3 nor T4 injection. Accession numbers of gene expression probe sets are listed in **Table 4**.

Table 4. Taqman probe sets used in quantitative PCR experiments

Gene	Name	Accession Nr.
TSHβ in T4 and T3 treated E18 and P2 chicken pituitary		
TSHβ	thyroid stimulating hormone beta	Gg03348479_m1
GAPDH	glyceraldehyde-3-phosphate dehydrogenase	Gg03346982_m1
Effect of cold stress on sympathetically denervated iBAT		
Luciferase	firefly luciferase enzyme	AIY9ZTZ
dio2	type 2 deiodinase	Mm00515664_m1
GAPDH	glyceraldehyde-3-phosphate dehydrogenase	Mm99999915_g1
TH action in hypothalamus in NTIS		
TRH	thyrotropin-releasing hormone	Mm01963590_s
Luciferase	firefly luciferase enzyme	AIY9ZTZ
dio2	type 2 deiodinase	Mm00515664_m1
GAPDH	glyceraldehyde-3-phosphate dehydrogenase	Mm99999915_g1

5.12 Analysis of norepinephrine content of iBAT

NE concentrations of mouse iBAT were measured using surfactant-assisted online solid phase extraction sample preparation followed column-switching liquid chromatographic separation with electrochemical detection, as described (Horváth et al., 2014). Prevention of fat-precipitation in the aqueous extraction solvent phase, the non-ionic surfactant Triton X-100 was used. The native tissue was homogenized by sonication in 300µl 0.1 M ice-cold perchloric acid which contained 10mM theophylline as internal standard, 0.1 % sodium metabisulfite as anti-oxidant and 0.01 % (v/v) Triton X-100 as emulsifier. The NE content was expressed as pmol/mg protein. NE measurement was performed by Mária Baranyi and Beáta Sperlágh, Molecular Pharmacology Research Group, Institute of Experimental Medicine, Budapest, Hungary.

5.13 Indirect calorimetric measurements

11-week-old old male THAI #4 and wild type control (FVB/Ant) mice were analysed for whole energy expenditure, oxygen consumption and carbon dioxide production using calorimetric cages (PhenoMaster/LabMaster, TSE Systems GmbH, Bad Homburg, Germany). Body composition analyses were performed using an EchoMRI Whole Body Composition Analyser (EchoMRI LLC, Houston, TX). Indirect calorimetric measurements were performed with the help of Mónika Tóth and Csaba Fekete in the Metabolic Phenotyping Center of the Institute of Experimental Medicine, Budapest, Hungary.

5.14 Serum thyroid hormone measurement

Serum free T4 and free T3 levels were measured with AccuLite CLIA Microwells kit (Monobind Inc., Lake Forest, CA USA) according to the manufacturer's instructions. Measurement is based on competitive chemiluminescence enzyme immunoassay methodology in a microplate format.

5.15 Statistics

All data are shown as mean ± SEM. Groups were compared with two-tailed t-test. Multiple comparisons were made by one way ANOVA followed by Newman-Keuls or (above group number higher than 3) the Tukey post-hoc tests. Results of denervated iBAT experiments were analysed by Repeated Measurements ANOVA followed by Tukey post-hoc test.

6. Results

The developmental mechanisms responsible for the onset of TH-evoked negative feedback on the HPT axis are poorly understood. Since rodents provide a suboptimal model for these studies due to their strikingly different kinetics of HPT axis development compared the humans, we used chicken embryos, a well-established developmental model for our studies.

6.1 Regulation of the onset of negative feedback in the developing chicken hypothalamus

6.1.1 T4 induced negative feedback of the chicken HPT axis forms between E19 and P2

First we aimed to determine the period of onset of hypothalamic negative feedback and assess the role of D2-mediated T4 activation in this process. We studied the effect of T4 and T3 challenges on the developing chicken hypothalamus and determined TRH expression in the PVN and TSHβ in the pituitary. Expression of the proTRH mRNA was significantly decreased by 25% in response to T4 treatment in the PVN of P2 chicken **(Figure 6D,E)**, while the same treatment did not induce a significant change in E19 embryos **(Figure 6A,B)**. In contrast, proTRH expression was responsive to T3 in both age groups **(Figure 6C,F)**. T3 decreased proTRH expression by 30% in E19 chicken PVN and by 25% in P2. Densitometric analysis of the data is presented in **Figure 6G**.

Expression of TSHβ mRNA was also monitored in the pituitary with TaqMan qPCR. TSHβ expression was not suppressed at E19 either by T4 or T3 injection, while in P2 animals both T4 and T3 reduced TSHβ mRNA (60% and 20%, respectively) **(Figure 6H)**.

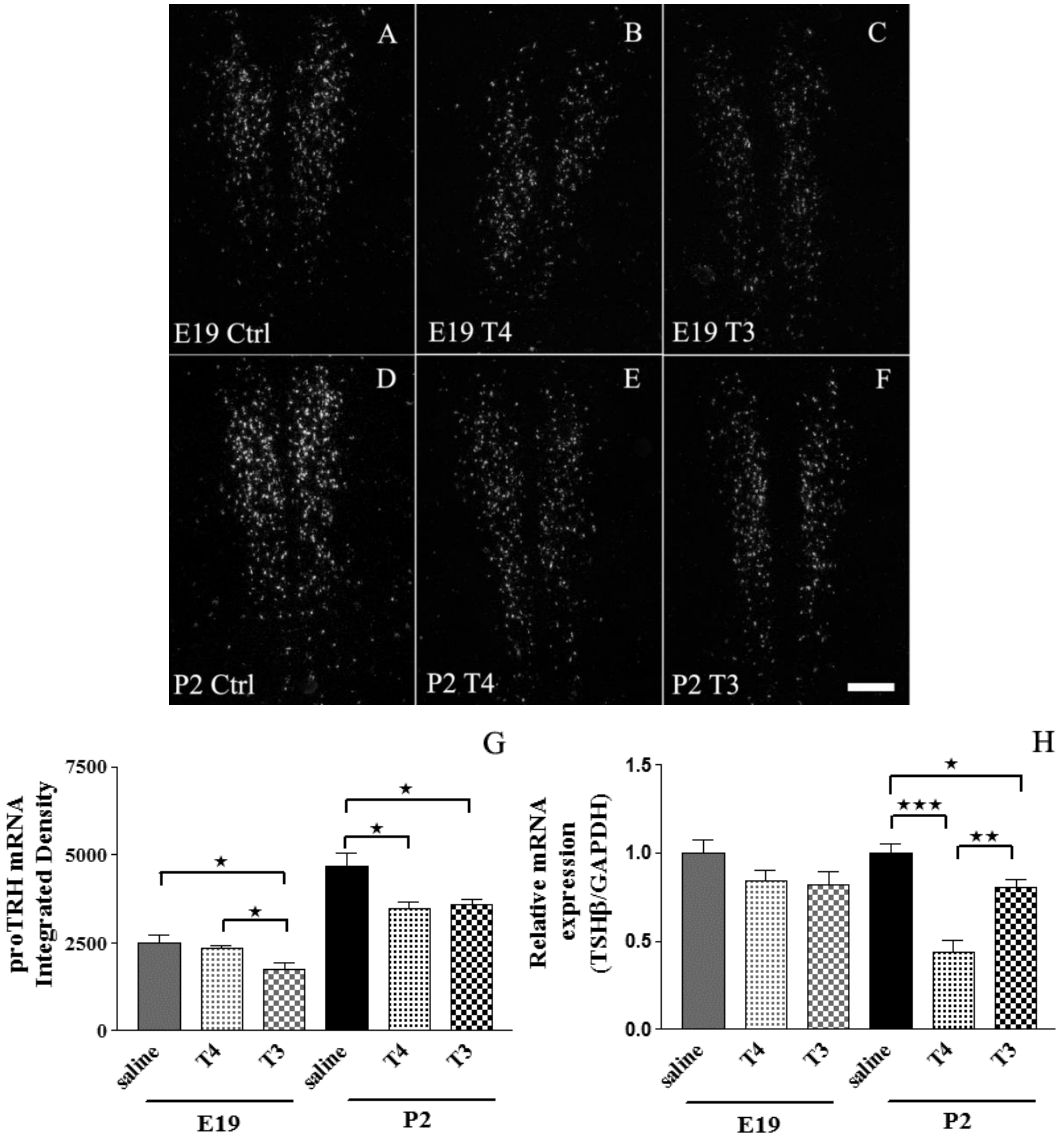

Figure 6. T4 and T3-induced negative feedback of the hypothalamus-pituitary-thyroid (HPT) axis in the developing chicken hypothalamus and pituitary. Dark-field images of proTRH *in situ* hybridization in (A,B,C) E19 and (D,E,F) P2 chicken paraventricular nucleus (PVN) 8 hours after (B,E) T4, (C,F) T3 or (A,D) saline injection. (G) Densitometric analysis of proTRH signal in E19 and P2 PVN. T3 decreased TRH expression in the PVN of both age groups while T4 could reduce proTRH expression only in P2. *P<0.05 (mean ± SEM, N=5) ANOVA followed by Newman-Keuls post-hoc test. (H) Taqman qPCR of TSHβ mRNA expression in E19 and P2 pituitaries, 8 hours after T4, T3 or saline treatment. In P2 animals, both T4 and T3 decreased thyroid stimulating hormone beta (TSHβ) expression, while no significant change was detected at E19. *P<0.05; **P<0.01; ***P<0.001 (mean ± SEM, N=5) by ANOVA followed by

Newman-Keuls post-hoc test. Scale bar, 200 μm E19: 19-day-old embryo; P2: 2-day-old posthatched chicken

6.1.2 D2 mRNA is expressed in E13 tanycytes

The presented difference between the responsiveness of TRH expression in the PVN to T4 and T3 at E19 suggested that developmental changes in D2-mediated TH activation could be an important factor in set point generation. Therefore the expression of D2 mRNA was assessed in the chicken hypothalamus with isotopic *in situ* hybridization during development before (E13) and after (P2) the onset of negative TH feedback. In all studied developmental stages, strong perivascular D2 mRNA hybridization signal appeared throughout the hypothalamus. In the E13 embryos, faint D2 hybridization signal was observed after six weeks exposure in β-tanycytes in "posterior" hypothalamic sections containing the region of the inferior hypothalamic nucleus **(Figure 7C).** However, the hybridization signal was absent in the β-tanycytes in "anterior" sections located between the optic chiasm and the inferior hypothalamic nucleus and in the α-tanycytes **(Figure 7A,C)** In later stages (P2), the D2 mRNA expression appeared in β-tanycytes in the "anterior" sections **(Figure 8A,C)** and became more dominant in the β-tanycytes of "posterior" sections, while D2 hybridization signal expanded to α-tanycytes in the wall in the more "posterior" region **(Figure 8E)** generating an expression pattern along the ependymal layer of the third ventricle **(Figure 8A,C,E)**.

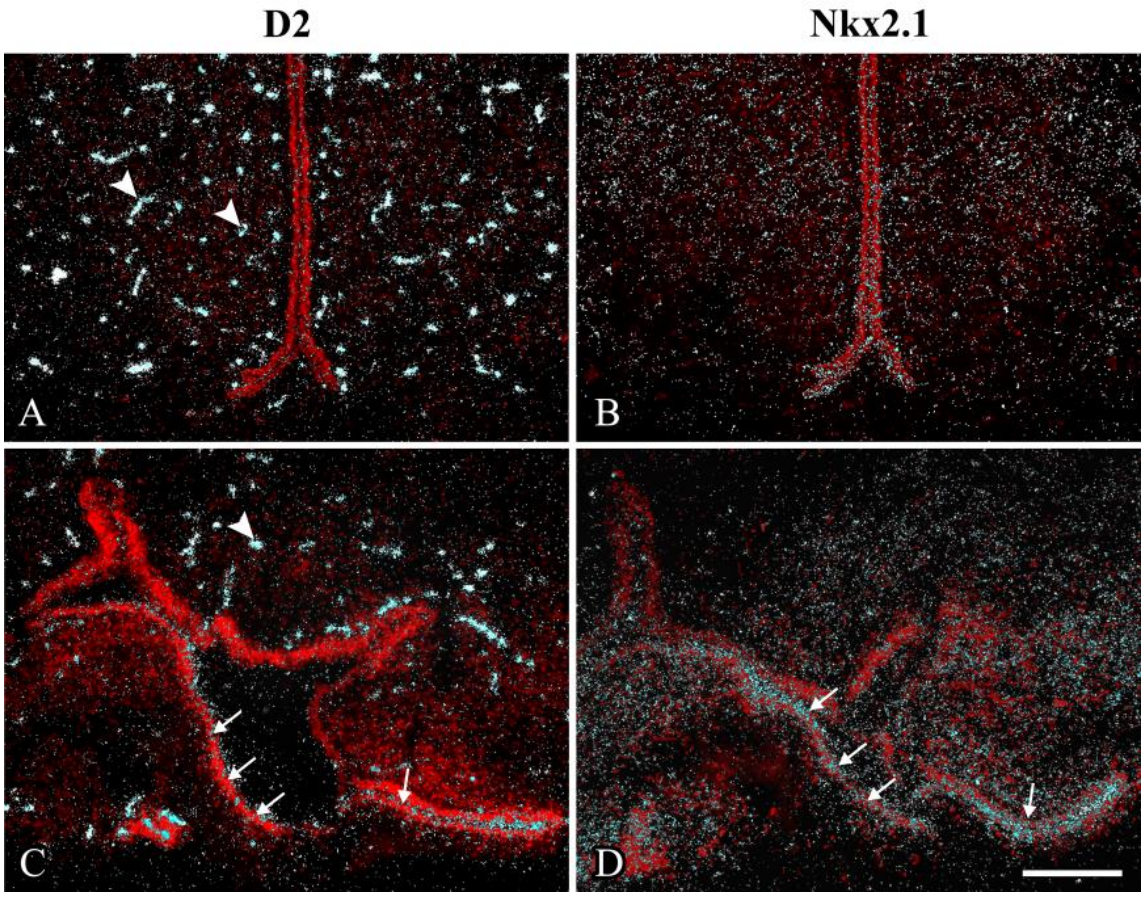

Figure 7. D2 and Nkx2.1 mRNA expression in the E13 chicken hypothalamus. Dark-field images of (A,C) type 2 deiodinase (D2) and (B,D) Nkx2.1 *in situ* hybridization in E13 chicken mediobasal hypothalamus (MBH) (blue). Cresyl violet background staining was used to visualize tissue pattern (red) under fluorescent light. (arrows: C) D2 mRNA signal was found in tanycytes in the floor and wall of the third ventricle in the "posterior" sections (see Methods), (A) while it was absent in "anterior" sections. (arrowheads: A,C) D2 was also expressed in the perivascular space. (arrows: D) Nkx2.1 mRNA was coexpressed with D2 in tanycytes, (B, D) while it was absent from the perivascular space. Scale bar, 200 μm

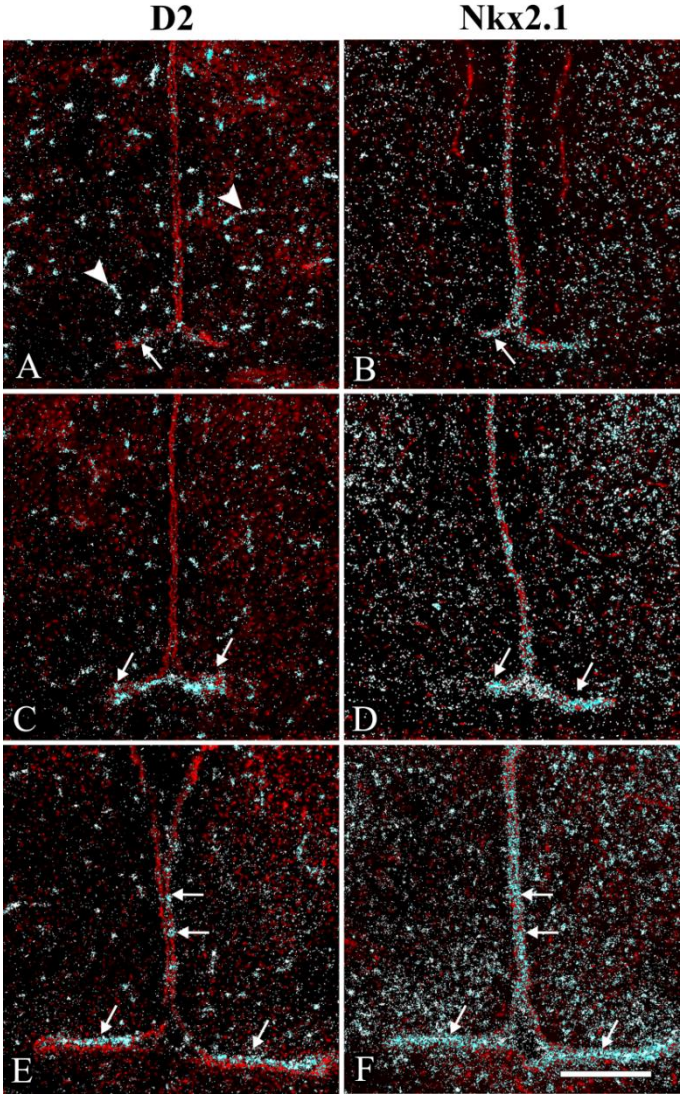

Figure 8. D2 and Nkx2.1 mRNA expression in P2 chicken hypothalamus**.** Dark-field images of (A,C,E) type 2 deiodinase (D2) and (B,D,F) Nkx2.1 *in situ* hybridization in P2 chicken mediobasal hypothalamus (MBH) (blue). Cresyl violet background staining was used to visualize tissue pattern (red) under fluorescent light. D2 and Nkx2.1 are coexpressed (arrows). (A,C,E) D2 expression shows an anterior-to-posterior expression pattern. (A) In "anterior" sections (see Methods) D2 expression starts in β-tanycytes at the floor and (E) it expands to α-tanycytes in the wall in more "posterior" sections. Strong perivascular signal appeared in all regions (arrowhead). (B,D,F) Nkx2.1 was expressed both on the floor and the wall of the ventricle. Scale bar 200 μm

6.1.3 *D2 activity markedly increased in the developing chicken hypothalamus between E15 and P2*

D2 activity was detected both in the MBH and in the MBH-lacking hypothalamic region at stage E15, E18 and P2. D2 activity showed an 11.6-fold increase in the MBH and a markedly lower but significant 3.9-fold increase in the MBH-lacking hypothalamic sample when P2 samples were compared to those of E15 **(Figure 9)**.

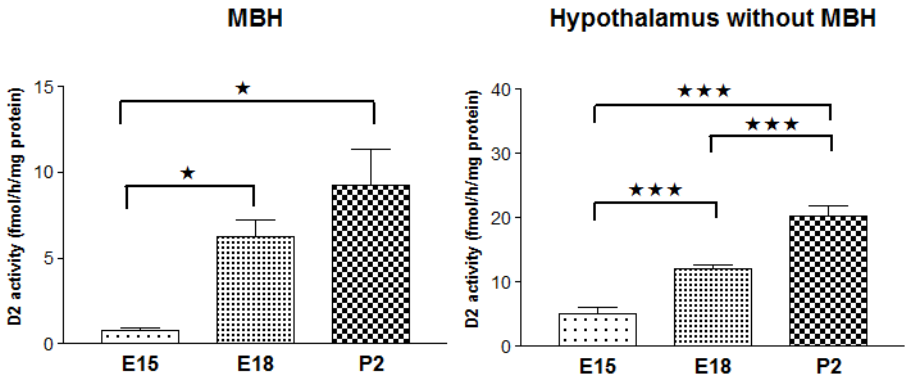

Figure 9. D2 activity in different regions of the developing chicken hypothalamus. Type 2 deiodinase (D2) enzyme activity in E15, E18 and P2 chicken mediobasal hypothalamus (MBH) and hypothalamic samples lacking MBH (Hypothalamus without MBH).*P<0.05; ***, P<0.001 (mean ± SEM, N=4) by ANOVA followed by Newman-Keuls post-hoc test.

6.1.4 *Nkx2.1 mRNA was expressed in the chicken tanycytes but not in perivascular elements*

We also tried to identify factors that could be involved in the expression of D2 in the developing hypothalamus. Nkx2.1 is a homeodomain-containing transcription factor that regulates the expression of thyroid-specific genes and is also expressed in the developing brain (Civitareale et al., 1989; Lazzaro et al., 1991), and was also found to induce the human *DIO2* gene (Gereben et al., 2001). Since Nkx2.1 is a potential regulator of D2 expression, we aimed to analyse the expression pattern of this transcription factor in developing chicken hypothalamus. Hybridization signal of the

Nkx2.1 transcription factor was strongly present in tanycytes of the hypothalamus of E13 chicken embryos. The Nkx2.1 mRNA was uniformly expressed in the tanycyte subtypes, both β and α-tanycytes expressed this mRNA abundantly in "anterior" and "posterior" sections of the MBH. The distribution of Nkx2.1 expression overlapped with that of D2 in E13 and P2 tanycytes both in the floor and the wall of the third ventricle, but Nkx2.1 was absent in D2-expressing cells of the perivascular space **(Figure 7B,D and Figure 8B,D,F)**. Nkx2.1 hybridization signal increased significantly in tanycytes during development and its intensity increased 1.5-fold from E13 to P2.

6.1.5 D3 is expressed in chicken tanycytes

Since neuronal D3 is a crucial component of the machinery regulating T3 availability in the brain, we also studied the D3 expression in the hypothalamus of E15, E18, P2 chicken using *in situ* hybridization. Beyond the expected neuronal localization, D3 mRNA was also detected in tanycytes at all stages studied **(Figure 10A,B for E18 and P2, respectively)**. All tanycyte subtypes demonstrated abundant hybridization signal after four days exposure suggesting that D3 is present at a high expression level in these cells. Immunohistochemistry also supported this finding, D3 immunoreactivity was detected both in tanycytes and in numerous hypothalamic neurons **(Figure 10C,D)**. However, we could not observe marked changes in D3 expression before and after the period of negative feedback formation.

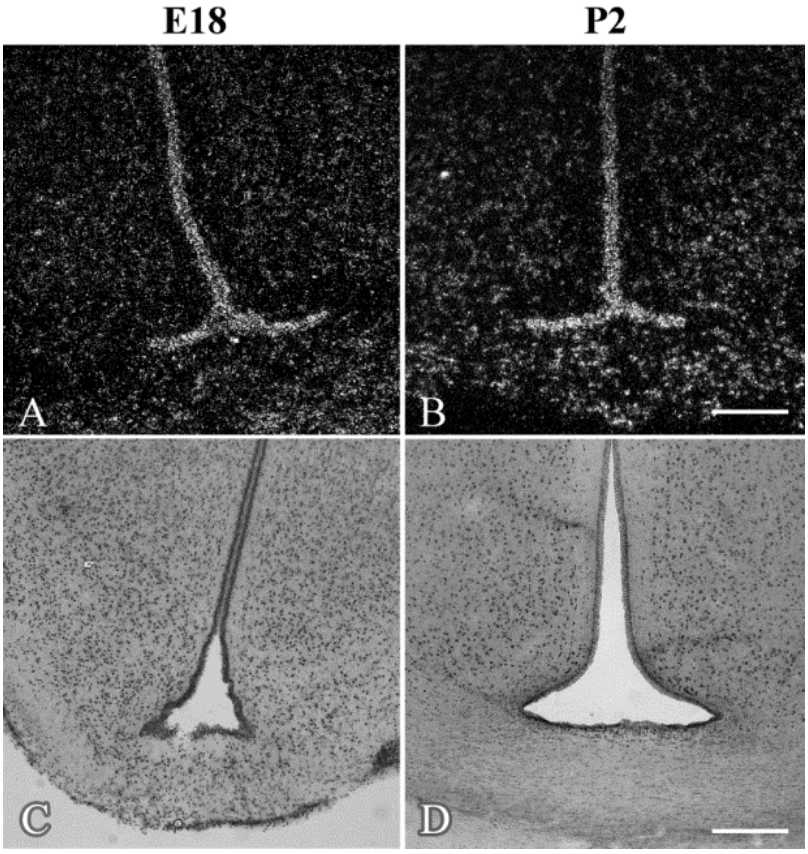

Figure 10. D3 protein and mRNA is expressed in E18 and P2 chicken tanycytes**.** Isotopic *in situ* hybridization revealed type 3 deiodinase (D3) mRNA in (A) E18 and (B) P2 tanycytes and hypothalamic neurons. D3 immunoreactivity was also detected in (C) E18 and (D) P2 hypothalamus in all tanycyte subtypes and hypothalamic neurons using diaminobenzidine (DAB) immunolabelling. Scale bar, 100 μm in B corresponds to A and B; scale bar, 200 μm in D corresponds to C and D. E18: 18-day-old embryo; P2: 2-day-old posthatch chicken

6.1.6 Nkx2.1 transcriptionally activates the chicken Dio2 promoter

To assess whether expression of Nkx2.1 in D2 expressing chicken tanycytes could lead to Nkx2.1-mediated transcriptional activation of the chicken *Dio2* gene, we performed promoter assay in U87 glioma cells. Nkx2.1 coexpression increased transcription of the *cDio2* 3.6kb and 588 bp long 5' FR by ~4-fold and 1.8-fold, respectively (fold response of pGL3-cDIO2(-3586/-1) *vs.* pGL3-cDIO2(-588/-1). The empty pGL3-basic vector remained unresponsive **(Figure 11)**. Sequence analysis of the used *cDio2* 5' FR fragment indicated five putative Nkx2.1 binding sites related to the transcriptional start

site (-18, -2872, -2587: TCAAGG; -2321, -1671; TCAAGT)**.** Since D3 was coexpressed with Nkx2.1 in chicken tanycytes, we cloned a 623 bp long *cdio3* 5'FR and studied its responsiveness to Nkx2.1 in U87 cells similarly to the approach used above **(Figure 11)**. In contrast to c*Dio2*, the studied c*Dio3* 5'FR fragment did not show responsiveness to Nkx2.1 (not shown).

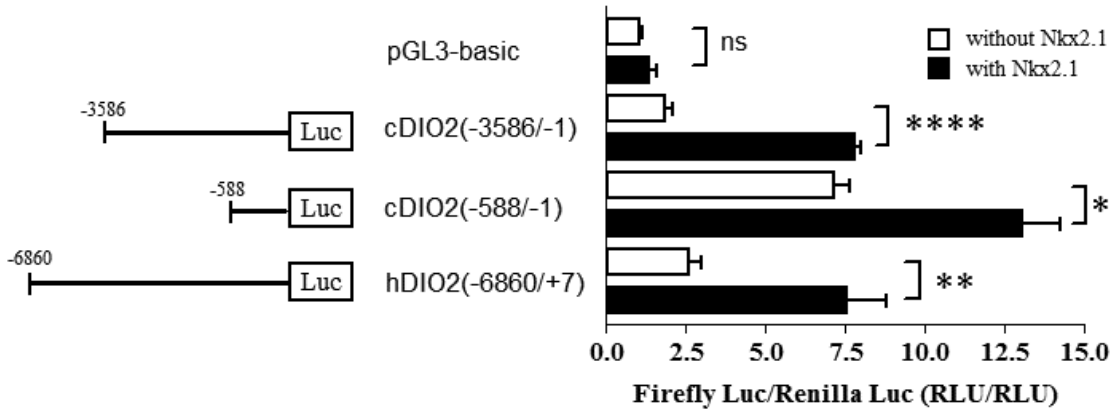

Figure 11. Nkx2.1 responsiveness of the *cDio2* gene. The chicken ~3.6 kb and 588 bp 5'flanking region containing *cDio2* luciferase vectors were transfected into U87 glioma cells in the presence of an Nkx2.1 expressing plasmid. For uninduced negative control a similar vector without the Nkx2.1 coding region co-transfected cytomegalovirus (CMV) -driven vector with the constructs, while a 6.8 kb of human *DIO2* promoter construct (hDIO2) was used as positive control. The chicken *Dio2* promoter showed ~2.5 fold induction to Nkx2.1 that was comparable to the *hDIO2* positive control while the empty pGL3-basic vector remained unresponsive. Truncated *cDio2* (-588/-1) containing one putative Nkx2.1 binding site at -18 remained responsive by ~1.8 fold. Data are shown as the mean ± SEM of the Luc to Ren ratios of Nkx2.1 or empty CMV vector co-transfected cells in at least four separate experiments. *P<0.05; **P<0.01; ****P<0.0001 vs. corresponding uninduced control by t-test (mean ± SEM, N≥4).

6.2 Regulation of thyroid hormone availability in parvocellular neurosecretory neurons of the rodent hypothalamus

Since neurons cannot generate T3, these cells need to import T3 from glial cells. Intracellular T3 level in neurons is fine-tuned by D3-mediated T3 degradation. We aimed to understand how this process works in neurosecretory neurons and understand its potential impact on the HPT axis.

6.2.1 Distribution of D3 protein in the ME of the rat

The D3 protein can be detected in the rat and human hypothalamus, as shown by western blot **(Figure 12).** At the cellular level, D3-immunoreactivity appeared as small puncta distributed unevenly in the hypothalamus. The highest density was observed in the external zone of the ME **(Figure 13A,B)**, where the axons of the hypophysiotropic neurons accumulated around the portal capillary system. D3 immunoreactivity was also observed in most hypothalamic regions including those known to project to the ME (i.e. MPOA, PVN and ARC), although less intense than the ME. The punctate appearance in these regions suggested localization in axons similar to that observed in axons in the ME as no D3 immunoreactivity was identified in neuronal perikarya.

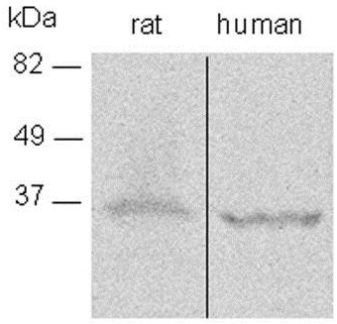

Figure 12 D3 detection by western blot in the rat and human hypothalamus. The blot showed bands of expected sizes of the rat and human type 3 deiodinase (D3) and also demonstrated the calculated 3 kDa size difference between the D3 proteins of the two species. After overexposure of the blot, faint bands of ~22 and 120 kDa bands also appeared in the rat but not in the human sample.

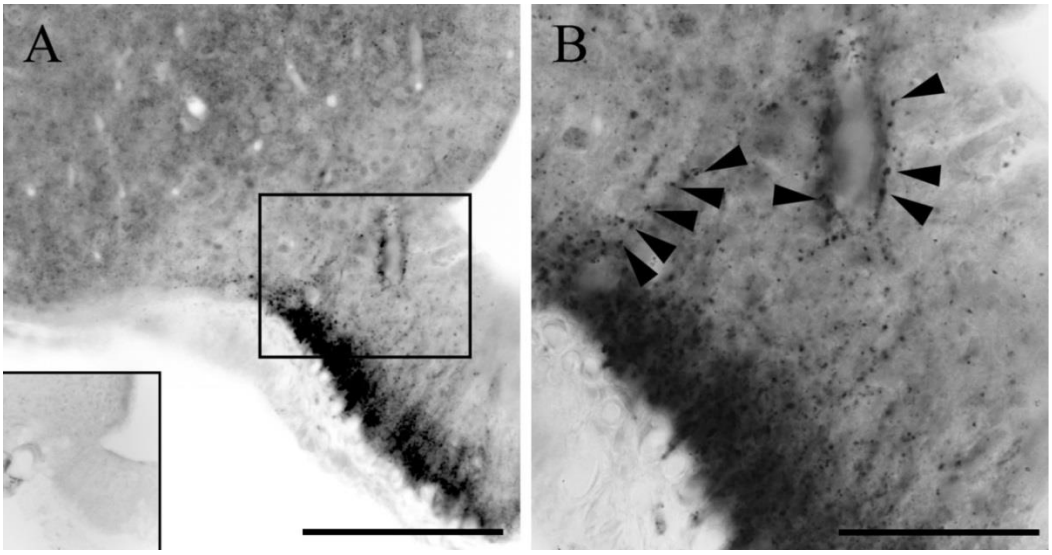

Figure 13 D3 immunoreactivity in the rat mediobasal hypothalamus (MBH). (A) Abundant type 3 deiodinase (D3) immunoreactive structures are seen in the external zone of the rat median eminence marked by silver grains. The inset on the left demonstrates the complete disappearance of D3- immunoractivity from the MBH when sections were incubated with D3 antisera previously preabsorbed with the corresponding peptide antigen. (B) The boxed region of A is enlarged.. Black arrowheads indicate immunoreactive loci located frequently adjacent to blood vessels. Scale bars: 50 μm in A, 20 μm in B.

6.2.2 D3 distribution at the subcellular level

Previous ultrastructural studies performed by our group revealed that D3 is localized exclusively to hypophysiotropic axon terminals in the external zone of the ME. The majority of D3-immunoreactivity was associated with dense core vesicles (DCV) ranging between 80–120nm. We continued this study by determining the topology of D3 in the DCV in the outer zone of the hypothalamic ME using N-STORM superresolution microscopy. For comparison, we used both GnRH that is located inside of DCV and RAB3, a protein covering the outer surface of these vesicles (Meldolesi et al., 2004). The C-terminal portion of D3 formed immunoreactive clusters of 83.9 nm diameter, that was significantly larger than the 65.6 nm of clusters containing intravesicular GnRH and only slightly larger than clusters containing RAB3 (81.4 nm)

(Figure 14). Thus N-STORM microscopy revealed that C-terminal active center of D3 is localized outside of the DCV surface and faces the cytoplasm, representing the main TH inactivation locus in the axon terminals. Importantly, DCV associated D3 is catalytically active in the axon terminals, as proved by the demonstration of authentic D3 activity using deiodinase assay on microdissected rat ME samples containing the axonal compartment of hypophysiotropic neurons. Furthermore, D3 activity was upregulated by ~4-fold in hyperthyroid rats **(Figure 15)**.

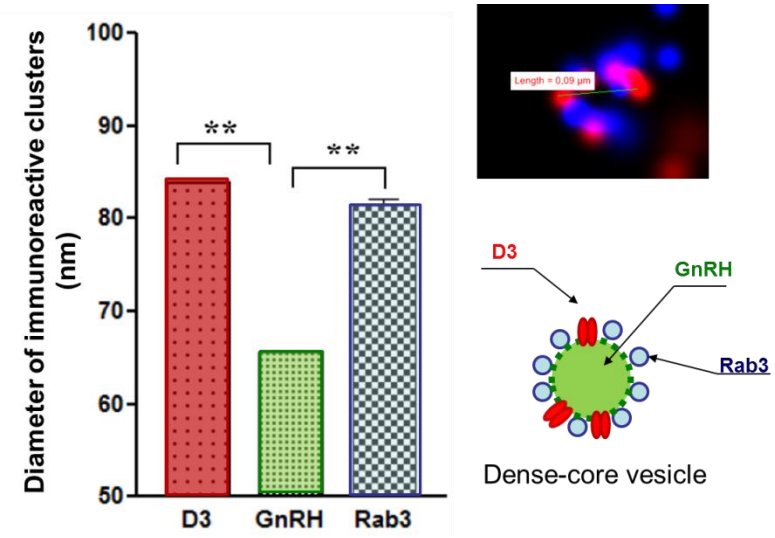

Figure 14 Diameter of immunoreactive clusters in the external zone of the rat hypothalamic median eminence stained for type 3 deiodinase (D3), GnRH or RAB3 detected by N-STORM superresolution microscopy. **P<0.001; by ANOVA followed by Newman-Keuls post-test. Data are shown as Mean ± SEM (N=500).

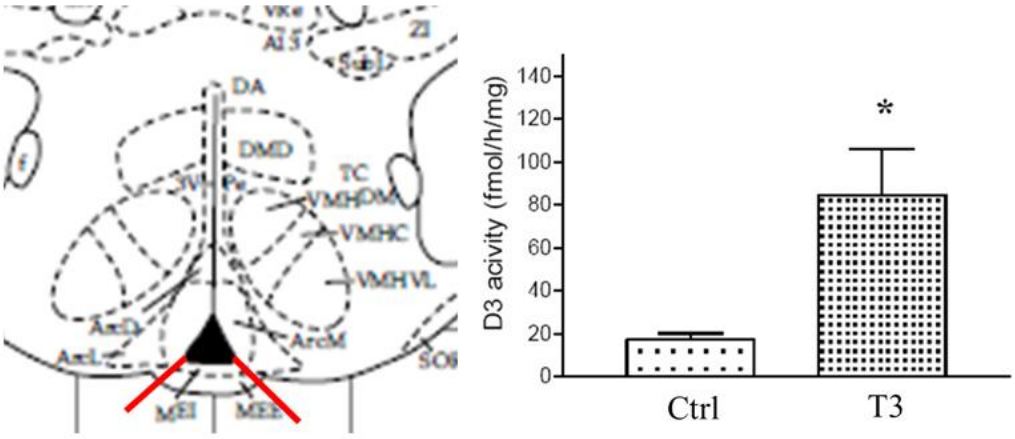

Figure 15 D3 enzyme activity in microdissected rat median eminence samples. Axonal D3 activity is increased by T3-treatment in the median eminence of male Wistar rats. Mean±SEM (N=9) *P<0.05 by t-test.

6.2.3 Phenotype of D3-immunoreactive hypophysiotropic terminals in the rat ME

To determine the phenotype of the D3-containing axon terminals in the ME, colocalization of D3-immunoreactivity with hypophysiotropic releasing- or inhibiting hormones was performed with double-labelling immunofluorescence and confocal microscopy **(Figure 16)**. D3-immunoreactivity was observed in 71.8±3.8% of GnRH axon terminals **(Figure 16A-C)**. The D3-immunoreactive loci appeared as small islands within axon varicosities. In addition, D3 immunoreactivity was also detected in 63.2±7.5% of CRH- and 64.2±2.7% GHRH-immunoreactive axons, mostly in distal varicosities and terminal portions **(Figure 16G,H)**. In contrast, D3 was present only in 26.6±5.0% of TRH-immunoreactive varicosities (**Figure 16D-F)**. The lower D3 occurrence in TRH axons was significantly different from that observed in GnRH, CRH and GHRH axons **(Figure 17)**. D3 was absent from somatostatin (SST)-immunoreactive axon varicosities **(Figure 16I)** and magnocellular neurons (not shown).

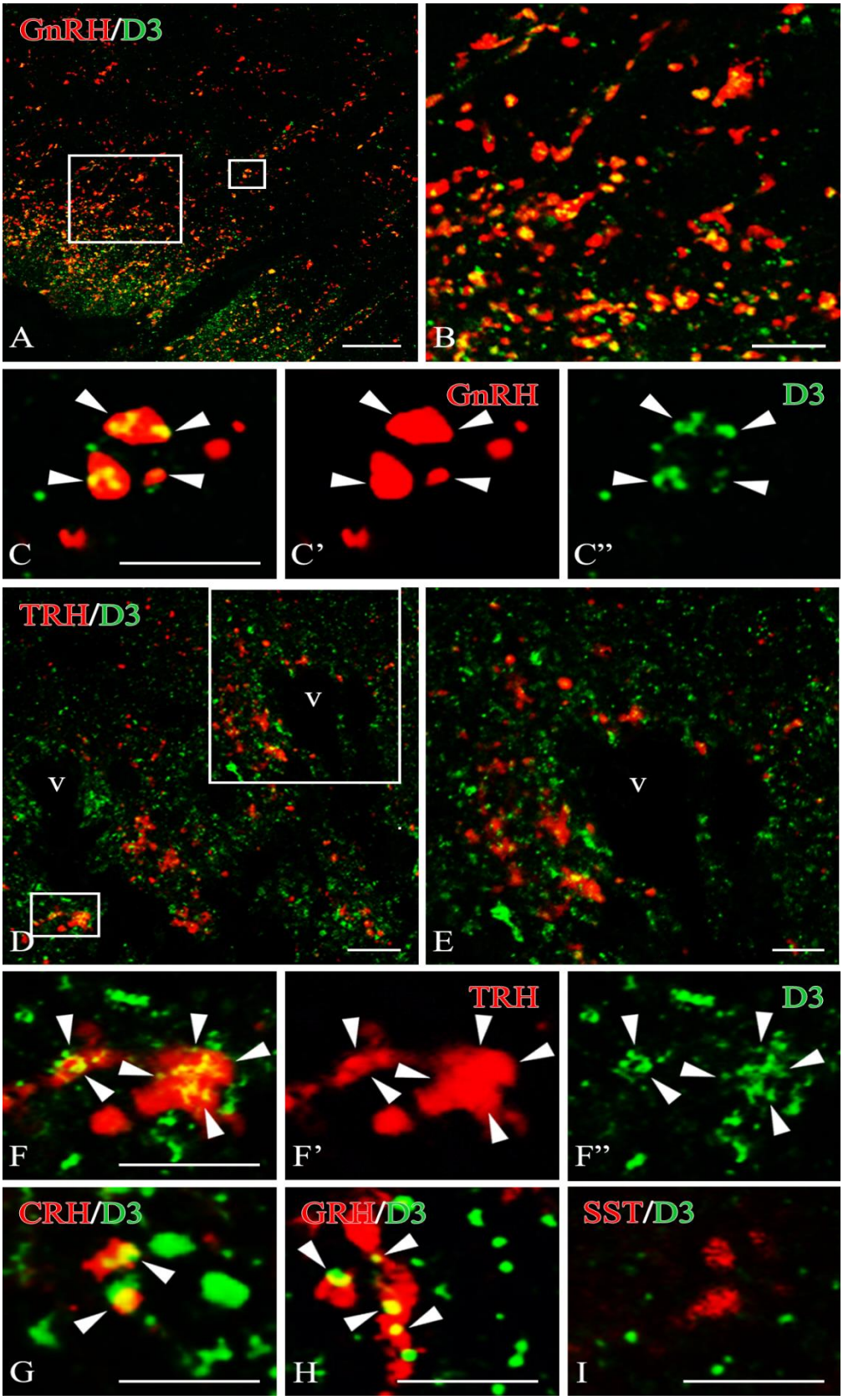
GnRH/D3
A
B
C
GnRH
C'
D3
C''
TRH/D3
v
v
D
v
E
F
TRH
F'
D3
F''
CRH/D3
G
GRH/D3
H
SST/D3
I

Figure 16 Dual-immunofluorescence illustrate the overlapping distribution of fibers immunoreactive for type 3 deiodinase (D3) (green colour) and (A) GnRH or (D) TRH (red) in the rat median eminence (ME). (B, E) Sites of overlap (yellow) occur along the axonal pathway in the ME. High power confocal images demonstrate dual-labelled axon varicosities (yellow in composite images) immunoreactive for (C) D3 and GnRH or (F) D3 and TRH. The D3 immunoreactivity appears as yellow patches (arrowheads) within the axon varicosities. Single channels are also shown in C', C" and F', F", respectively. High power dual-immunofluorescent images are also shown for fibers labelled for (G) D3 (green) and CRH, (H) GHRH or (I) somatostatin (SST) (red). (G, H) These D3-immunoreactive sites (arrowheads) correspond to axon varicosities. SST - immunoreactive axon varicosities show virtually no signal for D3. Scale bars: 20 μm in A, 5 μm in B, 5 μm in C, 10 μm in D,E, 5 μm in F–I.

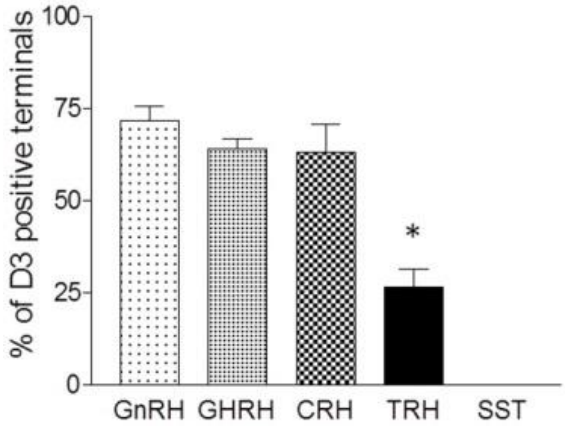

Figure 17 Quantification of D3 distribution in parvocellular axon terminals in the rat median eminence. (N=3; *P<0.01 TRH vs. GnRH, GHRH, CRH and somatostatin (SST) by ANOVA followed by Newman-Keuls post-test.)

6.2.4 Colocalization of MCT8 and D3 in a subpopulation of hypophysiotropic axons in the ME

We also aimed to understand T3 uptake and D3-mediated degradation in parvocellular hypophysiotropic neurons in a phenotype-specific context using triple-labelling immunohistochemistry. MCT8-immunoreactivity was associated with virtually all D3-immunoreactive axon varicosities containing either GnRH or CRH **(Figure 18A, B)**

TRH, or GHRH (not shown). In contrast, somatostatin containing axons contained MCT8 without the presence of D3 (not shown). Scale bars: 2 μm.

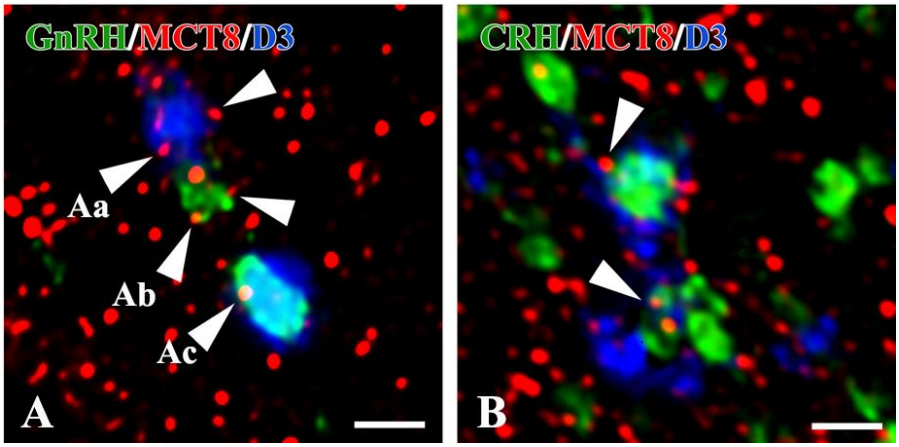

Figure 18. MCT8 and D3 immunoreactivities in axon varicosities of the rat parvocellular hypophysiotropic neurons. Confocal images were subjected to deconvolution. The immunofluorescent signal for monocarboxylate transporter 8 (MCT8) (red) is distributed as small dots throughout the external zone of median eminence and appears (arrowheads) on the surface of axon varicosities of parvocellular neurons (green) for example: (A) gonadotropin-releasing hormone (GnRH), (B) corticotropin-releasing hormone (CRH). MCT8-immunoreactive puncta (arrowheads) appear on the surface of the following categories of axon varicosities; (Aa) single-labelled for type 3 deiodinase (D3), (Ab) single-labelled for GnRH, and (Ac) double-labelled for D3 and GnRH or (B) CRH. Scale bars: 2 μm.

6.2.5 Distribution of D3 in axon varicosities of parvocellular neurons in LPS induced non-thyroidal illness syndrome

NTIS, observed after infection, fasting and in critically ill patients is characterized by falling serum TH levels that is not accompanied with the upregulation of the HPT axis (Boelen et al., 2011). LPS induced inflammation is a frequently used model of NTIS and hypothalamic TH action is known to be increased under these conditions (See also section VI 6.3.7) (Fekete et al., 2004). We used the LPS-induced NTIS model to assess how the T3 degradation capacity of parvocellular neurons is affected by this challenge and studied the distribution of D3 in axon terminals of parvocellular neurons by confocal imaging of double-labelled immunofluorescent sections. LPS significantly

decreased the number of D3 positive varicosities both in GHRH (10%) and CRH (25%) containing axons suggesting deceased T3 degradation and elevated T3 level in these compartments. Importantly, neither TRH, nor GnRH-containing axons were affected **(Figure 19A)**. The unchanged axonal D3 content of TRH neurons after LPS challenge along with the similarly unchanged number of MCT8 positive terminals of these neurons **(Figure 19B)** are indicating that TRH neurons are programmed to rely on hypothalamic T3 without significant further intracellular modulation of their T3 content.

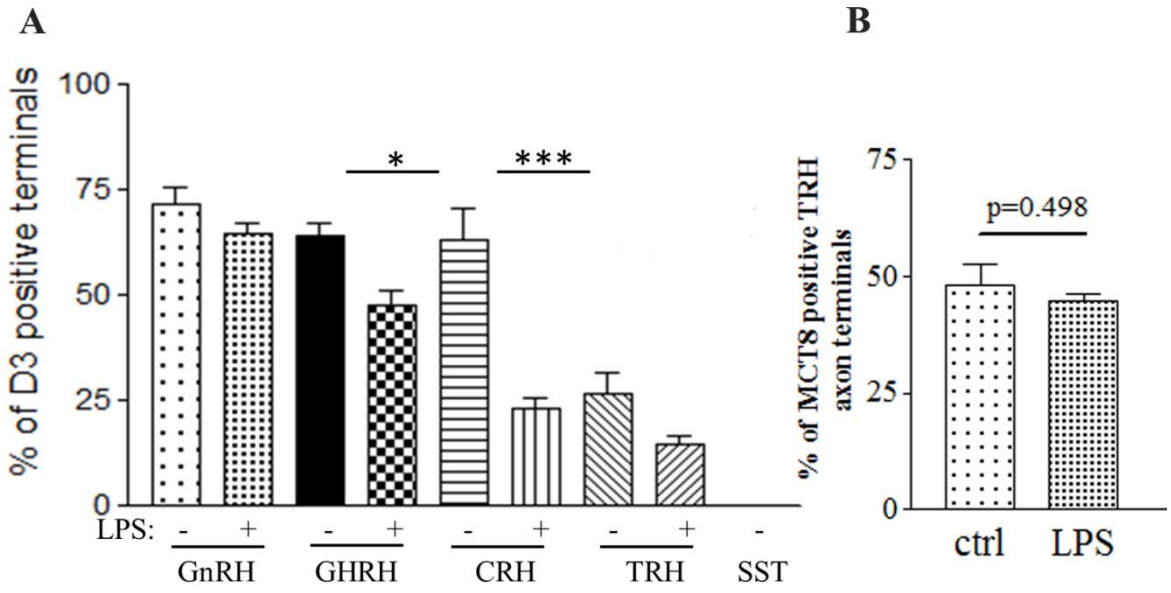

Figure 19. Quantification of D3 distribution in parvocellular axon varicosities during LPS challenge. (A) Number of type 3 deiodinase (D3) positive axon varicosities decreased significantly upon bacterial lipopolysaccharide (LPS) challenge in GHRH and CRH axons, while remained unchanged in GnRH and TRH expressing neurons. N=3; *P<0.05 GHRH +/- LPS; ***P<0.001 CRH +/- LPS, by ANOVA followed by Newman-Keuls post-test. (B) Number of MCT8 positive TRH axon terminals remained also unchanged in TRH neurons after LPS treatment. t-test (mean ± SEM, N=3).

6.3 Generation and characterization of Thyroid hormone action indicator mouse model

TH action is a net result of the activity of a complex molecular machinery that includes TH transport, TH metabolism and TR-mediated nuclear events. To asses mammalian TH action *in vivo* is confounded by technical limitations therefore we aimed to generate a transgenic mouse model to assess TH action in an *in vivo* context and study TH signalling in the hypothalamus and brown adipose tissue.

6.3.1 Transgenic construc

To generate the targeting constructs, we cloned three copies of a DR-4 TRE (of the human *DIO1* 5' FR) (Toyoda et al., 1995) 5' to the *Herpes simplex* virus thymidine kinase (TK) minimal promoter (Kollar et al., 2016). This DNA segment was linked upstream of the firefly luciferase coding region containing a codon-optimized and methylation-resistant dCpG Luciferase-ShBle fusion protein upstream of an EF1 pAn polyadenylation cassette. The cassette was then assembled in a pWHERE vector (Invivogen) that flanked the insert with H19 insulators and subcloned between EcoRI blunt sites of the pt2-BH plasmid to generate the THAI expression construct **(Figure 20).**

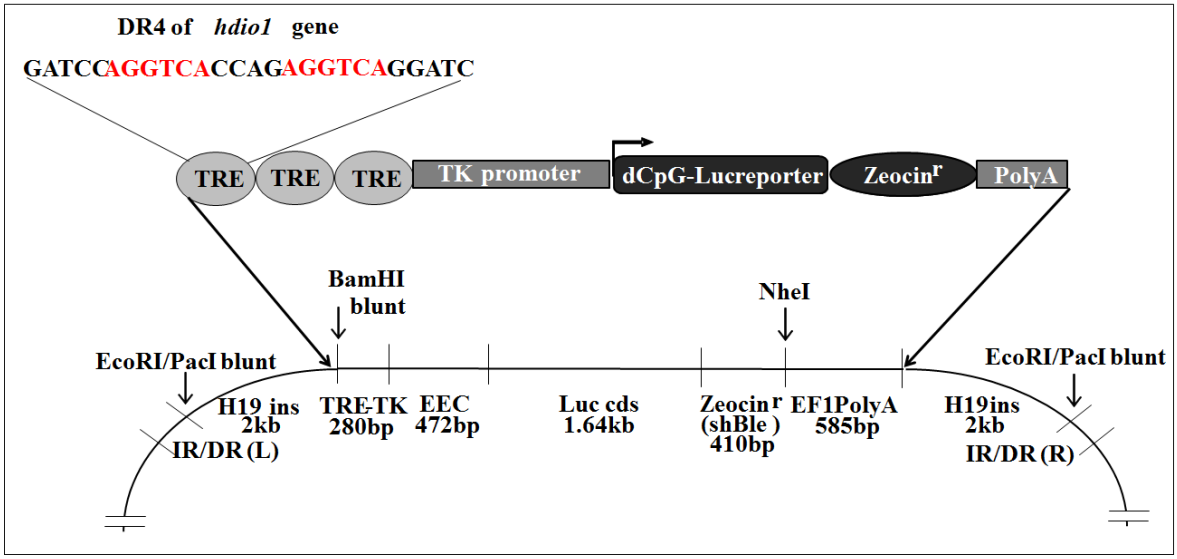

Figure 20. The recombinant THAI construct (THAIC). TK promoter: thymidine kinase minimal promoter; TRE: thyroid hormone response element; EEC: expression enhancer cassette; Luc reporter-zeocin sequences encoding a Luciferase/zeocin resistance fusion protein. The lower panel depicts the structure of the targeting construct generated in the pt2-BH vector. The coding sequence encodes Luciferase (62 kDa) fused to ShBle (14 kDa) allowing selection based on resistance to zeocin.

6.3.2 The thyroid hormone action indicator HEK-293T cell line

In order to test the targeting construct, we have created a TH action indicator HEK293T cell line (THAIC-HEK293T) stably expressing the THAI vector. To test TH induction of reporter cassette TRα was transiently expressed in THAIC-HEK293T line and cells were incubated with T3 for 24h. A readily measurable baseline luciferase activity was detected that was 3.7-fold stimulated after T3 exposure, while no stimulation was observed in the absence of TRα coexpression indicating that induction was TR dependent **(Figure 21)**.

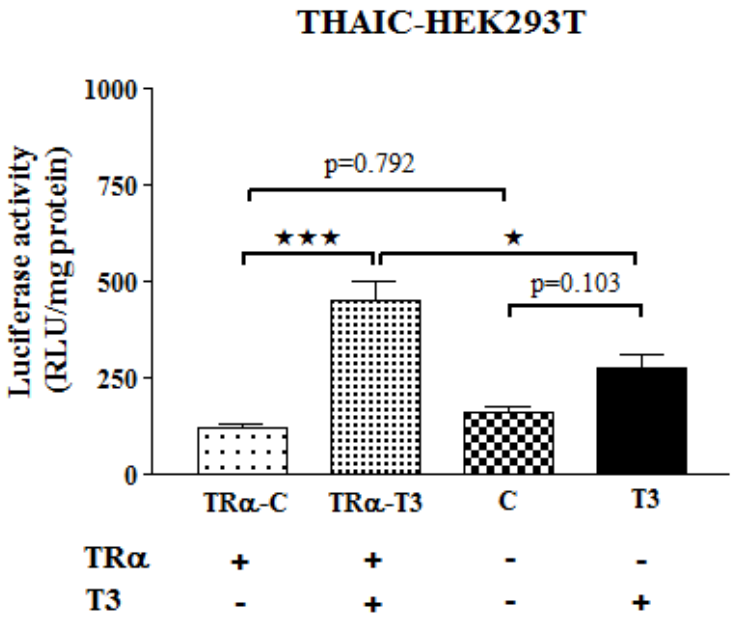

Figure 21. THAIC responds to T3 in a TR dependent manner. The thyroid hormone action indicator construct (THAIC) was expressed in HEK293T cells using Sleeping Beauty-mediated recombination followed by zeocin selection. THAIC-HEK293T cells were treated with 100nM T3 for 24h. Mean±SEM (N=3) *P<0.05 ***P<0.001 by one-way ANOVA followed by Tukey post-test.

6.3.3 Homozygote THAI-Mouse harbours two copies of transgene and represents systemic euthyroidism

Genomic insertion of the transgenic cassette was performed with pronuclear injection in the presence of *in vitro* transcribed mRNA encoding the Sleeping Beauty transposase (Ivics et al., 2014). Three transgenic mouse lines were generated, i.e. #4, #18 and #23. FISH revealed that homozygotes of all lines harbour two copies of the THAI transgenic construct indicating that a single copy was inserted into founders (not shown). Homozygote mice showed a 2-fold higher luciferase activity compared to heterozygotes animals demonstrating that activity of the reporter correlates directly with gene dosage, and were born following a Mendelian distribution **(Figure 22A)**. The reporter cassette was inserted into a region of repeat family L1 into the genome of THAI-Mouse line #4 as shown by Splinkerette PCR, indicating that the cassette did not alter the structure of

any endogenous gene. In accordance, the animals did not exhibit any identifiable phenotype. In THAI-Mouse #4, neither body weight nor systemic parameters highly dependent on thyroid status (lean body mass, fat mass, respiratory exchange ratio /RER/ and volume of oxygen consumption /VO2/) were significantly different from wild-type controls **(Figure 22C)**. In addition, the adult THAI-Mouse is biochemically euthyroid with normal fT4 and fT3 serum concentrations **(Figure 22B)**.

A

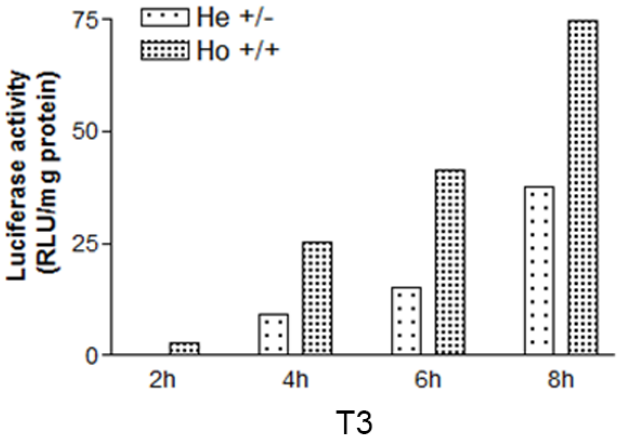

B

	WT	THAI #4	P value	THAI #23	P value	THAI #18	P value
fT4 (pmol/L)	13.44 ± 1.81	10.57 ± 1.96	0.325	12.86±1.44	0.811	12.89±2.03	0.846
fT3 (pmol/L)	5.33 ± 0.74	4.26 ± 0.41	0.249	4.27±0.36	0.247	4.40±0.39	0.309
body weight (g)	29.83 ± 1.27	32.93 ± 1.31	0.14	28.33±0.42	0.223	27.5±1.51	0.344

C

	WT	THAI #4	P value
lean body mass %	80.51 ± 2.03	81.92 ± 1.53	0.6
fat mass %	13.07 ± 2.27	12.79 ± 1.77	0.92
daily average RER VCO2/VO2	0.86 ± 0.03	0.86 ± 0.01	0.91
daily average VO2 (ml/kg lean body/h)	3746.49 ± 328	4072.59 ± 184	0.42

Figure 22. Luciferase activity of the transgenic animal model directly depends on copy number.(A) T3 was administered to mice from the THAI #4 mouse line (1µg/g bw, *i.p.*) and luciferase activity was assessed by luciferase assay at four different time points in brown adipose tissue. Homozygotes (Ho +/+) showed a 2-fold higher luciferase activity compared to heterozygotes (He +/-). (Data are shown as means of two closely agreeing duplicates of each group). (B) THAI #4, #23, #18 mice are systematically euthyroid,

and show no significant differences in body weight. (C) Metabolic characterization of THAI #4 mice. Results are expressed as means ± SEM (N=4). No significant difference was found (wt vs. THAI #4) by Student's t-test. RER: respiratory exchange ratio; VO2: volume of oxygen consumption; VCO2: carbon dioxide production

6.3.4 The THAI-Mouse model is an "indicator" of TH signalling

Three transgenic mouse lines were generated, i.e. #4, #18 and #23. In all lines, basal luciferase activity varied extensively among different tissues. Differences of ~6-orders of magnitude were observed between liver and testicle, while values of most tissues fall into a range within 2-orders of magnitude **(Table 5)**. These differences are likely to reflect the overall transcriptional activity of the DNA insertion site that is cell-specific.
Various tissues of homozygote male mice with modulated TH status were harvested and processed for measurement of luciferase activity **(Table 5)**. To test the responsiveness of the THAI-Mouse to TH, all mouse lines were treated with TH (L-T4) for 3 days and killed 16h after the last L-T4 injection. Line #4 exhibited a great deal of variability in tissue responsiveness to TH when treated with L-T4 , from 0.8-fold in the testicle, 1.5-2 fold in brain (hypothalamus, hippocampus, cerebellum, cortex), to 64-fold in iBAT, while other highly responsive tissues were skeletal muscle, heart, mandibular salivary gland and skin (4-11-fold) **(Table 5A)**. The pattern of TH responsiveness was distinct in the other THAI-Mice, with line #23 only exhibiting a ~7-fold L-T4 responsiveness in the iBAT and no detectable activity at all in this tissue of line #18. However, line #23 and #18 exhibited marked response to TH in the pituitary, and line #18 showed the highest brain baseline activity **(Table 5A)**. Under the used treatment conditions, the lines showed greater response to L-T3 compared to that of L-T4, e.g. the line #4 responded to L-T3 5-fold in the liver and 46-fold in the heart, while the MBH of line #23 responded to L-T3 by ~12-fold **(Table 5 B)**. Thus, line #4 permits the study of TH action in a wide variety of tissues, whereas the two other lines hold additional value for specific applications represented by high reporter response in the pituitary (lines #18 and #23) and higher basal activity in the brain (#18) due to their different insertion sites.

Table 5 Responsiveness of different tissues and brain regions of THAI #4, #23 and #18 mouse lines to TH. Euthyroid animals were treated with (A) T4 (*i.p.* 5µg/day/animal for 3 d), (B) T3 (*i.p.* 1µg/g bw for 1 d). Luciferase activity was assessed with a luciferase assay and expressed as Relative Light Unit (RLU)/mg protein. Luciferase activity of corresponding tissues of TH *vs.* vehicle treated animals was performed by Student's t-test (N ≥ 4). Pit: pituitary; MBH: mediobasal hypothalamus; HC: hippocampus; HT: hypothalamus; CTX: cerebral cortex; CER: cerebellum; BAT: interscapular brown adipose tissue; MSG: mandibular salivary gland

A

Tissue	#4				#23				#18			
	basal (RLU/mg protein)	induced (RLU/mg protein)	Fold (mean±SEM)	p value	basal (RLU/mg protein)	induced (RLU/mg protein)	Fold (mean±SEM)	p value	basal (RLU/mg protein)	induced (RLU/mg protein)	Fold (mean±SEM)	p value
Pit	0.337	0.791	2.3±0.16	*0.0001	1.932	16.926	8.8±0.62	*0.0001	0.066	0.540	8.2±0.36	*0.0001
MBH	0.206	0.368	1.8±0.20	* 0.013	0.142	0.240	1.7±0.29	0.103	0.372	0.602	2.2±0.25	*0.005
HC	0.060	0.116	1.9±0.03	*0.0001	0.035	0.047	1.5±0.35	0.201	2.308	3.756	2.1±0.25	*0.013
HT	0.377	0.488	1.3±0.08	*0.031	0.650	0.780	1.2±0.11	0.176	0.755	1.589	2.8±0.35	*0.004
CTX	0.194	0.359	1.9±0.30	* 0.035	0.179	0.253	1.4±0.13	*0.017	1.617	2.586	1.9±1.18	*0.005
CER	0.938	2.162	2.3±0.41	*0.019	0.012	0.023	1.9±0.28	*0.045	0.045	0.063	1.8±0.31	0.073
Liver	0.002	0.005	1.9±0.14	*0.0007	0.001	0.003	2.9±0.86	0.064	No detectable expression			
Heart	0.004	0.030	8.5±0.31	*0.0001	0.001	0.001	1.0±0.25	-				
BAT	0.028	1.820	64.6±8.1	*0.0002	0.005	0.038	7.2±1.54	*0.007				
Bone	0.031	0.066	2.2±0.18	*0.0015	0.010	0.011	0.7±0.11	0.057				
Muscle	0.025	0.276	11.2±5.7	*0.0041	0.004	0.003	0.7±0.18	0.115				
MSG	0.052	0.399	7.6±2.60	*0.044	0.004	0.011	2.7±0.77	0.072	Not determined			
Thyroid	0.115	0.176	1.5±0.07	*0.002	0.026	0.030	0.8±0.18	0.734				
Testicle	4876	4086	0.8±0.06	0.108	2909	2509	0.9±0.11	0.253				
Intestine	4.571	9.480	2.1±0.30	*0.012	0.041	0.212	5.2±1.6	*0.029				
Skin	0.696	2.798	4.0±0.76	*0.001	2.358	1.878	0.8±0.17	0.544				

B

#4 (T3)				
Tissue	basal (RLU/mg protein)	induced (RLU/mg protein)	Fold (mean±SEM)	p value
Liver	0.003	0.017	5.0±0.6	*0.009
Heart	0.006	0.284	45.9±5.65	*0.002

#23 (T3)				
Tissue	basal (RLU/mg protein)	induced (RLU/mg protein)	Fold (mean ± SEM)	p value
MBH	0.180	2.222	12.31±2.4	*0.003

6.3.5 The THAI-Mouse model detects tissue hypothyroidism

To test the responsiveness of the THAI-Mouse #4 to a decrease in tissue TH action, animals were chemically rendered hypothyroid for 3 weeks and luciferase activity was measured in various tissues and brain regions. Approximately 2-3 fold decrease in TH signalling could be detected in different brain regions (e.g. the hypothalamus and cerebral cortex), the liver and in white blood cells, 4-fold in iBAT, 5-fold in the pituitary, 6-fold in heart and bone and 10-fold in small intestine **(Table 6)**. Thus THAI-Mouse allows detection of tissue hypothyroidism in various tissues.

Table 6 Responsiveness of different tissues and brain regions of THAI #4 to hypothyroidism. Animals were rendered hypothyroid by adding 0.1% sodium perchlorate and 0.5% methimazole in drinking water for 3 weeks combined with low iodine diet. Luciferase activity was assessed with luciferase assay and expressed as Relative Light Unit (RLU)/mg protein in tissue samples. Luciferase activity of corresponding tissues of hypothyroid vs. euthyroid animals was compared with Student's t-test (N=6).

Pit: pituitary; MBH: mediobasal hypothalamus; HT: hypothalamus; CTX: cerebral cortex; iBAT: interscapular brown adipose tissue; WBC: white blood cell

Tissue	#4 (Hypothyroid)			
	Eu (RLU/mg protein)	Hypo (RLU/mg protein)	Fold (mean±SEM)	p value
Pit	0.347	0.072	0.21±0.02	*0.0005
MBH	0.153	0.076	0.49±0.04	* 0.0099
HT	0.315	0.136	0.43±0.05	*0.0032
CTX	0.163	0.056	0.34±0.06	* 0.0003
Liver	0.003	0.001	0.44±0.07	*0.0446
Heart	0.009	0.001	0.16±0.06	*0.0001
BAT	0.037	0.008	0.23±0.1	*0.0051
Bone	0.031	0.008	0.26±0.04	*0.0034
Muscle	0.008	0.007	-	0.776
Thyroid	0.071	0.078	-	0.439
Intestine	1.683	0.166	0.1±0.01	*0.0001
WBC	0.013	0.005	0.42±0.08	*0.0412

6.3.6 TH signalling can be assessed in the live THAI-Mouse

We also studied whether THAI mouse can be used to detect TH action in live animals. We used *in vivo* bioluminescence imaging to measure TH signalling in live line #4 THAI-Mice, 15 min after luciferin injection. Baseline luciferase activity was detected in the iBAT, anterior and posterior foot pads, tail, small intestine, *saccus caecum* of the stomach, mandibular salivary gland, mouth, nose, skin and testicles **(Figure 23A)** In the duodenum and jejunum, hypothyroidism decreased luciferase activity by ~80% **(Figure 23A,B)**. A single L-T3 injection 24h before imaging induced luciferase activity in iBAT by ~9-fold, in the small intestine (predominantly the duodenum and jejunum, analysed by *ex vivo* imaging) (not shown) by ~3-fold, and to a lesser extent in mandibular salivary gland, foot pads and tail **(Figure 23A,B)**. Notably, despite very high basal reporter activity, luciferase activity in testicles was not inducible by L-T3 injection **(Figure 23A)**.

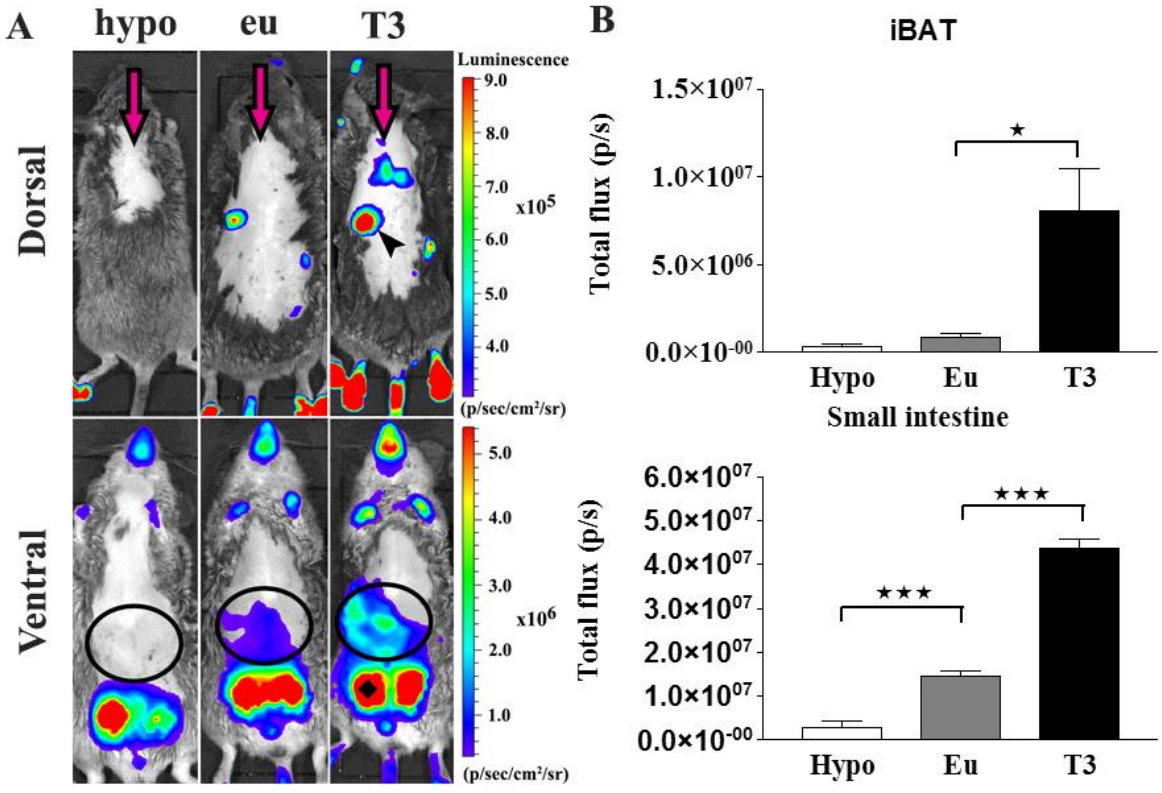

Figure 23. Detection of TH action in live animals. *In vivo* bioluminescence imaging on euthyroid, T3-treated (1 µg/g bw injected *i.p.* 24h before imaging), and hypothyroid line #4 THAI-Mice followed by *i.p.* luciferin administration. (A) Representative images of hypothyroid (Hypo), euthyroid (Eu) and T3 treated mice and light intensity diagram of

interscapular brown adipose tissue (iBAT) and small intestine. T3 injection increased light intensity in iBAT. In the small intestine, hypothyroidism decreased while T3 treatment increased light intensity. Dorsal image arrow: iBAT, arrowhead: *saccus caecum* of the stomach; Ventral image circle: small intestine; ♦ testicles (B) Light intensity diagram (photon/sec) of luciferase activity in iBAT and small intestine of Hypo, Eu and T3-treated THAI #4 mice. Mean of photon/sec ± SEM (N=3) * P<0.05 ***P<0.001 by one-way ANOVA followed by Newman-Keuls post-hoc test.)

6.3.7 Assessment of tissue-specific TH action in discrete brain regions: implications for pathogenesis of NTIS

The NTIS is characterized by a suppressed response of the HPT axis despite low serum TH levels in critically ill patients. (Boelen et al., 2011). The syndrome is at least partially caused by central inhibition of TRH secretion and the resulting decrease of TSH release. To test whether this is caused by increased D2-mediated TH signalling in the hypothalamus, as previously suggested (Fekete et al., 2004), the THAI-Mouse line #23 was treated with LPS, which triggers NTIS. Luciferase expression in hypothalamic ARC-ME region, where TH activation occurs in D2 expressing tanycytes, increased 6h after LPS injection, reaching statistical significance by 8h **(Figure 24A)**. D2 expression was markedly elevated in all time points in ARC-ME region **(Figure 24B)**, preceding the increase of luciferase expression. TRH mRNA levels decreased significantly between 6h-8h after LPS treatment in PVN samples **(Figure 24D)**. These data provide direct evidence that accelerated D2 activity increases TH signalling in the ARC-ME region that can inhibit TRH expression in the PVN during pathogenesis of NTIS.

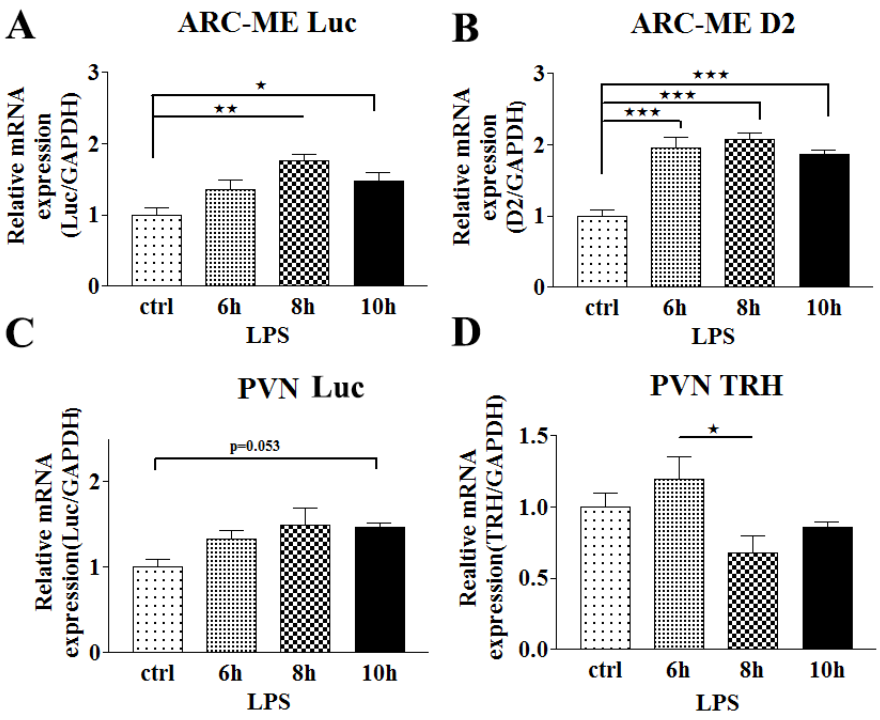

Figure 24 Detection of tissue-specific TH action in a model of non-thyroidal illness syndrome in the THAI #23 mouse line. TH action was assessed at three different time points after *i.p.* injection of 150µg/mouse bacterial lipopolysaccharide (LPS) (E. coli 0127:B8) by real time PCR analysis of luciferase mRNA in microdissected samples of hypothalamic arcuate nucleus-median eminence (ARC-ME) region in the THAI #23 mouse line. (A) In the ARC-ME region, LPS evoked a significant increase in luciferase mRNA level after 8h. (B) D2 mRNA in the ARC-ME was already elevated 6h after treatment and remained significantly increased in all time points. (C) In the paraventricular nucleus (PVN), luciferase mRNA tended to increase, while (D) TRH mRNA level markedly decreased after 8h, at the time point when TH action reached the maximum in the ARC-ME *P<0.05, **P<0.01, *** P<0.001; by one-way ANOVA followed by Tukey post-test. Data are shown as Mean ± SEM (N =5)

6.3.8 THAI-Mouse reveals strong activation of TH signalling in cold-stimulated iBAT

The iBAT is under synergistic control of NE and TH signalling and is under the regulation of the CNS. TH signalling in iBAT is expected to increase as a result of

certain physiological stimuli such as cold exposure (Contreras et al., 2015). To test whether this change of endogenous TH signalling could be captured in THAI-Mouse and differences between the regulation of basal and cold-induced TH signalling could be observed, THAI animals were exposed to cold (4°C) for 9 and 24h and then sacrificed. Line #4 mice exhibited an ~3.4-fold increase in luciferase activity in dissected iBAT and 2.8- fold in luciferase mRNA **(Figure 25A,B)**. Similar induction of TH action was detected *in vivo*, with the iBAT of live animals exhibiting a 3.2-fold increase in bioluminescence signal after 24h of cold exposure. At all times, TH action in foot pad skin remained unchanged. This indicates that the observation in the iBAT is specific and is not the consequence of general change in tissue blood flow **(Figure 25C,D)**.

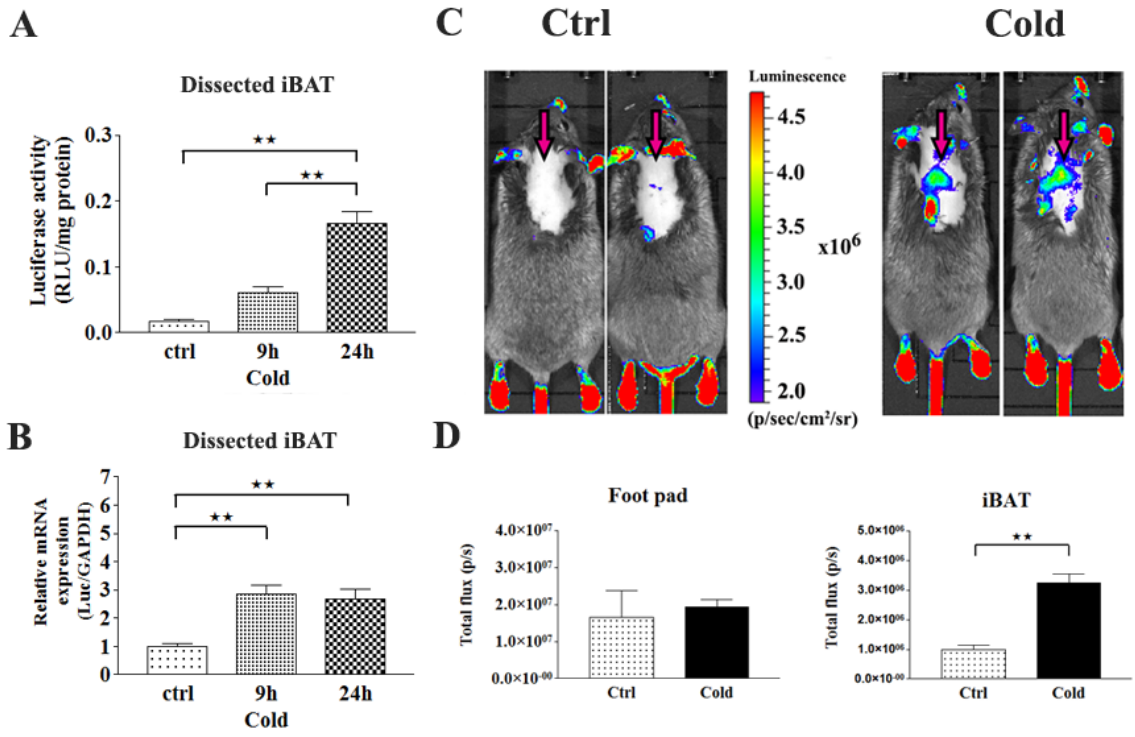

Figure 25. TH action in iBAT during cold stress. (A) Luciferase activity shows a tendency to increase in dissected interscapular brown adipose tissue (iBAT) of THAI #4 line after 9 hours at 4°C and is significantly increased after 24 hours of cold stress. (B) Luciferase mRNA is significantly increased after 9 hours in dissected iBAT of THAI #4 line. **P<0.01; by one-way ANOVA followed by Newman-Keuls post-test. Mean ± SEM (N =5). (C) *In vivo* bioluminescence imaging on iBAT of THAI #4 subjected to

cold stress for 24 h at 4°C followed by *i.p.* luciferin administration. Representative images of two control and two cold exposed mice. Arrows indicate iBAT. (D) Light intensity diagram of luciferase activity in iBAT and foot pads of control and cold induced THAI #4 mice. Luciferase activity of skin above non-iBAT containing region was deducted from iBAT reporter values. Mean of photon/sec ± SEM (N=4) **P<0.001 by Student's t-test.

To address the role of sympathetic inputs on TH action under basal and cold induced condition, THAI-Mice were subjected to unilateral surgical denervation of iBAT followed by cold exposure. Notably, unilateral denervation resulted in a strong tendency of decrease in NE levels in iBAT **(Figure 26A)**, and prevented the 9-hour cold exposure induced ~2-fold increase of NE content that was only observed in the intact iBAT lobe. Furthermore, only the intact iBAT lobe exhibited a 9-fold increase in D2 expression and 18-fold acceleration in D2 activity **(Figure 26C,B)**, that increased local TH availability. Indeed, only in the intact lobe did luciferase mRNA levels increase by ~2.7-fold **(Figure 26D)**. It is notable that baseline TH action was not affected by denervation in the animals kept at room temperature indicating that in contrast to the cold induced TH action basal TH action was less dependent on sympathetic inputs. Thus, THAI mice allow the detection of changes in TH action caused by physiological stimuli e.g. cold evoking the alteration of local, endogenous TH availability in the iBAT of live animals and in tissue samples and revealed that basal and cold-induced TH actions are differently regulated by the sympathetic nervous system.

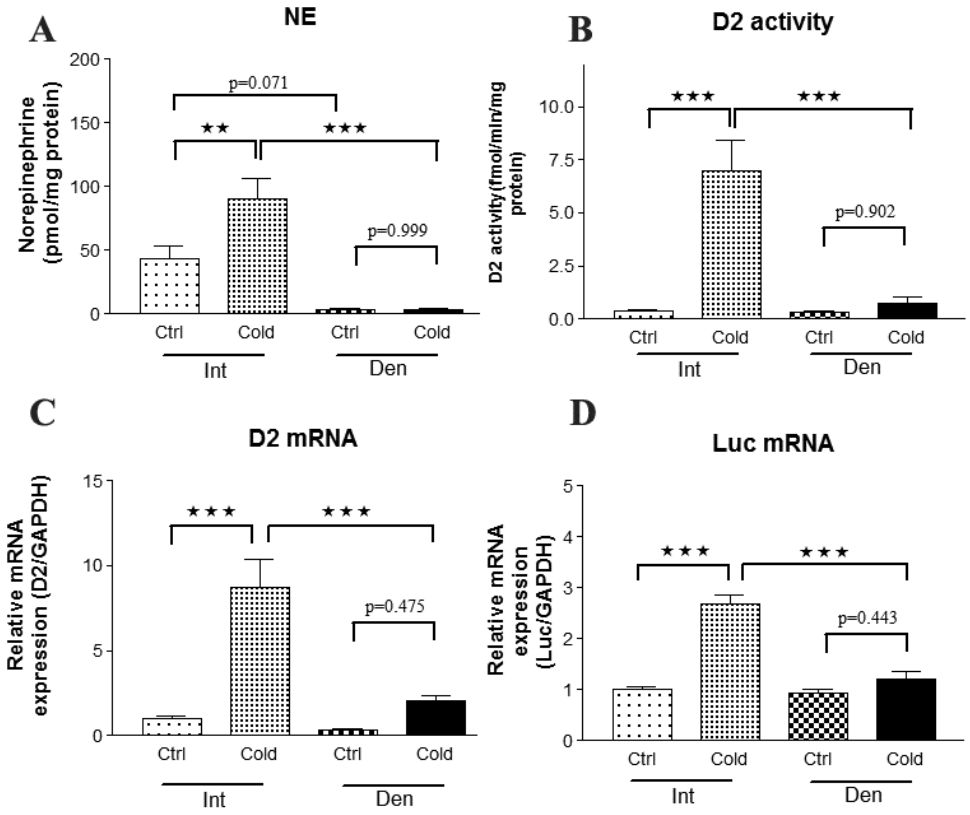

Figure 26. Sympathetic regulation of TH action in iBAT of THAI #4 mice. (A) 9h cold stress increased norepinephrine (NE) levels by 2-fold in intact lobe, while the NE level was not induced in the denervated lobe. (B) Type 2 deiodinase (D2) enzymatic activity and (C) mRNA levels were increased by cold stress in dissected intact interscapular brown adipose tissue (iBAT) while the denervated side remained unresponsive. (D) Luciferase mRNA level increased 2.7-fold in the intact lobe in response to cold, but TH action remained unresponsive to cold on the denervated side. Despite sympathetic denervation, luciferase expression did not decrease at room temperature in the denervated lobe compared to the intact lobe. ***P<0.001; **P<0.01 by repeated measurement ANOVA followed by Tukey post-hoc test. Data are shown as Mean ± SEM (N=6).

6.3.9 THAI-Mouse can test the performance of TR isoform-specific TH analogues

Industrial efforts are being paid to develop TR isoform-specific compounds to evoke the beneficial effects of TH (e.g. lowering of cholesterol and induce weight loss) without

unwanted cardiac effects. This is based on the phenomenon that TRα and TRβ isoforms are unevenly distributed in different tissues. E.g. TRβ predominates in liver, whereas the TRα isoform predominates in brain, skeletal muscle and heart (Zhang and Lazar, 2000; Moran and Chatterjee, 2015). However, no model is available for *in vivo* testing of these compounds. To learn whether TR isoform specificity of a thyromimetic compound can be assessed in THAI-Mouse, line #4 animals were treated with GC24, TRβ selective agonist (Borngraeber et al., 2003). Treatment with GC24 increased luciferase activity by ~2.5-fold in liver **(Figure 27A)**, however it did not increase TH signalling in the heart **(Figure 27B).** Therefore, it is anticipated that this mouse model could be used in the *in vivo* screening and testing of such compounds.

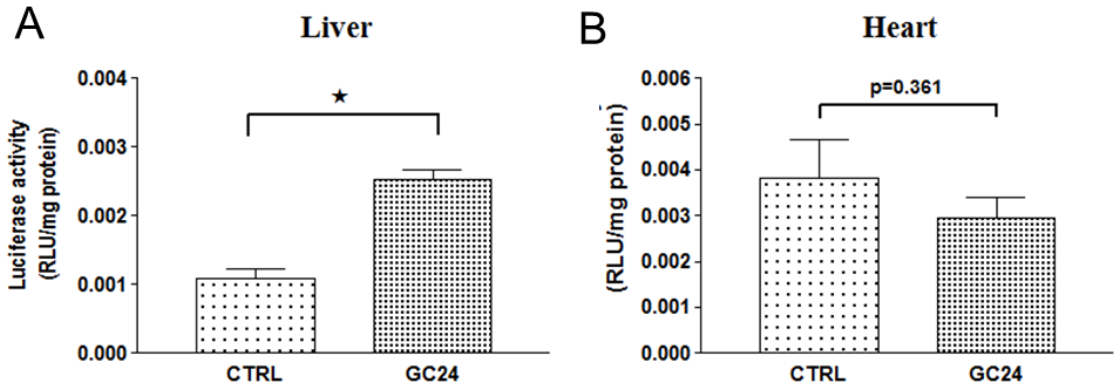

Figure 27. Detection of TR isoform-specific TH action in THAI-Mouse. (A) Single injection of the thyroid hormone receptor β (TRβ) agonist GC24 (1.53 nM/g BW *i.p.*) significantly increased luciferase activity after 24 h in hypothyroid (0.1% sodium perchlorate and 0.5% methimazole in drinking water for 3 weeks combined with low iodine diet) THAI #4 animals in the TRβ isoform dominant liver, while (B) luciferase activity did not change in TRα isoform dominant heart. Luciferase activity was assayed 24h after GC24 injection. Mean ± SEM (N=10) **P<0.0001 by Student's t-test.

7. Discussion

7.1 Mechanisms contributing to formation of negative feedback during the development of HPT axis

While significant progress had been made in understanding the regulation of the HPT axis, the mechanisms responsible for its set point formation during development remained poorly understood. In humans, embryonic studies are impaired by ethical concerns while rodent models face also limitations due to the slow development of their HPT axis (Oppenheimer and Schwartz, 1997). In the current study, chicken was used as model organism, since the developmental kinetics of the HPT axis of this species is relatively similar to that of humans (Darras et al., 1999; De Groef et al., 2008; Debonne et al., 2008). In addition, similarly to mammals, TRβ2 serves as the mediator of negative feedback on TRH neurons in the chicken hypothalamus (Lezoualc'h et al., 1992). Essential components of the HPT axis are already present at early embryonic development in chicken, e.g. TRβ2 is expressed at least from E14 in the developing chicken diencephalon, pituitary and thyroid gland (Grommen et al., 2008). TRH is expressed already in the E4.5 infundibulum before the formation of the hypothalamus and its level was found to continuously increase from E16 in the hypothalamus during embryonic development (Thommes et al., 1985; Geris et al., 1998). Consequently, the level of circulating T4 increases from E15 to hatching (De Groef et al., 2006).

Despite these findings, while TSH could be detected from E6.5 in the chicken pars distalis (Thommes et al., 1983), the TSHβ mRNA reached its maximal level only at E19 followed by a drop (Gregory et al., 1998) suggesting the lack of negative feedback on anterior pituitary before E19. Our TH injection study provided direct evidence that negative TH feedback on the developing chicken hypothalamus forms between the stages of E19 and P2. Importantly, the finding that proTRH expression in the E19 PVN responded with down-regulation to T3 but not T4 indicated that the hypothalamus is already sensitive to T3 at this stage. It also suggested that insufficient conversion of T4 to T3 would be a crucial rate-limiting factor in this process.

We aimed to better understand why negative feedback is impaired before E19 despite the presence of crucial elements of T3 signalling. Thus, we studied whether anticipated changes in hypothalamic TH metabolism follow a pattern that would enable increased

hypothalamic T3 generation to suppress the TRH neurons in the PVN around E19, the period of the onset of feedback.

Local hypothalamic TH availability for TRH neurons in the PVN is a crucial factor that is under the control of members of the deiodinase enzyme family (Fekete and Lechan, 2014). Earlier, non-isotopic *in situ* hybridization could not reveal D2 expression in E15 tanycytes (Gereben et al., 2004) that allowed to speculate that onset of D2 expression in this location before E19 and the consequent T3 production of the enzyme could be the trigger for the formation of negative feedback on TRH neurons. However, the more sensitive isotopic *in situ* hybridization approach used in the current study detected D2 mRNA already from E13, showing that the onset of D2 expression in the tanycytes cannot be a trigger of the T3-mediated negative feedback on TRH neurons. However, we also detected intense perivascular D2 expression during the entire E13-P2 period that confirms our observations in this compartment at earlier stages of development (Gereben et al., 2004; Geysens et al., 2012). This situation is clearly different both from that found in the adult chicken where perivascular expression is faint and also from the adult rodent brain where hypothalamic D2 expression is confined to tanycytes lining the floor and walls of the third ventricle in the MBH (Abe et al., 1998; Gereben et al., 2004). This led us to conclude that around set point formation T4 conversion in the hypothalamic perivascular compartment could also significantly contribute to T3 generation.

In accordance with this assumption, D2 activity measurement demonstrated that the T3 generating capacity intensively increased from E15 to P2 both in the MBH (by 11.6-fold) and in the non-tanycyte containing hypothalamic region (by 3.9-fold). This finding indicates that a continuously increasing local T3 level is present in the developing chicken hypothalamus. Presently no established transgenic or transient approach is available that would allow specific *in vivo* ablation of D2 expression in chickens, thus loss-of-function studies could not be performed to assess T3-mediated feedback formation in developing chicken hypothalamus in the absence of D2. However, the presented data on impaired response of proTRH expression to T4 but not to T3 in the E19 PVN along with the presented pattern of D2 activity changes strongly indicate that the elevation of D2-mediated hypothalamic T3 generation is a critical factor for the

onset of T3-evoked negative feedback of the hypothalamus. As to the cell-type specific contribution of hypothalamic D2 elevation, the presence of tanycytes in the MBH represents the major difference in cellular composition between this region and the rest of the hypothalamus. Therefore it can be suggested that the more intense increase in D2 expression in the MBH between E15 and P2 compared to the rest of the hypothalamus is the consequence of changes in D2 expression in tanycytes.

We also investigated which factor could be involved in the developmental increase of D2 in the chicken hypothalamus. We studied the expression of the Nkx2.1 homeodomain containing transcription factor, a known transcriptional modulator of TH activation (Gereben et al., 2001). The presented *in situ* hybridization data revealed cell-type specific Nkx2.1 expression, suggesting that this factor could play a role in promoting D2 expression in developing tanycytes but not in perivascular elements. This observation was further supported by coordinated elevation of Nkx2.1 and D2 expression in E13-P2 in tanycytes. The applied luciferase promoter assay in the U87 glioma cell line proved that Nkx2.1 is indeed capable to increase the transcriptional rate of the chicken *Dio2* gene ~4 fold. The Nkx2.1 binding site contains a CAAG core in vertebrates but its binding capacity is heavily affected by flanking nucleotides; a 5' T and 3' G or T is usually required for strong binding (Damante and Di Lauro, 1994; Fabbro et al., 1995). The identified five putative Nkx2.1 binding sites of the ~3.6 kb *cDio2* 5' FR meet these criteria but none of them overlapped with the C1 and D Nkx2.1 binding sites of the human *DIO2* 5'FR (Gereben et al., 2001). The C1 Nkx2.1 binding site of the *hDIO2* site was not present in the *cDio2* 5'FR while the CAAG core of the D site was destroyed by insertion CA*G*AAG. The finding that the proximal 588 bp *cDio2* 5'FR, containing only one of the five putative Nkx2.1 binding sites remained responsive to Nkx2.1 but in a lesser extent than the 3.6 kb 5'FR suggests that the putative binding site at -18 bp is functional. It also indicates that more than one binding site contributes to the Nkx2.1 responsiveness of the *cDio2* 5'FR, similarly to the observations on the *hDIO2 5'*FR (Gereben et al., 2001). The obtained *in vivo* and *in vitro* data suggest that Nkx2.1 could be involved in the developmental increase of D2 expression in tanycytes.

TH inactivating D3 is another crucial participant in fine tuning of local TH levels (Abel et al., 1999; Freitas et al., 2010). Thus we also studied D3 expression in the developing chicken hypothalamus. Interestingly, the intense D3 mRNA and protein expression at E15 and P2 was not confined only to neurons, but it was also present in tanycytes. In contrast to this finding, tanycytes express just a limited amount of D3 in adult mammals (Abel et al., 1999; Escamez et al., 1999; Kallo et al., 2012). Only specific species of seasonal breeders (CBA/N mouse, Siberian hamster *(Phodopus sungorus),* F344 rats and also Japanese quail (*Coturnix japonica)* were reported to show significant D3 expression in tanycytes when kept under short day condition (Yoshimura et al., 2003; Yasuo et al., 2005; Barrett et al., 2007; Ono et al., 2008; Ross et al., 2011). D2 and D3 coexpression in developing chicken tanycytes suggests tightly controlled intracellular T3 availability in this cell-type. Since no marked changes could be observed in the tanycytal D3-mediated T3-degrading capacity it can be assumed that D2-catalyzed T3 activation is the dynamic factor in tanycyte-assisted regulation of hypothalamic T3 availability. In contrast to the *cDio*2 promoter we found that the used *cDio3* 5'FR remained unresponsive to Nkx2.1. However, we cannot exclude the potential existence of more 5' located bindings sites located more 5' to the region present in the cloned 623bp long 5'FR *cDio*3 fragment.

7.2 D3-mediated TH inactivation represents a novel mechanism in regulation of local TH levels in hypophysiotropic parvocellular neurons

Although serum TH concentrations are remarkably constant under physiological conditions, many biological processes require rapid and spatially controlled TH action. To meet the requirement of quick and cell-type specifically customized regulation of TH availability, intracellular TH levels are subjected to D2 and D3-mediated activation and inactivation, respectively, accompanied by TH transporters assisted active cellular influx and outflux of TH (Bianco et al., 2002; Visser et al., 2008).The deiodinase enzymes act in concert to fine-tune intracellular TH levels and play an especially important role in the brain to maintain TH levels required for normal neuronal development and function (Gereben et al., 2008). This concept is remarkably supported by findings obtained on the D3 knock-out mouse where the absence of D3 results in

altered hypothalamic function and the consequences persist through the entire lifespan (Hernandez et al., 2006).

These findings also demonstrate that TH also plays a critical role in the regulation of hypothalamic function. Beyond its well-described role in regulation of hypophysiotropic TRH neurons, TH has a complex impact on the regulation of other hypothalamic-pituitary axes (Lechan and Fekete, 2006; Murphy and Ebling, 2011) including, the reproductive axis, adrenal axis and GH secretion (Dawson, 1993; Giustina and Wehrenberg, 1995; Baumgartner et al., 1998; Araki et al., 2003; Lechan and Fekete, 2005; Nakao et al., 2008). To deepen our understanding on the TH-mediated regulation of these neurohormonal systems we identified the location and subcellular distribution of D3 and the major neuronal T3 transporter, MCT8 in hypophysiotropic neurons. These neurosecretory neurons have a common locus of termination in the external zone of the ME in close juxtapositon to the fenestrated portal capillaries in order to modulate hormone production in the anterior pituitary. However, cell bodies of neurosecretory neurons are located at various hypothalamic subdivisions, including e.g. the PVN (TRH and CRH), ARC (GHRH), and POA (GnRH) (Wiegand and Price, 1980; Merchenthaler et al., 1984).

D3-immunoreactivity was highly enriched in the external zone of the ME, and the authenticity of the signal was confirmed by Western blot, showing a band of expected size. Earlier D3 was considered to be a plasma membrane protein (Baqui et al., 2003) but interestingly previous ultrastructural studies of our group localized D3 primarily in DCV of neurosecretory granules of hypophysiotropic axon varicosities, while only limited immunostaining was present in the plasma membrane of axon terminals. In the present study we used N-STORM superresolution microscopy to further analyse D3 topology in DCV. N-STORM superresolution microscopy revealed that the size of the D3-immunoreactive clusters had similar size as the RAB3-immunoreactive clusters and had significantly larger diameter than the GnRH-immunoreactive clusters. Since RAB3 is known to be located on the outer surface of the DCV and GnRH is packaged inside the DCV, this data indicate that similarly to RAB3, the C-terminal of D3, containing the peptide that was used for the generation of the antiserum, is also located on the outer

surface of the DCV. As the C-terminal globular domain of D3 containing the active center of the enzyme is located in the cytosol, this localization allows an easy access to substrate. The transmembrane proteins with single transmembrane domain are classified according to their membrane orientation. Type 1 transmembrane proteins are single pass molecules with their C-terminus exposed to the cytosol (Chou and Elrod, 1999). Since D3 has one transmembrane domain on its N-terminal end (Callebaut et al., 2003), our findings provide *in vivo* evidence that D3 is a type 1 transmembrane protein and suggest that in hypophysiotropic neurons D3 exerts its biologic effects primarily in the membrane of DCV. Functional importance of D3 in axon terminals was proved by the demonstration that elevated T3-levels evoke increased D3-medited axonal TH inactivation in the rat ME.

We aimed to characterize the phenotype of D3 positive axon terminals, and performed double-labelling immunohistochemistry for D3 and hypophysiotropic peptides of parvocellular neurons in the external zone of rat ME. Our analysis revealed, that number of D3 positive axon varicosities strongly depends on cell-type. High proportion (approx. 70%) of GnRH, GHRH, CRH axon terminals contained D3 while only 30% of TRH varicosities were D3 positive. No signal was detected in SST containing axon terminals. TH is known to have critical role in the regulation of the reproductive axis both in adult and developing animals (Mann and Plant, 2010). Transient hypothyroidism during development has a major impact on the number and distribution of GnRH neurons in the hypothalamus (Lehman et al., 1997). Furthermore, TH is essential for the photoperiod induced transition between the breeding phase and anestrus in seasonal breeding animals (Yoshimura, 2010). Since GnRH neurons express TH receptors (Jansen et al., 1997), the presence of D3 contained within GnRH terminals indicates that TH may have an essential role in the regulation of reproductive function through direct effects on GnRH neurons. Thus, under certain conditions, controlling the amount of T3 within the GnRH neurons may be important to maintain normal function of the reproductive axis. This is supported by the phenotype of the D3 KO mouse in which deficits in reproductive function are observed (Hernandez et al., 2006).

Hypophysiotropic CRH neurons are well known to be regulated by TH. Hypothyroidism decreases CRH gene expression in the PVN, while T4 replacement induces upregulation of CRH mRNA levels (Ceccatelli et al., 1992). Furthermore,

experimental hyperthyroidism results in a hyperexcitability of the hypothalamic-pituitary-adrenal axis (Johnson et al., 2005). Therefore, prevention of an increase in T3 concentration by axonal D3 may be beneficial for normal functioning of the adrenal axis. Relatively less is known about thyroid regulation of the GHRH neurons, although hypothyroidism results in increased GHRH synthesis and release (Bluet-Pajot et al., 1998), and the severe growth retardation of the D3 KO mice (Hernandez et al., 2006) suggests the importance of D3 in the regulation of the GHRH neurons. The presence of D3 in GHRH axon terminals raises the possibility that some of these effects may be exerted directly on the GHRH neurons.

At first glance, the relative paucity of D3 in axon terminals of hypophysiotropic TRH neurons (26.6%) might seem surprising, given that negative feedback effects of TH on these neurons are so important for regulation of the HPT axis (Fekete and Lechan, 2007). The presence of D3 in neurons, however, may serve to modulate intracellular TH levels, perhaps as a way to maintain constant TH levels despite alterations in circulating levels. This type of regulation would not be to the advantage of hypophysiotropic TRH neurons that must sense increases or decreases in circulating levels of TH to enhance or diminish anterior pituitary TSH secretion. Nevertheless, a small subpopulation of TRH-containing axon terminals did co-contain D3, indicating a heterogeneity among hypophysiotropic TRH axon terminals. A heterogeneity of the hypophysiotropic TRH neurons was also suggested earlier indicating that a different subset of hypophysiotropic TRH neurons are responsible for the response to cold and suckling (Sanchez et al., 2001). Further studies are required to test the hypothesis, that D3 expressing TRH neurons represent the subpopulation that are activated by cold environment.

We were also interested in TH uptake capacity of the axon terminals, belonging to neurosecretory neurons of different peptidergic phenotype so we studied the presence of the MCT8 transporter in hypophysiotropic axon terminals.in accordance with previous findings of our group demonstrating MCT8 in TRH axon terminals. Since the perikarya of the hypophysiotropic neurons are located relatively far from the tanycytes, the question arises how T3 gains access to the nucleus. Tanycyte processes are often embedded by axonal segments of neurosecretory neurons in the ME and this allows the formation of a unique microenvironment between the two cell compartments (Rethelyi and Fockter, 1982). It can be suggested that T3 is subjected to retrograde axonal

transport that could represent a major route of T3 from the ME to hypophysiotropic perikarya. According to this model, the amount of axonal D3 will determine the local T3 level in axon varicosities, and would serve as a gate keeper to control the amount of T3 reaching the nucleus **(Figure 1)**.

T3 influx may also be directed to axonal mitochondria, affecting mitochondrial biogenesis and/or modulation of uncoupling proteins with important consequences on oxygen consumption, ATP generation and heat production (Martinez et al., 2009; Cheng et al., 2010). Modulation of neuronal energy homeostasis via mitochondrium-coupled mechanisms is known to affect neurotransmission, a process that is highly energy dependent (Laughlin et al., 1998). In agreement with this, robust uncoupling protein-2 (UCP2) expression has been demonstrated in the neuronal processes of the hypothalamic-pituitary system, paralleled with decreased mitochondrial respiration and elevated hypothalamic temperature compared to the non-UCP2 expressing thalamus (Horvath et al., 1999). It can be hypothesized that T3-mediated changes of mitochondrial function in hypothalamic axons could serve as potential regulator of neurotransmission but this hypothesis needs to be tested experimentally.

Based on the MCT8 and D3 content in hypophysiotropic terminals, we propose that hypophysiotropic axons in the ME can be divided into two categories **(Figure 28)**. The first are axon terminals that can uptake T3 and regulate the intracellular T3 concentration by axonal D3 (e.g. GnRH). This type of axon can be protected from sudden changes of T3 concentration by maintaining normal levels of cytoplasmic T3. In contrast, the second type of axon terminals accumulate T3 but unable to regulate their intracellular T3 due to the lack of D3 (e.g. TRH neurons). These axons may be very sensitive to changes in local T3 concentration that may be important for normal function of hypophysiotropic neuronal networks.

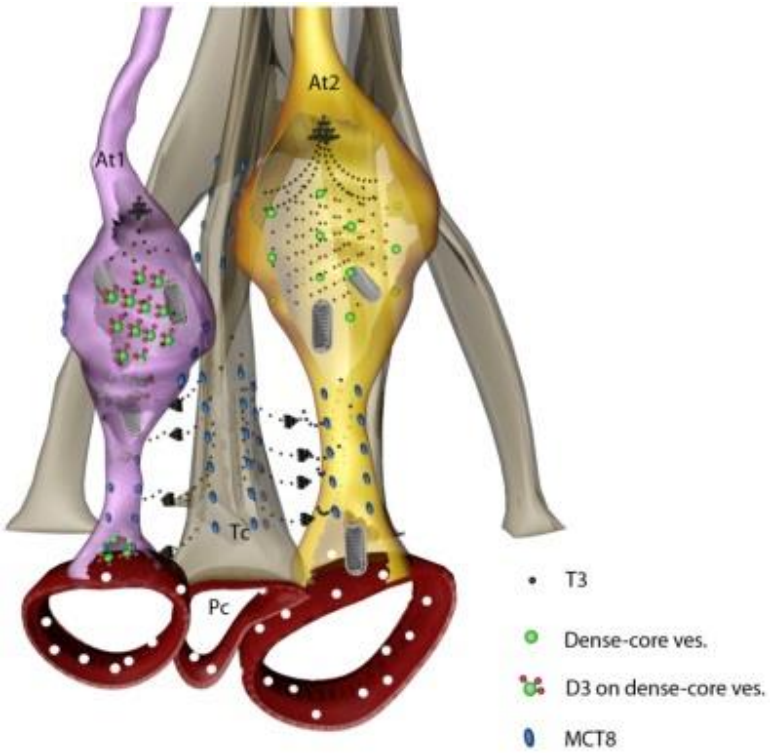

Figure 28 Schematic depiction of axonal uptake and regulation of T3 in the mediobasal hypothalamus. We suggest that T3 generated by type 2 deiodinase (D2) is released from tanycyte processes and taken up by monocarboxylate transporter 8 (MCT8) into axons of hypophysiotropic neurons. T3 concentrations are subjected to local regulation by type 3 deiodinase (D3)-containing axon varicosities (At1), but absent in D3-negative axons (At2). T3 could be subjected to retrograde transport to reach the soma and nucleus of hypophysiotropic neurons and/or could act locally by affecting mitochondrial function and local thermogenesis. At: axon terminal; Tc: tanycyte; Pc: portal capillary

Although D3 is normally distributed as described above, challenges affecting TH economy in the hypothalamus may change D3 content cell-type specifically. LPS challenge, a frequently used model of NTIS, is known to be modulate hypothalamic TH activation by increasing the expression and activity of D2 in tanycytes (Fekete et al., 2004). Thus under these conditions local T3 content of the ME is shifted towards locally generated T3 compared to T3 that arrives form the circulation to this region located outside of the BBB. Thus we used this experimental paradigm to investigate the functional flexibility of the TH inactivating machinery of hypophysiotropic neurons. We studied axonal D3 distribution in parvocellular neurons using the same

immunolabelling and confocal imaging based approach as for animals without LPS challenge. Our studies suggest that LPS treatment exerts a regulatory effect on intracellular T3 availability in hypophysiotropic neurons via cell-type specific alterations of axonal D3 content. The LPS induced marked decrease in D3 content of GHRH and CRH axon terminals suggests that these neurons are exposed to an elevated TH availability due to increased TH activation and decreased intracellular TH inactivation capacity. TH responsive genes in CRH and GHRH neurons may need to be activated to manage LPS challenge as it indeed happens with CRH expression. In contrast, GnRH and TRH expressing neurons are programmed not to modify their TH availability upon LPS challenge and keep their high and low (GnRH and TRH neurons, respectively) T3 degradation rate unchanged under these conditions. Our findings demonstrate that D3 content of hypophysiotropic axon varicosities is regulated dynamically within hours represents a novel mechanism for tightly controlled, cell-type specific TH availability.

7.3 Generation and characterization of thyroid hormone action indicator mouse model

Up to now, one could only assess tissue-specific TH signalling by measuring the expression of TH-responsive genes (Bianco et al., 2014). However, this approach is highly limited due to multiple factors affecting the expression of endogenously expressed TH-responsive genes. For example, well-known TH-responsive genes such as spot-14, malic enzyme and ectonucleotide pyrophosphatase/phosphodiesterase 2 (ENPP2) are also regulated by many other factors beyond TH, including insulin and 17β-estradiol (Ishihara et al., 2007; Sarvari et al., 2015). Thus, an experimental model that would allow the authentic assessment of TH signalling in mammals would be invaluable to reveal TH-related changes in health and disease. No such system has been available since the FINDT3 mouse model is based on an artificial chimeric Gal4DNA-binding domain-TRα ligand-binding domain fusion protein that works independently of endogenous TR and TRE (Quignodon et al., 2004). Thus, this system detects only T3 availability, but cannot assess physiologically relevant TH action. A 2xTRE β-galactosidase mouse model has been also reported to assess TH action at embryonic stages, but this model does not work in adults, cannot be used in live animals. More

importantly this model is severely biased since it is an uncharacterized mixture of different lines with enormously different copy numbers of the transgene thus it cannot be used for quantification of TH action (Nucera et al., 2010). Thus, our goal was to create a transgenic mouse that overcomes these shortcomings and allows the quantification of tissue-specific TH action under different conditions.

Our novel transgenic mouse THAI model allows semiquantitative assessment of TH action in both live animals and in tissue samples using a reporter cassette that operates in the context of endogenously expressed levels of transcriptional factors.

The reporter cassette was designed to achieve detectable basal expression of the reporter protein and achieve the highest sensitivity to TH both in live animals and in tissue samples. At the same time, we wanted to avoid genomic silencing of the reporter. To do so, we used an expression enhancer cassette (EEC), triplets of TRE elements isolated from the 5' flanking region of the most TH responsive human *DIO1* gene and a minimal TK promoter to express a codon-optimized, methylation-resistant firefly luciferase reporter protein and the whole insert was flanked by insulators. FISH studies revealed that thank to the applied Sleeping Beauty-mediated transgene delivery (Ivics et al., 2014) all three generated founders (THAI #4, #18, #23) harbour only one copy of the transgene. In addition, in case of the #4 line, we demonstrated with Splinkerette PCR (Potter and Luo, 2010) that the cassette was inserted into the L1 repeat region without any known role in protein expression. This region is often preferred for insertion by the SB transposase (Yant et al., 2005). Due to this favourable genomic context the #4 transgenic animals shown systemic euthyroidism and do not have any significant difference in metabolic parameters.

Using this model, TH signalling could be readily assessed in samples originating from most classical TH-responsive tissues including the brain, iBAT, liver, heart, small intestine and skeletal muscle. Basal luciferase activity values were fairly variable in different tissues, reflecting the local promoter activity within a tissue, but most of them fall in a 2-order of magnitude interval. We tested the TH responsiveness of different tissues and brain regions in all transgenic lines, using exogenous T4 and T3. Our measurements demonstrated that luciferase expression is inducible in all tissues of THAI line #4 mice, and can be used both in the CNS and in various peripheral tissues for a broad range of studies. The two other lines hold additional values for specific

studies; line #23 is especially suitable for studies on the hypothalamus/pituitary, due to the high responsiveness in HF and brain, while #18, having the highest basal activity in brain, is more appropriate to study decreased TH action in different brain regions.

When TRs are unoccupied by their ligands, e.g. in hypothyroidism, the TR remains bound to the regulatory regions of TH-dependent genes, repressing the gene transcription. Measuring TR-mediated gene repression could provide an entirely new approach to physiological studies of TH signalling and the impact of the deiodinases and transporters. The present studies indicate that the THAI-Mouse can be instrumental in achieving this goal as the THAI-Mouse exhibits sufficient signal-to-noise ratio to assess co-repression, i.e. a decrease in TH signalling observed during hypothyroidism. Indeed, in the hypothyroid THAI-Mouse there is ~2-10 fold decrease in TH signalling in different brain regions, the pituitary and other peripheral organs including liver, heart, bone, iBAT, white blood cells and small intestine. The latter is particularly interesting as it illustrates the high degree of TH responsiveness exhibited by the intestinal epithelium, which is consistent with the observation that patients carrying TRα inactivating mutations exhibit marked constipation (Bochukova et al., 2012). More than 100 million patients with hypothyroidism are treated with levothyroxine replacement therapy worldwide (Jonklaas et al., 2014). The rationale for using only levothyroxine is based on the idea that the deiodinases, which activate T4 to T3, will regulate the amount of T3 required by individual tissues. It has recently been recognized that there are tissue-specific limits of the efficiency of this process to the extent that deiodinases normalize systemic and intracellular T3 during treatment with levothyroxine, which probably explains residual symptoms in 10-15% of these patients (Gereben et al., 2015). It is hypothesized that despite normal serum TSH local tissue hypothyroidism persists in these patients. THAI-Mouse could serve as powerful tool to understand tissue-specific TH action that is required to study the efficiency of TH replacement therapies to restore tissue euthyroidism.

Importantly, in specific organs, like iBAT, small intestine and mandibular salivary gland, we could study TH action even in live animals by *in vivo* imaging, that was the first approach to quantitatively visualize TH action live. Importantly, *in vivo* imaging in THAI-Mice could not only detect the marked effect of supraphysiological doses (34) of TH-s and severe hypothyroidism, but alterations of TH signalling could be also capture

and quantified after cold stress in the iBAT, thus the system also works under physiological challenges. In addition, the THAI-Mouse responds to TH within a timeframe – a few hours - that is compatible with current view of the kinetics on TH action.

Although the dosage of L-T4 and L-T3 used in the present studies meet professional standards still it is certainly well above the physiological range (Bianco et al., 2014). Remarkably, the THAI-Mouse model is sufficiently sensitive for detection of tissue-specific alterations in TH signalling-mediated by physiological changes in local TH metabolism. Using this model, we provided direct evidence in tissue samples and also in live animal, that the cold-stimulated iBAT undergoes rapid D2-mediated increase in TH signalling, that was only indirectly documented in previous studies (Bianco and Silva, 1987). We also revealed that not basal only cold induced increase of TH signalling is dependent on NE in iBAT. Likewise, we also provided the first direct evidence that TH action is elevated in the MBH during LPS induced NTIS. This was only hypothesized before by circumstantial data(Boelen et al., 2004; Fekete et al., 2005a; Zeold et al., 2006a). The doubling of luciferase expression in hypothalamic areas of the LPS-treated mice also proves that the THAI-Mouse can also assess TH signalling within a physiological/pathophysiological context in the brain. THAI-Mice revealed marked tissue-specific differences in TH action during the development of NTIS directly demonstrating that increase of TH action in the MBH plays a role in TRH suppression in the PVN. Beyond providing further insight into the pathogenesis of the syndrome, these data importantly demonstrated the remarkable advantage of the THAI reporter in the assessment of TH action in contrast to endogenous TH-responsive genes that are also controlled by TH independent factors.

TH-s, the key regulators of cellular energetics and basal metabolic rate could be used to enhance weight loss in obesity but this treatment cannot be performed due to unwanted, mostly cardiac side effects (Kahaly and Dillmann, 2005). An intense effort is being paid to achieve organ-specific TH action. Since TR-subtypes are differently expressed in specific tissues, one option is to develop TH analogues called thyromimetics that should regulate TH metabolism in the target tissue in a TR-subtype (mainly TRβ1) specific manner and would allow to avoiding TRα-mediated cardiac side effects (Grover et al., 2003). The THAI-Mouse works in the context of endogenously expressed receptors, and

co-regulators, therefore it is appropriate to report TH availability in any kind of TR expressing tissues. Our data obtained with TRβ selective GC24 compound clearly demonstrated the effectiveness of THAI-Mouse for *in vivo* testing of TR-subtype selective agonists as it evoked increased TH action in TRβ dominant liver while not affected TRα dominant heart.

Our data provided clear evidence that THAI-Mice reveal local tissue-specific up- or downregulation of TH action even in conditions when serum TH levels are unchanged. Thus, the THAI-Mouse model provides a novel way to study tissue-specific TH action both from a basic science and from translational perspective.

8. Conclusions

The presented results aimed to contribute to the better understanding of mechanisms underlying TH action in the developing and adult brain and in related peripheries along with the generation of a novel transgenic mouse model for these studies.

TH-mediated hypothalamic set point formation is poorly understood despite its fundamental impact on TH economy and consequently on tissue function persisting throughout the entire lifespan. Our studies in chicken model determined the period of set point formation and demonstrated that tight regulation of local hypothalamic TH availability via a dramatic developmental increase in hypothalamic D2-mediated T3 generation plays a crucial role in the formation of negative feedback on TRH neurons. Since maternal TH status impacts fetal TH availability and altered TH levels during development could result in shifted HPT set point with persisting effects, our data could provide novel arguments to the ongoing debate whether maternal TH levels should be routinely monitored during human pregnancy, especially in the sensitive period when set point of the HPT axis is formed. Studies on primates would be useful to confirm the importance of the presented mechanism in higher vertebrates.

Neurosecretory neurons represent a major hypothalamic target of TH. The revealed abundant presence of functional D3 in axon terminals of hypophysiotropic parvocellular neurons on the outer surface of dense core vesicles represents a novel regulation of neuroendocrine axes by TH. We could classify two types of axon terminals based on their D3 content. Number of D3-positive axon varicosities was found highly variable in different neurosecretory systems and was subjected to intense and quick changes in response to challenges like bacterial LPS-induced inflammation. This indicated the existence of axon-type specific regulation of intracellular T3 availability in axon terminals of neurosecretory neurons. Tanycyte processes in the median eminence represent the main source of hypothalamic T3 while the cell bodies of hypophysiotropic neurons are located in distinct brain nuclei. Thus it can be hypothesized that the pathway along TH can gain access to the nuclear compartment of these neurons involves uptake by axon terminals in the median eminence and retrograde transport along neurosecretory axons to the soma. We suggest that D3-mediated T3 inactivation in the varicosities can serve as a gate keeper that dynamically regulates the amount of T3 reaching the nucleus by retrograde transport. Furthermore D3 may have also local

effect on axonal neurosecretion by affecting mitochondrial biogenesis, and function, however more studies are still needed to support this hypothesis. Monocarboxylate transporter 8-mediated axonal T3 uptake and neuron-type specific regulation of intracellular T3 concentration via D3 in the rodent median eminence could represent a novel pathway for the modulation of hypothalamic control of reproduction, growth, stress and metabolism.

The generated Thyroid Hormone Action Indicator (THAI) Mouse model has the potential greatly facilitate the investigation of tissue-specific TH action by providing an unbiased *in vivo* model for these studies. The THAI-Mouse model is based on a firefly luciferase reporter and uses a fully endogenous set of regulators of TH action. The model allows quantification of TH action in a live mammal for the first time along with the assessment of TH action in samples originating from various brain regions and peripheral tissues. While endogenous TH responsive genes are also controlled by various non-TH related factors, THAI-Mouse authentically reports TH action. The model can detect endogenous changes in TH availability and reports both tissue hyper- and hypothyroidism in the brain and in peripheral tissues. Using this model we could demonstrate that TH action is tissue-specifically regulated in hypothalamic subdivisions during the development of infection-induced non-thyroidal illness syndrome. The model was also used to better understand TH regulated mechanism in the cold-induced iBAT. Moreover our studies demonstrated, that THAI-Mouse could be used in testing TR isoform-selective compounds in the presence of endogenously expressed receptors, and could support the efforts to develop thyromimetics to treat obesity, and high cholesterol levels. THAI-Mouse could be also highly useful to study tissue hypothyroidism during TH replacement therapy. These studies can provide novel data to advance the ongoing debate on TH replacement that could potentially affect future treatment of tens of millions of patients worldwide.

9. Summary

Serum thyroid hormone (TH) levels are kept relatively stable by the hypothalamus-pituitary-thyroid (HPT) axis. However, TH exerts is biological effect on cells in tissue niches that undergoes vigorous changes of tissue and cell-type specific TH availability customized by local TH metabolizing enzymes and transporters. Our aim was to better understand the regulation of tissue-specific TH action in the brain and related peripheries. We studied the onset of the set point of the HPT axis, a poorly understood event exerting impact on the entire lifespan. We demonstrated that negative TH feedback on thyrotropin releasing hormone (TRH) neurons forms between embryonic day 19 and two days after hatching during chicken ontogenesis. Our studies on the underlying mechanisms revealed that feedback formation is accompanied by intense and coordinated hypothalamic increase of type 2 deiodinase (D2) activity required to build the sufficient T3 gradient for set point formation. We also provided evidence that Nkx2.1-mediated transcriptional events could play a role in this process. Our studies on the regulation of TH action in the hypothalamic neurosecretory system identified enzymatically active type 3 deiodinase (D3) in axon terminals of hypophysiotropic parvocellular neurons on the outer surface of dense core vesicle in the rodent hypothalamus. The occurrence of D3 in axon varicosities was phenotype dependent in neurosecretory neurons indicating a strikingly different capacity for intracellular T3 regulation in these neuronal subtypes. This diversity could be further refined based on the difference in response to bacterial lipopolysaccharide (LPS) evoked challenge in a rat model of non-thyroidal illness syndrome (NTIS). We generated and characterized a firefly luciferase reporter expressing TH action indicator (THAI)-Mouse model that works in the intact context of endogenously expressed factors and allows the detection of tissue/cell-type specific TH action in live animals and tissue samples. Our studies using THAI-Mouse revealed that a D2-mediated increase of TH action in hypothalamic subdivisions contributes to the pathogenesis of LPS-induced NTIS. Using THAI mice we also demonstrated that norepinephrine signalling impacts TH action in interscapular brown adipose tissue during cold stress while does not affect basal TH action. The THAI-Mouse model also allows *in vivo* testing of TH receptor isoform-specific thyromimetics. In conclusion, our data contribute to the better understanding of the regulation of cell-type specific TH action in the brain and related peripheries.

10. Összefoglalás

A szérum pajzsmirigyhormon (PMH) szint viszonylagos stabilitását a hipotalamusz-hipofízis-pajzsmirigy tengely (HHP) szavatolja. A PMH-ok biológiai hatásukat azonban a szövetekben fejtik ki, ahol a szövet és sejttípus-specifikus PMH elérhetőséget a PMH metabolizáló enzimek és transzporterek helyben alakítják ki. Célunk e szövetspecifikus szabályozás mélyebb megértése volt az agyban és ezzel összefüggésben egyes perifériás szövetekben. Tanulmányoztuk a HHP tengely „set point"-jának kialakulását ami az egész élettartamra kiható hatása ellenére kevéssé feltárt. Megmutattuk, hogy a csirke egyedfejlődése során a PMH-függő negatív visszacsatolás a 19. embrionális nap és két napos kor között alakul ki a TRH neuronokon. Az ennek hátterében álló mechanizmusokat vizsgálva megállapítottuk, hogy a folyamatot erőteljes és szabályozott hipotalamikus kettes típusú dejodáz (D2) aktivitás növekedés kíséri, ami elengedhetetlen a „set point" beállításhoz szükséges T3 gradiens létrehozásához. Bizonyítékot szolgáltattunk arra is, hogy az Nkx2.1-mediált transzkripcionális folyamatok szerepet játszhatnak ennek szabályozásában. A hipotalamikus neuroszekretoros rendszer PMH jelátvitel szabályozását célzó vizsgálataink során enzimatikusan aktív, hármas típusú dejodázt (D3) azonosítottunk rágcsáló hipotalamusz hipofizeotróf parvocelluláris neuronjainak axon terminálisaiban a dense core vezikulák külső felszínén. A D3 jelenléte neuroszekretoros neuronok fenotípusától függően változott, ami jelentősen eltérő intracelluláris T3 bontó kapacitásra enged következtetni a különböző neuron altípusokban. Ez a változatosság a neuronok D3 válasz készségének alapján további csoportokra oszlott a bakteriális lipopoliszacharid (LPS) indukált „alacsony T3 szindróma" (NTIS) rágcsáló modelljében. Létrehoztunk és jellemeztünk egy PMH indikátor (THAI) egér modellt, ami érintetlen szabályozó faktorok jelenlétében méri a szövet/sejttípus-specifikus PMH jelátvitelt élő állatban és szövetmintákban. A THAI-egérben igazoltuk, hogy az LPS-indukált NTIS patogenezisében szerepet játszik a D2-mediált hipotalamikus PMH jelátvitel növekedése és igazoltuk, hogy a noradrenalin jelpálya nincs hatással a lapockák közti barna zsírszövet alap PMH jelátvitelére, de hidegstresszben befolyásolja azt. A THAI modell továbbá PMH receptor izoforma specifikus tiromimetikumok *in vivo* tesztelését is lehetővé teszi. Adataink hozzájárulnak az agy és egyes érintett perifériás szövetek sejttípus specifikus PMH jelátvitelének mélyebb megértéséhez.

11. References

Abe T, Kakyo M, Sakagami H, Tokui T, Nishio T, Tanemoto M, Nomura H, Hebert SC, Matsuno S, Kondo H, Yawo H. 1998. Molecular characterization and tissue distribution of a new organic anion transporter subtype (oatp3) that transports thyroid hormones and taurocholate and comparison with oatp2. The Journal of biological chemistry 273(35):22395-22401.

Abel ED, Ahima RS, Boers ME, Elmquist JK, Wondisford FE. 2001. Critical role for thyroid hormone receptor beta2 in the regulation of paraventricular thyrotropin-releasing hormone neurons. The Journal of clinical investigation 107(8):1017-1023.

Abel ED, Boers ME, Pazos-Moura C, Moura E, Kaulbach H, Zakaria M, Lowell B, Radovick S, Liberman MC, Wondisford F. 1999. Divergent roles for thyroid hormone receptor beta isoforms in the endocrine axis and auditory system. The Journal of clinical investigation 104(3):291-300.

Alkemade A, Friesema EC, Unmehopa UA, Fabriek BO, Kuiper GG, Leonard JL, Wiersinga WM, Swaab DF, Visser TJ, Fliers E. 2005. Neuroanatomical pathways for thyroid hormone feedback in the human hypothalamus. The Journal of clinical endocrinology and metabolism 90(7):4322-4334.

Almazan G, Honegger P, Matthieu JM. 1985. Triiodothyronine stimulation of oligodendroglial differentiation and myelination. A developmental study. Dev Neurosci 7(1):45-54.

Alonso M, Goodwin C, Liao X, Ortiga-Carvalho T, Machado DS, Wondisford FE, Refetoff S, Weiss RE. 2009. In Vivo Interaction of Steroid Receptor Coactivator (SRC)-1 and the Activation Function-2 Domain of the Thyroid Hormone Receptor (TR) β in TRβ E457A Knock-In and SRC-1 Knockout mice. Endocrinology 150(8):3927-3934.

Alvarez-Buylla A, Ling CY, Kirn JR. 1990. Cresyl violet: a red fluorescent Nissl stain. Journal of neuroscience methods 33(2-3):129-133.

Alvarez-Dolado M, Iglesias T, Rodríguez-Peña A, Bernal J, Muñoz A. 1994. Expression of neurotrophins and the trk family of neurotrophin receptors in normal and hypothyroid rat brain. Brain Res Mol Brain Res 27(2):249-257.

Aquila H, Link TA, Klingenberg M. 1985. The uncoupling protein from brown fat mitochondria is related to the mitochondrial ADP/ATP carrier. Analysis of sequence homologies and of folding of the protein in the membrane. The EMBO journal 4(9):2369-2376.

Araki O, Morimura T, Ogiwara T, Mizuma H, Mori M, Murakami M. 2003. Expression of type 2 iodothyronine deiodinase in corticotropin-secreting mouse pituitary tumor cells is stimulated by glucocorticoid and corticotropin-releasing hormone. Endocrinology 144(10):4459-4465.

Astapova I, Lee LJ, Morales C, Tauber S, Bilban M, Hollenberg AN. 2008. The nuclear corepressor, NCoR, regulates thyroid hormone action in vivo. Proceedings of the National Academy of Sciences of the United States of America 105(49):19544-19549.

Baqui M, Botero D, Gereben B, Curcio C, Harney JW, Salvatore D, Sorimachi K, Larsen PR, Bianco AC. 2003. Human type 3 iodothyronine selenodeiodinase is located in the plasma membrane and undergoes rapid internalization to endosomes. The Journal of biological chemistry 278(2):1206-1211.

Baqui MM, Gereben B, Harney JW, Larsen PR, Bianco AC. 2000. Distinct subcellular localization of transiently expressed types 1 and 2 iodothyronine deiodinases as determined by immunofluorescence confocal microscopy. Endocrinology 141(11):4309-4312.

Barrett P, Ebling FJ, Schuhler S, Wilson D, Ross AW, Warner A, Jethwa P, Boelen A, Visser TJ, Ozanne DM, Archer ZA, Mercer JG, Morgan PJ. 2007. Hypothalamic thyroid hormone catabolism acts as a gatekeeper for the seasonal control of body weight and reproduction. Endocrinology 148(8):3608-3617.

Bartha T, Kim S-W, Salvatore D, Gereben B, Tu HM, Harney JW, Rudas P, Larsen PR. 2000. Characterization of the 5′-Flanking and 5′-Untranslated Regions of the Cyclic Adenosine 3′,5′-Monophosphate-Responsive Human Type 2 Iodothyronine Deiodinase Gene. Endocrinology 141(1):229-237.

Bates JM, St Germain DL, Galton VA. 1999. Expression profiles of the three iodothyronine deiodinases, D1, D2, and D3, in the developing rat. Endocrinology 140(2):844-851.

Baumgartner A, Hiedra L, Pinna G, Eravci M, Prengel H, Meinhold H. 1998. Rat brain type II 5'-iodothyronine deiodinase activity is extremely sensitive to stress. J Neurochem 71(2):817-826.

Berbel P, Guadańo-Ferraz A, Angulo A, Ramón Cerezo J. 1994. Role of thyroid hormones in the maturation of interhemispheric connections in rats. Behav Brain Res 64(1-2):9-14.

Bernal J, Guadańo-Ferraz A, Morte B. 2003. Perspectives in the study of thyroid hormone action on brain development and function. Thyroid : official journal of the American Thyroid Association 13(11):1005-1012.

Berry MJ, Kieffer JD, Harney JW, Larsen PR. 1991. Selenocysteine confers the biochemical properties of the type I iodothyronine deiodinase. The Journal of biological chemistry 266:14155-14158.

Berry MJ, Maia AL, Kieffer JD, Harney JW, Larsen PR. 1992. Substitution of cysteine for selenocysteine in type I iodothyronine deiodinase reduces the catalytic efficiency of the protein but enhances its translation. Endocrinology 131(4):1848-1852.

Bianco AC, Anderson G, Forrest D, Galton VA, Gereben B, Kim BW, Kopp PA, Liao XH, Obregon MJ, Peeters RP, Refetoff S, Sharlin DS, Simonides WS, Weiss RE, Williams GR. 2014. American thyroid association guide to investigating thyroid hormone economy and action in rodent and cell models. Thyroid : official journal of the American Thyroid Association 24(1):88-168.

Bianco AC, Salvatore D, Gereben B, Berry MJ, Larsen PR. 2002. Biochemistry, cellular and molecular biology and physiological roles of the iodothyronine selenodeiodinases. Endo Rev 23(1):38-89.

Bianco AC, Sheng X, Silva JE. 1988. Triiodothyronine amplifies norepinephrine stimulation of uncoupling protein gene transcription by a mechanism not requiring protein synthesis. The Journal of biological chemistry 263:18168-18175.

Bianco AC, Silva JE. 1987. Intracellular conversion of thyroxine to triiodothyronine is required for the optimal thermogenic function of brown adipose tissue. The Journal of clinical investigation 79(1):295-300.

Bluet-Pajot MT, Epelbaum J, Gourdji D, Hammond C, Kordon C. 1998. Hypothalamic and hypophyseal regulation of growth hormone secretion. Cell Mol Neurobiol 18(1):101-123.

Bochukova E, Schoenmakers N, Agostini M, Schoenmakers E, Rajanayagam O, Keogh JM, Henning E, Reinemund J, Gevers E, Sarri M, Downes K, Offiah A, Albanese A, Halsall D, Schwabe JW, Bain M, Lindley K, Muntoni F, Vargha-Khadem F, Dattani M, Farooqi IS, Gurnell M, Chatterjee K. 2012. A mutation in the thyroid hormone receptor alpha gene. The New England journal of medicine 366(3):243-249.

Boelen A, Kwakkel J, Fliers E. 2011. Beyond low plasma T3: local thyroid hormone metabolism during inflammation and infection. Endocrine reviews 32(5):670-693.

Boelen A, Kwakkel J, Thijssen-Timmer DC, Alkemade A, Fliers E, Wiersinga WM. 2004. Simultaneous changes in central and peripheral components of the hypothalamus-pituitary-thyroid axis in lipopolysaccharide-induced acute illness in mice. The Journal of endocrinology 182(2):315-323.

Borngraeber S, Budny MJ, Chiellini G, Cunha-Lima ST, Togashi M, Webb P, Baxter JD, Scanlan TS, Fletterick RJ. 2003. Ligand selectivity by seeking hydrophobicity in thyroid hormone receptor. Proceedings of the National Academy of Sciences of the United States of America 100(26):15358-15363.

Brent GA. 2012. Mechanisms of thyroid hormone action. The Journal of clinical investigation 122(9):3035-3043.

Brent GA, Harney JW, Chen Y, Warne RL, Moore DD, Larsen PR. 1989. Mutations of the rat growth hormone promoter which increase and decrease response to thyroid hormone define a consensus thyroid hormone response element. Mol Endocrinol 3(12):1996-2004.

Burgunder JM, Taylor T. 1989. Ontogeny of thyrotropin-releasing hormone gene expression in the rat diencephalon. Neuroendocrinology 49(6):631-640.

Callebaut I, Curcio-Morelli C, Mornon JP, Gereben B, Buettner C, Huang S, Castro B, Fonseca TL, Harney JW, Larsen PR, Bianco AC. 2003. The iodothyronine selenodeiodinases are thioredoxin-fold family proteins containing a glycoside

hydrolase clan GH-A-like structure. The Journal of biological chemistry 278(38):36887-36896.

Canettieri G, Celi FS, Baccheschi G, Salvatori L, Andreoli M, Centanni M. 2000. Isolation of human type 2 deiodinase gene promoter and characterization of a functional cyclic adenosine monophosphate response element. Endocrinology 141(5):1804-1813.

Cannon B, Nedergaard J. 2004. Brown adipose tissue: function and physiological significance. Physiological reviews 84(1):277-359.

Ceccatelli S, Giardino L, Calza L. 1992. Response of hypothalamic peptide mRNAs to thyroidectomy. Neuroendocrinology 56(5):694-703.

Chassande O, Fraichard A, Gauthier K, Flamant F, Legrand C, Savatier P, Laudet V, Samarut J. 1997. Identification of Transcripts Initiated from an Internal Promoter in the c-erbAα Locus That Encode Inhibitors of Retinoic Acid Receptor-α and Triiodothyronine Receptor Activities. Molecular Endocrinology 11(9):1278-1290.

Cheng SY, Leonard JL, Davis PJ. 2010. Molecular aspects of thyroid hormone actions. Endocrine reviews 31(2):139-170.

Chou KC, Elrod DW. 1999. Prediction of membrane protein types and subcellular locations. Proteins 34(1):137-153.

Christoffolete MA, Doleschall M, Egri P, Liposits Z, Zavacki AM, Bianco AC, Gereben B. 2010. Regulation of thyroid hormone activation via the liver X-receptor/retinoid X-receptor pathway. The Journal of endocrinology 205(2):179-186.

Christoffolete MA, Linardi CC, de Jesus L, Ebina KN, Carvalho SD, Ribeiro MO, Rabelo R, Curcio C, Martins L, Kimura ET, Bianco AC. 2004. Mice with targeted disruption of the Dio2 gene have cold-induced overexpression of the uncoupling protein 1 gene but fail to increase brown adipose tissue lipogenesis and adaptive thermogenesis. Diabetes 53(3):577-584.

Civitareale D, Lonigro R, Sinclair AJ, Di Lauro R. 1989. A thyroid-specific nuclear protein essential for tissue-specific expression of the thyroglobulin promoter. The EMBO journal 8(9):2537-2542.

Contreras C, Gonzalez F, Ferno J, Dieguez C, Rahmouni K, Nogueiras R, Lopez M. 2015. The brain and brown fat. Annals of medicine 47(2):150-168.

Crantz FR, Silva JE, Larsen PR. 1982. Analysis of the sources and quantity of 3,5,3'-triiodothyronine specifically bound to nuclear receptors in rat cerebral cortex and cerebellum. Endocrinology 110:367-375.

Croteau W, Davey JC, Galton VA, St Germain DL. 1996. Cloning of the mammalian type II iodothyronine deiodinase. A selenoprotein differentially expressed and regulated in human and rat brain and other tissues. The Journal of clinical investigation 98(2):405-417.

Curcio-Morelli C, Gereben B, Zavacki AM, Kim BW, Huang S, Harney JW, Larsen PR, Bianco AC. 2003a. In vivo dimerization of types 1, 2, and 3 iodothyronine selenodeiodinases. Endocrinology 144(3):937-946.

Curcio-Morelli C, Zavacki AM, Christofollete M, Gereben B, de Freitas BC, Harney JW, Li Z, Wu G, Bianco AC. 2003b. Deubiquitination of type 2 iodothyronine deiodinase by von Hippel-Lindau protein-interacting deubiquitinating enzymes regulates thyroid hormone activation. The Journal of clinical investigation 112(2):189-196.

Dahl GE, Evans NP, Thrun LA, Karsch FJ. 1994. A central negative feedback action of thyroid hormones on thyrotropin-releasing hormone secretion. Endocrinology 135(6):2392-2397.

Damante G, Di Lauro R. 1994. Thyroid-specific gene expression. Biochimica et Biophysica Acta (BBA)-Gene Structure and Expression 1218(3):255-266.

Dani A, Huang B, Bergan J, Dulac C, Zhuang X. 2010. Superresolution imaging of chemical synapses in the brain. Neuron 68(5):843-856.

Darimont BD, Wagner RL, Apriletti JW, Stallcup MR, Kushner PJ, Baxter JD, Fletterick RJ, Yamamoto KR. 1998. Structure and specificity of nuclear receptor–coactivator interactions. Genes & development 12(21):3343-3356.

Darras VM, Hume R, Visser TJ. 1999. Regulation of thyroid hormone metabolism during fetal development. Molecular and cellular endocrinology 151(1-2):37-47.

Dawson A. 1993. Thyroidectomy progressively renders the reproductive system of starlings (Sturnus vulgaris) unresponsive to changes in daylength. The Journal of endocrinology 139(1):51-55.

De Groef B, Grommen SV, Darras VM. 2006. Increasing plasma thyroxine levels during late embryogenesis and hatching in the chicken are not caused by an increased sensitivity of the thyrotropes to hypothalamic stimulation. The Journal of endocrinology 189(2):271-278.

De Groef B, Grommen SV, Darras VM. 2008. The chicken embryo as a model for developmental endocrinology: Development of the thyrotropic, corticotropic, and somatotropic axes. Molecular and cellular endocrinology 293(1-2):17-24.

De Groot LJ. 2015. The Non-Thyroidal Illness Syndrome. Endotext. Vol PMID: 25905425. South Dartmouth (MA).

de Jesus LA, Carvalho SD, Ribeiro MO, Schneider M, Kim SW, Harney JW, Larsen PR, Bianco AC. 2001. The type 2 iodothyronine deiodinase is essential for adaptive thermogenesis in brown adipose tissue. The Journal of clinical investigation 108(9):1379-1385.

Debonne M, Baarendse PJJ, Van Den Brand H, Kemp B, Bruggeman V, Decuypere E. 2008. Involvement of the hypothalamicpituitary-thyroid axis and its interaction with the hypothalamic-pituitary-adrenal axis in the ontogeny of avian thermoregulation: a review. World's Poultry Science Association 64:309-321.

Doleschall M, Mayer B, Cervenak J, Cervenak L, Kacskovics I. 2007. Cloning, expression and characterization of the bovine p65 subunit of NFkappaB. Dev Comp Immunol 31(9):945-961.

Dumitrescu AM, Liao XH, Best TB, Brockmann K, Refetoff S. 2004. A novel syndrome combining thyroid and neurological abnormalities is associated with mutations in a monocarboxylate transporter gene. Am J Hum Genet 74(1):168-175.

Egri P, Gereben B. 2014. Minimal requirements for ubiquitination-mediated regulation of thyroid hormone activation. Journal of molecular endocrinology 53(2):217-226.

Errijgers V, Van Dam D, Gantois I, Van Ginneken CJ, Grossman AW, D'Hooge R, De Deyn PP, Kooy RF. 2007. FVB.129P2-Pde6b(+) Tyr(c-ch)/Ant, a sighted variant of the FVB/N mouse strain suitable for behavioral analysis. Genes, brain, and behavior 6(6):552-557.

Escamez MJ, Guadano-Ferraz A, Cuadrado A, Bernal J. 1999. Type 3 iodothyronine deiodinase is selectively expressed in areas related to sexual differentiation in the newborn rat brain. Endocrinology 140(11):5443-5446.

Fabbro D, Tell G, Pellizzari L, Leonardi A, Pucillo C, Lonigro R, Damante G. 1995. Definition of the DNA-Binding Specificity of TTF-1 Homeodomain by Chromatographic Selection of Binding Sequences. Biochemical and Biophysical Research Communications 213(3):781-788.

Farsetti A, Lazar J, Phyillaier M, Lippoldt R, Pontecorvi A, Nikodem VM. 1997. Active repression by thyroid hormone receptor splicing variant alpha2 requires specific regulatory elements in the context of native triiodothyronine-regulated gene promoters. Endocrinology 138(11):4705-4712.

Fedorenko A, Lishko PV, Kirichok Y. 2012. Mechanism of Fatty-Acid-Dependent UCP1 Uncoupling in Brown Fat Mitochondria. Cell 151(2):400-413.

Fekete C, Freitas BC, Zeold A, Wittmann G, Kadar A, Liposits Z, Christoffolete MA, Singru P, Lechan RM, Bianco AC, Gereben B. 2007. Expression patterns of WSB-1 and USP-33 underlie cell-specific posttranslational control of type 2 deiodinase in the rat brain. Endocrinology 148(10):4865-4874.

Fekete C, Gereben B, Doleschall M, Harney JW, Dora JM, Bianco AC, Sarkar S, Liposits Z, Rand W, Emerson C, Kacskovics I, Larsen PR, Lechan RM. 2004. Lipopolysaccharide induces type 2 iodothyronine deiodinase in the mediobasal hypothalamus: implications for the nonthyroidal illness syndrome. Endocrinology 145(4):1649-1655.

Fekete C, Lechan RM. 2007. Negative feedback regulation of hypophysiotropic thyrotropin-releasing hormone (TRH) synthesizing neurons: role of neuronal afferents and type 2 deiodinase. Front Neuroendocrinol 28(2-3):97-114.

Fekete C, Lechan RM. 2014. Central regulation of hypothalamic-pituitary-thyroid axis under physiological and pathophysiological conditions. Endocrine reviews 35(2):159-194.

Fekete C, Mihaly E, Luo LG, Kelly J, Clausen JT, Mao Q, Rand WM, Moss LG, Kuhar M, Emerson CH, Jackson IM, Lechan RM. 2000. Association of cocaine- and amphetamine-regulated transcript-immunoreactive elements with thyrotropin-releasing hormone-synthesizing neurons in the hypothalamic paraventricular

nucleus and its role in the regulation of the hypothalamic-pituitary-thyroid axis during fasting. The Journal of neuroscience : the official journal of the Society for Neuroscience 20(24):9224-9234.

Fekete C, Sarkar S, Christoffolete MA, Emerson CH, Bianco AC, Lechan RM. 2005a. Bacterial lipopolysaccharide (LPS)-induced type 2 iodothyronine deiodinase (D2) activation in the mediobasal hypothalamus (MBH) is independent of the LPS-induced fall in serum thyroid hormone levels. Brain research 1056(1):97-99.

Fekete C, Singru PS, Sarkar S, Rand WM, Lechan RM. 2005b. Ascending brainstem pathways are not involved in lipopolysaccharide-induced suppression of thyrotropin-releasing hormone gene expression in the hypothalamic paraventricular nucleus. Endocrinology 146(3):1357-1363.

Fekkes D, Hennemann G, Visser TJ. 1982. Evidence for a single enzyme in rat liver catalysing the deiodination of the tyrosyl and the phenolic ring of iodothyronines. Biochemical Journal 201(3):673-676.

Ferrara AM, Onigata K, Ercan O, Woodhead H, Weiss RE, Refetoff S. 2012. Homozygous Thyroid Hormone Receptor β-Gene Mutations in Resistance to Thyroid Hormone: Three New Cases and Review of the Literature. The Journal of clinical endocrinology and metabolism 97(4):1328-1336.

Fisher DA, Klein AH. 1981. Thyroid development and disorders of thyroid function in the newborn. The New England journal of medicine 304(12):702-712.

Flament-Durand J. 1980. The hypothalamus: anatomy and functions. Acta psychiatrica Belgica 80(4):364-375.

Fonseca TL, Correa-Medina M, Campos MP, Wittmann G, Werneck-de-Castro JP, Arrojo e Drigo R, Mora-Garzon M, Ueta CB, Caicedo A, Fekete C, Gereben B, Lechan RM, Bianco AC. 2013. Coordination of hypothalamic and pituitary T3 production regulates TSH expression. The Journal of clinical investigation 123(4):1492-1500.

Fonseca TL, Fernandes GW, McAninch EA, Bocco BM, Abdalla SM, Ribeiro MO, Mohacsik P, Fekete C, Li D, Xing X, Wang T, Gereben B, Bianco AC. 2015. Perinatal deiodinase 2 expression in hepatocytes defines epigenetic susceptibility

to liver steatosis and obesity. Proceedings of the National Academy of Sciences of the United States of America.

Forrest D, Erway LC, Ng L, Altschuler R, Curran T. 1996a. Thyroid hormone receptor beta is essential for development of auditory function. Nature genetics 13(3):354-357.

Forrest D, Golarai G, Connor J, Curran T. 1996b. Genetic analysis of thyroid hormone receptors in development and disease. Recent progress in hormone research 51:1-22.

Forrest D, Hanebuth E, Smeyne RJ, Everds N, Stewart CL, Wehner JM, Curran T. 1996c. Recessive resistance to thyroid hormone in mice lacking thyroid hormone receptor beta: evidence for tissue-specific modulation of receptor function. The EMBO journal 15(12):3006-3015.

Freitas BC, Gereben B, Castillo M, Kallo I, Zeold A, Egri P, Liposits Z, Zavacki AM, Maciel RM, Jo S, Singru P, Sanchez E, Lechan RM, Bianco AC. 2010. Paracrine signaling by glial cell-derived triiodothyronine activates neuronal gene expression in the rodent brain and human cells. The Journal of clinical investigation 120(6):2206-2217.

Friesema EC, Docter R, Moerings EP, Verrey F, Krenning EP, Hennemann G, Visser TJ. 2001. Thyroid hormone transport by the heterodimeric human system L amino acid transporter. Endocrinology 142(10):4339-4348.

Friesema EC, Ganguly S, Abdalla A, Manning Fox JE, Halestrap AP, Visser TJ. 2003. Identification of monocarboxylate transporter 8 as a specific thyroid hormone transporter. The Journal of biological chemistry 278(41):40128-40135.

Friesema EC, Grueters A, Biebermann H, Krude H, von Moers A, Reeser M, Barrett TG, Mancilla EE, Svensson J, Kester MH, Kuiper GG, Balkassmi S, Uitterlinden AG, Koehrle J, Rodien P, Halestrap AP, Visser TJ. 2004. Association between mutations in a thyroid hormone transporter and severe X-linked psychomotor retardation. Lancet 364(9443):1435-1437.

Friesema EC, Jansen J, Jachtenberg JW, Visser WE, Kester MH, Visser TJ. 2008. Effective cellular uptake and efflux of thyroid hormone by human monocarboxylate transporter 10. Mol Endocrinol 22(6):1357-1369.

Galton VA, Martinez E, Hernandez A, St Germain EA, Bates JM, St Germain DL. 1999. Pregnant rat uterus expresses high levels of the type 3 iodothyronine deiodinase. The Journal of clinical investigation 103(7):979-987.

Ganong WF. 2000. Circumventricular organs: definition and role in the regulation of endocrine and autonomic function. Clinical and experimental pharmacology & physiology 27(5-6):422-427.

Gereben B, Bartha T, Tu HM, Harney JW, Rudas P, Larsen PR. 1999. Cloning and expression of the chicken type 2 iodothyronine 5'-deiodinase. The Journal of biological chemistry 274(20):13768-13776.

Gereben B, Goncalves C, Harney JW, Larsen PR, Bianco AC. 2000. Selective proteolysis of human type 2 deiodinase: a novel ubiquitin- proteasomal mediated mechanism for regulation of hormone activation. Mol Endocrinol 14(11):1697-1708.

Gereben B, McAninch EA, Ribeiro MO, Bianco AC. 2015. Scope and limitations of iodothyronine deiodinases in hypothyroidism. Nature reviews Endocrinology 11(11):642-652.

Gereben B, Pachucki J, Kollar A, Liposits Z, Fekete C. 2004. Ontogenic redistribution of type 2 deiodinase messenger ribonucleic acid in the brain of chicken. Endocrinology 145(8):3619-3625.

Gereben B, Salvatore D, Harney JW, Tu HM, Larsen PR. 2001. The Human, but Not Rat, dio2 Gene Is Stimulated by Thyroid Transcription Factor-1 (TTF-1). Mol Endocrinol 15(1):112-124.

Gereben B, Zavacki AM, Ribich S, Kim BW, Huang SA, Simonides WS, Zeold A, Bianco AC. 2008. Cellular and molecular basis of deiodinase-regulated thyroid hormone signaling. Endocrine reviews 29(7):898-938.

Gereben Balázs FC. 2016. Az alacsony T3 szindróma kialakulásának idegrendszeri mechanizmusai. Magyar Belorvosi Archivum 2-3:76-82.

Geris KL, Berghman LR, Kuhn ER, Darras VM. 1998. Pre- and posthatch developmental changes in hypothalamic thyrotropin-releasing hormone and somatostatin concentrations and in circulating growth hormone and thyrotropin levels in the chicken. The Journal of endocrinology 159(2):219-225.

Geysens S, Ferran JL, Van Herck SL, Tylzanowski P, Puelles L, Darras VM. 2012. Dynamic mRNA distribution pattern of thyroid hormone transporters and deiodinases during early embryonic chicken brain development. Neuroscience 221:69-85.

Giustina A, Wehrenberg WB. 1995. Influence of thyroid hormones on the regulation of growth hormone secretion. European journal of endocrinology / European Federation of Endocrine Societies 133(6):646-653.

Gregory CC, Dean CE, Porter TE. 1998. Expression of chicken thyroid-stimulating hormone beta-subunit messenger ribonucleic acid during embryonic and neonatal development. Endocrinology 139(2):474-478.

Grommen SV, Arckens L, Theuwissen T, Darras VM, De Groef B. 2008. Thyroid hormone receptor beta2 is strongly up-regulated at all levels of the hypothalamo-pituitary-thyroidal axis during late embryogenesis in chicken. The Journal of endocrinology 196(3):519-528.

Grover GJ, Mellstrom K, Ye L, Malm J, Li YL, Bladh LG, Sleph PG, Smith MA, George R, Vennstrom B, Mookhtiar K, Horvath R, Speelman J, Egan D, Baxter JD. 2003. Selective thyroid hormone receptor-beta activation: a strategy for reduction of weight, cholesterol, and lipoprotein (a) with reduced cardiovascular liability. Proceedings of the National Academy of Sciences of the United States of America 100(17):10067-10072.

Guadano-Ferraz A, Escamez MJ, Rausell E, Bernal J. 1999. Expression of type 2 iodothyronine deiodinase in hypothyroid rat brain indicates an important role of thyroid hormone in the development of specific primary sensory systems. The Journal of neuroscience : the official journal of the Society for Neuroscience 19(9):3430-3439.

Guadano-Ferraz A, Obregon MJ, St Germain DL, Bernal J. 1997. The type 2 iodothyronine deiodinase is expressed primarily in glial cells in the neonatal rat brain. Proceedings of the National Academy of Sciences of the United States of America 94(19):10391-10396.

Guazzi S, Price M, De Felice M, Damante G, Mattei MG, Di Lauro R. 1990. Thyroid nuclear factor 1 (TTF-1) contains a homeodomain and displays a novel DNA binding specificity. The EMBO journal 9(11):3631-3639.

Harbers M, Wahlström GM, Vennström B. 1996. Transactivation by the thyroid hormone receptor is dependent on the spacer sequence in hormone response elements containing directly repeated half-sites. Nucleic acids research 24(12):2252-2259.

Hashimoto Y, Furukawa S, Omae F, Miyama Y, Hayashi K. 1994. Correlative regulation of nerve growth factor level and choline acetyltransferase activity by thyroxine in particular regions of infant rat brain. J Neurochem 63(1):326-332.

Hernandez A, Martinez ME, Fiering S, Galton VA, St Germain D. 2006. Type 3 deiodinase is critical for the maturation and function of the thyroid axis. The Journal of clinical investigation 116(2):476-484.

Hillier AP. 1970. The binding of thyroid hormones to phospholipid membranes. The Journal of Physiology 211(3):585-597.

Horváth G, Gölöncsér F, Csölle C, Király K, Andó RD, Baranyi M, Koványi B, Máté Z, Hoffmann K, Algaier I, Baqi Y, Müller CE, Von Kügelgen I, Sperlágh B. 2014. Central P2Y12 receptor blockade alleviates inflammatory and neuropathic pain and cytokine production in rodents. Neurobiology of disease 70:162-178.

Horvath TL, Warden CH, Hajos M, Lombardi A, Goglia F, Diano S. 1999. Brain uncoupling protein 2: uncoupled neuronal mitochondria predict thermal synapses in homeostatic centers. The Journal of neuroscience : the official journal of the Society for Neuroscience 19(23):10417-10427.

Hrabovszky E, Molnar CS, Sipos M, Vida B, Ciofi P, Borsay BA, Sarkadi L, Herczeg L, Bloom SR, Ghatei MA, Dhillo WS, Kallo I, Liposits Z. 2011. Sexual dimorphism of kisspeptin and neurokinin B immunoreactive neurons in the infundibular nucleus of aged men and women. Frontiers in Endocrinology 2(Article 80).

Hrabovszky E, Turi GF, Liposits Z. 2005. Presence of vesicular glutamate transporter-2 in hypophysiotropic somatostatin but not growth hormone-releasing hormone neurons of the male rat. Eur J Neurosci 21(8):2120-2126.

Huang SA, Dorfman DM, Genest DR, Salvatore D, Larsen PR. 2003. Type 3 iodothyronine deiodinase is highly expressed in the human uteroplacental unit and in fetal epithelium. The Journal of clinical endocrinology and metabolism 88(3):1384-1388.

Huang TS, Chopra IJ, Beredo A, Solomon DH, Chua Teco GN. 1985. Skin is an active site for the inner ring monodeiodination of thyroxine to 3,3',5'-triiodothyronine. Endocrinology 117(5):2106-2113.

Hull D. 1977. Brown adipose tissue and the newborn infant's response to cold. In Scientific foundation of obstetrics and gynaecology E.E. Philipp, J. Barnes, and M. Newton, editors. London: William Heinemann. 545-550.

Hyyppä M. 1969. Differentiation of the hypothalamic nuclei during ontogenetic development in the rat. Zeitschrift für Anatomie und Entwicklungsgeschichte 129(1):41-52.

Ibarrola N, Rodríguez-Peña A. 1997. Hypothyroidism coordinately and transiently affects myelin protein gene expression in most rat brain regions during postnatal development. Brain research 752(1-2):285-293.

Ishihara A, Matsumoto E, Horikawa K, Kudo T, Sakao E, Nemoto A, Iwase K, Sugiyama H, Tamura Y, Shibata S, Takiguchi M. 2007. Multifactorial regulation of daily rhythms in expression of the metabolically responsive gene spot14 in the mouse liver. Journal of biological rhythms 22(4):324-334.

Ivics Z, Mates L, Yau TY, Landa V, Zidek V, Bashir S, Hoffmann OI, Hiripi L, Garrels W, Kues WA, Bosze Z, Geurts A, Pravenec M, Rulicke T, Izsvak Z. 2014. Germline transgenesis in rodents by pronuclear microinjection of Sleeping Beauty transposons. Nature protocols 9(4):773-793.

Jansen HT, Lubbers LS, Macchia E, DeGroot LJ, Lehman MN. 1997. Thyroid hormone receptor (alpha) distribution in hamster and sheep brain: colocalization in gonadotropin-releasing hormone and other identified neurons. Endocrinology 138(11):5039-5047.

Japon MA, Rubinstein M, Low MJ. 1994. In situ hybridization analysis of anterior pituitary hormone gene expression during fetal mouse development. The journal of histochemistry and cytochemistry : official journal of the Histochemistry Society 42(8):1117-1125.

Johnson EO, Kamilaris TC, Calogero AE, Gold PW, Chrousos GP. 2005. Experimentally-induced hyperthyroidism is associated with activation of the rat hypothalamic-pituitary-adrenal axis. European journal of endocrinology / European Federation of Endocrine Societies 153(1):177-185.

Jonklaas J, Bianco AC, Bauer AJ, Burman KD, Cappola AR, Celi FS, Cooper DS, Kim BW, Peeters RP, Rosenthal MS, Sawka AM, American Thyroid Association Task Force on Thyroid Hormone R. 2014. Guidelines for the treatment of hypothyroidism: prepared by the american thyroid association task force on thyroid hormone replacement. Thyroid : official journal of the American Thyroid Association 24(12):1670-1751.

Jost A, Dupouy JP, Rieutort M. 1974. The ontogenetic development of hypothalamo-hypophyseal relations. Progress in brain research 41:209-219.

Kahaly GJ, Dillmann WH. 2005. Thyroid hormone action in the heart. Endocrine reviews 26(5):704-728.

Kallo I, Butler JA, Barkovics-Kallo M, Goubillon ML, Coen CW. 2001. Oestrogen receptor beta-immunoreactivity in gonadotropin releasing hormone-expressing neurones: regulation by oestrogen. Journal of neuroendocrinology 13(9):741-748.

Kallo I, Mohacsik P, Vida B, Zeold A, Bardoczi Z, Zavacki AM, Farkas E, Kadar A, Hrabovszky E, Arrojo EDR, Dong L, Barna L, Palkovits M, Borsay BA, Herczeg L, Lechan RM, Bianco AC, Liposits Z, Fekete C, Gereben B. 2012. A novel pathway regulates thyroid hormone availability in rat and human hypothalamic neurosecretory neurons. PloS one 7(6):e37860.

Kaplan MM, Visser TJ, Yaskoski KA, Leonard JL. 1983. Characteristics of iodothyronine tyrosyl ring deiodination by rat cerebral cortical microsomes. Endocrinology 112(1):35-42.

Kester MH, Martinez de Mena R, Obregon MJ, Marinkovic D, Howatson A, Visser TJ, Hume R, Morreale de Escobar G. 2004. Iodothyronine levels in the human developing brain: major regulatory roles of iodothyronine deiodinases in different areas. The Journal of clinical endocrinology and metabolism 89(7):3117-3128.

Kim SW, Harney JW, Larsen PR. 1998. Studies of the hormonal regulation of type 2 5'-iodothyronine deiodinase messenger ribonucleic acid in pituitary tumor cells using semiquantitative reverse transcription-polymerase chain reaction. Endocrinology 139(12):4895-4905.

Kollar A, Kvarta-Papp Z, Egri P, Gereben B. 2016. Different Types of Luciferase Reporters Show Distinct Susceptibility to T3-Evoked Downregulation. Thyroid : official journal of the American Thyroid Association 26(1):179-182.

Koutcherov Y, Mai JK, Ashwell KWS, Paxinos G. 2002. Organization of human hypothalamus in fetal development. The Journal of Comparative Neurology 446(4):301-324.

Larsen PR, Davies TF, Hay ID. 1998. The Thyroid Gland. In: Wilson JD, Foster DW, Kronenberg HM, Larsen PR, eds. Williams Textbook of Endocrinology. 9th. ed. Philadelphia: W.B. Saunders Co. p 389-515.

Laughlin SB, de Ruyter van Steveninck RR, Anderson JC. 1998. The metabolic cost of neural information. Nature neuroscience 1(1):36-41.

Lazzaro D, Price M, de Felice M, Di Lauro R. 1991. The transcription factor TTF-1 is expressed at the onset of thyroid and lung morphogenesis and in restricted regions of the foetal brain. Development 113(4):1093-1104.

Lechan RM, Fekete C. 2005. Role of thyroid hormone deiodination in the hypothalamus. Thyroid : official journal of the American Thyroid Association 15(8):883-897.

Lechan RM, Fekete C. 2006. The TRH neuron: a hypothalamic integrator of energy metabolism. Progress in brain research 153:209-235.

Lehman MN, Goodman RL, Karsch FJ, Jackson GL, Berriman SJ, Jansen HT. 1997. The GnRH system of seasonal breeders: anatomy and plasticity. Brain Res Bull 44(4):445-457.

Lennard DE, Eckert WA, Merchenthaler I. 1993. Corticotropin-Releasing Hormone Neurons in the Paraventricular Nucleus Project to the External Zone of the Median Eminence: A Study Combining Retrograde Labeling with Immunocytochemistry. Journal of neuroendocrinology 5(2):175-181.

Leonard JL, Simpson G, Leonard DM. 2005. Characterization of the protein dimerization domain responsible for assembly of functional selenodeiodinases. The Journal of biological chemistry 280(12):11093-11100.

Leonard JL, Visser TJ, Leonard DM. 2001. Characterization of the subunit structure of the catalytically active type I iodothyronine deiodinase. The Journal of biological chemistry 276(4):2600-2607.

Lezoualc'h F, Hassan AH, Giraud P, Loeffler JP, Lee SL, Demeneix BA. 1992. Assignment of the beta-thyroid hormone receptor to 3,5,3'-triiodothyronine-dependent inhibition of transcription from the thyrotropin-releasing hormone promoter in chick hypothalamic neurons. Mol Endocrinol 6(11):1797-1804.

Lima FR, Gervais A, Colin C, Izembart M, Neto VM, Mallat M. 2001. Regulation of microglial development: a novel role for thyroid hormone. The Journal of neuroscience : the official journal of the Society for Neuroscience 21(6):2028-2038.

Lindsay RM. 1979. Adult rat brain astrocytes support survival of both NGF-dependent and NGF-insensitive neurones. Nature 282(5734):80-82.

Liposits Z, Setalo G, Flerko B. 1984. Application of the silver-gold intensified 3,3'-diaminobenzidine chromogen to the light and electron microscopic detection of the luteinizing hormone-releasing hormone system of the rat brain. Neuroscience 13(2):513-525.

Lopez M, Varela L, Vazquez MJ, Rodriguez-Cuenca S, Gonzalez CR, Velagapudi VR, Morgan DA, Schoenmakers E, Agassandian K, Lage R, Martinez de Morentin PB, Tovar S, Nogueiras R, Carling D, Lelliott C, Gallego R, Oresic M, Chatterjee K, Saha AK, Rahmouni K, Dieguez C, Vidal-Puig A. 2010. Hypothalamic AMPK and fatty acid metabolism mediate thyroid regulation of energy balance. Nature medicine 16(9):1001-1008.

LoPresti JS, Eigen A, Kaptein E, Anderson KP, Spencer CA, Nicoloff JT. 1989. Alterations in 3,3'5'-triiodothyronine metabolism in response to propylthiouracil, dexamethasone, and thyroxine administration in man. The Journal of clinical investigation 84(5):1650-1656.

Lowell BB, Spiegelman BM. 2000. Towards a molecular understanding of adaptive thermogenesis. Nature 404(6778):652-660.

Maciel RM, Ozawa Y, Chopra IJ. 1979. Subcellular localization of thyroxine and reverse triiodothyronine outer ring monodeiodinating activities. Endocrinology 104(2):365-371.

Maia AL, Harney JW, Larsen PR. 1995. Pituitary cells respond to thyroid hormone by discrete, gene-specific pathways. Endocrinology 136(4):1488-1494.

Maia AL, Kim BW, Huang SA, Harney JW, Larsen PR. 2005. Type 2 iodothyronine deiodinase is the major source of plasma T3 in euthyroid humans. The Journal of clinical investigation 115(9):2524-2533.

Mann DR, Plant TM. 2010. The role and potential sites of action of thyroid hormone in timing the onset of puberty in male primates. Brain research 1364:175-185.

Martinez B, Rodrigues TB, Gine E, Kaninda JP, Perez-Castillo A, Santos A. 2009. Hypothyroidism decreases the biogenesis in free mitochondria and neuronal oxygen consumption in the cerebral cortex of developing rats. Endocrinology 150(8):3953-3959.

Martinez de Mena R, Scanlan TS, Obregon MJ. 2010. The T3 receptor beta1 isoform regulates UCP1 and D2 deiodinase in rat brown adipocytes. Endocrinology 151(10):5074-5083.

Martinez R, Gomes FC. 2002. Neuritogenesis induced by thyroid hormone-treated astrocytes is mediated by epidermal growth factor/mitogen-activated protein kinase-phosphatidylinositol 3-kinase pathways and involves modulation of extracellular matrix proteins. The Journal of biological chemistry 277(51):49311-49318.

Mates L. 2011. Rodent transgenesis mediated by a novel hyperactive Sleeping Beauty transposon system. Methods in molecular biology 738:87-99.

Mates L, Chuah MK, Belay E, Jerchow B, Manoj N, Acosta-Sanchez A, Grzela DP, Schmitt A, Becker K, Matrai J, Ma L, Samara-Kuko E, Gysemans C, Pryputniewicz D, Miskey C, Fletcher B, VandenDriessche T, Ivics Z, Izsvak Z. 2009. Molecular evolution of a novel hyperactive Sleeping Beauty transposase enables robust stable gene transfer in vertebrates. Nature genetics 41(6):753-761.

Mayerl S, Muller J, Bauer R, Richert S, Kassmann CM, Darras VM, Buder K, Boelen A, Visser TJ, Heuer H. 2014. Transporters MCT8 and OATP1C1 maintain murine brain thyroid hormone homeostasis. The Journal of clinical investigation 124(5):1987-1999.

Meldolesi J, Chieregatti E, Luisa Malosio M. 2004. Requirements for the identification of dense-core granules. Trends Cell Biol 14(1):13-19.

Merchenthaler I, Gorcs T, Setalo G, Petrusz P, Flerko B. 1984. Gonadotropin-releasing hormone (GnRH) neurons and pathways in the rat brain. Cell Tissue Res 237(1):15-29.

Merchenthaler I, Kovacs G, Lavasz G, Setalo G. 1980. The preoptico-infundibular LH-RH tract of the rat. Brain research 198(1):63-74.

Merchenthaler I, Liposits Z. 1994. Mapping of thyrotropin-releasing hormone (TRH) neuronal systems of rat forebrain projecting to the median eminence and the OVLT. Immunocytochemistry combined with retrograde labeling at the light and electron microscopic levels. Acta biologica Hungarica 45(2-4):361-374.

Mohácsik P, Zeöld A, Bianco AC, Gereben B. 2011. Thyroid hormone and the neuroglia: both source and target. Journal of Thyroid Research (in press).

Moran C, Agostini M, Visser WE, Schoenmakers E, Schoenmakers N, Offiah AC, Poole K, Rajanayagam O, Lyons G, Halsall D, Gurnell M, Chrysis D, Efthymiadou A, Buchanan C, Aylwin S, Chatterjee KK. 2014. Resistance to thyroid hormone caused by a mutation in thyroid hormone receptor (TR)α1 and TRα2: clinical, biochemical, and genetic analyses of three related patients. The Lancet Diabetes & Endocrinology 2(8):619-626.

Moran C, Chatterjee K. 2015. Resistance to thyroid hormone due to defective thyroid receptor alpha. Best practice & research Clinical endocrinology & metabolism 29(4):647-657.

Murphy M, Ebling FJP. 2011. The role of hypothalamic tri-Iodothyronine availability in seasonal regulation of energy balance and body weight. Journal of Thyroid Research (in press).

Müller J, Heuer H. 2014. Expression Pattern of Thyroid Hormone Transporters in the Postnatal Mouse Brain. Frontiers in Endocrinology 5(92).

Nakao N, Ono H, Yamamura T, Anraku T, Takagi T, Higashi K, Yasuo S, Katou Y, Kageyama S, Uno Y, Kasukawa T, Iigo M, Sharp PJ, Iwasawa A, Suzuki Y, Sugano S, Niimi T, Mizutani M, Namikawa T, Ebihara S, Ueda HR, Yoshimura T. 2008. Thyrotrophin in the pars tuberalis triggers photoperiodic response. Nature 452(7185):317-322.

Nedergaard J, Bengtsson T, Cannon B. 2007. Unexpected evidence for active brown adipose tissue in adult humans. American journal of physiology Endocrinology and metabolism 293(2):E444-452.

Nucera C, Muzzi P, Tiveron C, Farsetti A, La Regina F, Foglio B, Shih SC, Moretti F, Della Pietra L, Mancini F, Sacchi A, Trimarchi F, Vercelli A, Pontecorvi A. 2010. Maternal thyroid hormones are transcriptionally active during embryo-foetal development: results from a novel transgenic mouse model. Journal of cellular and molecular medicine 14(10):2417-2435.

Ono H, Hoshino Y, Yasuo S, Watanabe M, Nakane Y, Murai A, Ebihara S, Korf HW, Yoshimura T. 2008. Involvement of thyrotropin in photoperiodic signal transduction in mice. Proceedings of the National Academy of Sciences of the United States of America 105(47):18238-18242.

Oppenheimer JH, Schwartz HL. 1997. Molecular basis of thyroid hormone-dependent brain development. Endocrine reviews 18(4):462-475.

Oppenheimer JH, Schwartz HL, Surks MI. 1972. Propylthiouracil inhibits the conversion of L-thyroxine to L-triiodothyronine: An explanation of the antithyroxine effect of propylthiouracil and evidence supporting the concept that triiodothyronine is the active thyroid hormone. The Journal of clinical investigation 51:2493-2497.

Palkovits M. 1986. Microdissection of Individual Brain Nuclei and Areas. Neuromethods. Vol 1. p 1-17.

Pope C, McNeilly JR, Coutts S, Millar M, Anderson RA, McNeilly AS. 2006. Gonadotrope and thyrotrope development in the human and mouse anterior pituitary gland. Developmental Biology 297(1):172-181.

Potter CJ, Luo L. 2010. Splinkerette PCR for mapping transposable elements in Drosophila. PloS one 5(4):e10168.

Prati M, Calvo R, Morreale G, Morreale de Escobar G. 1992. L-thyroxine and 3,5,3'-triiodothyronine concentrations in the chicken egg and in the embryo before and after the onset of thyroid function. Endocrinology 130(5):2651-2659.

Pulinilkunnil T, He H, Kong D, Asakura K, Peroni OD, Lee A, Kahn BB. 2011. Adrenergic regulation of AMP-activated protein kinase in brown adipose tissue in vivo. The Journal of biological chemistry 286(11):8798-8809.

Quignodon L, Legrand C, Allioli N, Guadano-Ferraz A, Bernal J, Samarut J, Flamant F. 2004. Thyroid hormone signaling is highly heterogeneous during pre- and postnatal brain development. Journal of molecular endocrinology 33(2):467-476.

Ramadan T, Camargo SM, Summa V, Hunziker P, Chesnov S, Pos KM, Verrey F. 2006. Basolateral aromatic amino acid transporter TAT1 (Slc16a10) functions as an efflux pathway. Journal of cellular physiology 206(3):771-779.

Rance NE, Young WS, 3rd, McMullen NT. 1994. Topography of neurons expressing luteinizing hormone-releasing hormone gene transcripts in the human hypothalamus and basal forebrain. J Comp Neurol 339(4):573-586.

Refetoff S, Weiss RE, Usala SJ. 1993. The syndromes of resistance to thyroid hormone. Endocrine reviews 14(3):348-399.

Reichlin S. 1967. Function of the hypothalamus. The American Journal of Medicine 43(4):477-485.

Rethelyi M, Fockter V. 1982. The fiber architecture of the rat median eminence with some accidental observations on the significance of tanycyte processes. Acta Biol Acad Sci Hung 33(2-3):289-300.

Ribeiro MO, Bianco SD, Kaneshige M, Schultz JJ, Cheng SY, Bianco AC, Brent GA. 2010. Expression of uncoupling protein 1 in mouse brown adipose tissue is thyroid hormone receptor-beta isoform specific and required for adaptive thermogenesis. Endocrinology 151(1):432-440.

Richard K, Hume R, Kaptein E, Sanders JP, van Toor H, De Herder WW, den Hollander JC, Krenning EP, Visser TJ. 1998. Ontogeny of iodothyronine deiodinases in human liver. The Journal of clinical endocrinology and metabolism 83(8):2868-2874.

Ritchie JW, Peter GJ, Shi YB, Taylor PM. 1999. Thyroid hormone transport by 4F2hc-IU12 heterodimers expressed in Xenopus oocytes. The Journal of endocrinology 163(2):R5-9.

Roberts LM, Woodford K, Zhou M, Black DS, Haggerty JE, Tate EH, Grindstaff KK, Mengesha W, Raman C, Zerangue N. 2008. Expression of the thyroid hormone transporters monocarboxylate transporter-8 (SLC16A2) and organic ion transporter-14 (SLCO1C1) at the blood-brain barrier. Endocrinology 149(12):6251-6261.

Rosene ML, Wittmann G, Arrojo e Drigo R, Singru PS, Lechan RM, Bianco AC. 2010. Inhibition of the Type 2 Iodothyronine Deiodinase Underlies the Elevated Plasma TSH Associated with Amiodarone Treatment. Endocrinology 151(12):5961-5970.

Ross AW, Helfer G, Russell L, Darras VM, Morgan PJ. 2011. Thyroid hormone signalling genes are regulated by photoperiod in the hypothalamus of F344 rats. PloS one 6(6):e21351.

ROTI E, GNUDI A, BRAVERMAN LE. 1983. The Placental Transport, Synthesis and Metabolism of Hormones and Drugs which Affect Thyroid Function. Endocrine reviews 4(2):131-149.

Rubio A, Raasmaja A, Silva JE. 1995. Thyroid hormone and norepinephrine signaling in brown adipose tissue. II: Differential effects of thyroid hormone on beta 3-adrenergic receptors in brown and white adipose tissue. Endocrinology 136(8):3277-3284.

Sagar GD, Gereben B, Callebaut I, Mornon JP, Zeold A, Curcio-Morelli C, Harney JW, Luongo C, Mulcahey MA, Larsen PR, Huang SA, Bianco AC. 2008. The thyroid hormone-inactivating deiodinase functions as a homodimer. Mol Endocrinol 22(6):1382-1393.

Sagar GD, Gereben B, Callebaut I, Mornon JP, Zeold A, da Silva WS, Luongo C, Dentice M, Tente SM, Freitas BC, Harney JW, Zavacki AM, Bianco AC. 2007. Ubiquitination-induced conformational change within the deiodinase dimer is a switch regulating enzyme activity. Molecular and cellular biology 27(13):4774-4783.

Sanchez E, Uribe RM, Corkidi G, Zoeller RT, Cisneros M, Zacarias M, Morales-Chapa C, Charli JL, Joseph-Bravo P. 2001. Differential responses of thyrotropin-releasing hormone (TRH) neurons to cold exposure or suckling indicate functional heterogeneity of the TRH system in the paraventricular nucleus of the rat hypothalamus. Neuroendocrinology 74(6):407-422.

Sarvari M, Kallo I, Hrabovszky E, Solymosi N, Rodolosse A, Vastagh C, Auer H, Liposits Z. 2015. Hippocampal Gene Expression Is Highly Responsive to Estradiol Replacement in Middle-Aged Female Rats. Endocrinology 156(7):2632-2645.

Sawchenko PE, Swanson LW, Rivier J, Vale WW. 1985. The distribution of growth-hormone-releasing factor (GRF) immunoreactivity in the central nervous system of the rat: an immunohistochemical study using antisera directed against rat hypothalamic GRF. J Comp Neurol 237(1):100-115.

Sawyer CH. 1978. History of the neurovascular concept of hypothalamo-hypophysial control. Biology of reproduction 18(3):325-328.

Schnell C, Shahmoradi A, Wichert SP, Mayerl S, Hagos Y, Heuer H, Rossner MJ, Hulsmann S. 2015. The multispecific thyroid hormone transporter OATP1C1 mediates cell-specific sulforhodamine 101-labeling of hippocampal astrocytes. Brain structure & function 220(1):193-203.

Schonbaum E, Sellers EA, Johnson GE. 1963. Noradrenaline and survival of rats in a cold environment. Canadian journal of biochemistry and physiology 41:975-983.

Schoonover CM, Seibel MM, Jolson DM, Stack MJ, Rahman RJ, Jones SA, Mariash CN, Anderson GW. 2004. Thyroid hormone regulates oligodendrocyte accumulation in developing rat brain white matter tracts. Endocrinology 145(11):5013-5020.

Schwartz CE, May MM, Carpenter NJ, Rogers RC, Martin J, Bialer MG, Ward J, Sanabria J, Marsa S, Lewis JA, Echeverri R, Lubs HA, Voeller K, Simensen RJ, Stevenson RE. 2005. Allan-Herndon-Dudley syndrome and the monocarboxylate transporter 8 (MCT8) gene. Am J Hum Genet 77(1):41-53.

Schwartz CE, Stevenson RE. 2007. The MCT8 thyroid hormone transporter and Allan-Herndon-Dudley syndrome. Best practice & research Clinical endocrinology & metabolism 21(2):307-321.

Segerson TP, Kauer J, Wolfe HC, Mobtaker H, Wu P, Jackson IM, Lechan RM. 1987. Thyroid hormone regulates TRH biosynthesis in the paraventricular nucleus of the rat hypothalamus. Science 238(4823):78-80.

Shibusawa N, Hollenberg AN, Wondisford FE. 2003. Thyroid hormone receptor DNA binding is required for both positive and negative gene regulation. The Journal of biological chemistry 278(2):732-738.

Silva JE, Larsen PR. 1978. Contributions of plasma triiodothyronine and local thyroxine monodeiodination to triiodothyronine to nuclear triiodothyronine receptor

saturation in pituitary, liver, and kidney of hypothyroid rats. Further evidence relating saturation of pituitary nuclear triiodothyronine receptors and the acute inhibition of thyroid-stimulating hormone release. The Journal of clinical investigation 61(5):1247-1259.

Silva JE, Larsen PR. 1983. Adrenergic activation of triiodothyronine production in brown adipose tissue. Nature 305(5936):712-713.

Simonides WS, Mulcahey MA, Redout EM, Muller A, Zuidwijk MJ, Visser TJ, Wassen FW, Crescenzi A, da-Silva WS, Harney J, Engel FB, Obregon MJ, Larsen PR, Bianco AC, Huang SA. 2008. Hypoxia-inducible factor induces local thyroid hormone inactivation during hypoxic-ischemic disease in rats. The Journal of clinical investigation 118(3):975-983.

Simpson GI, Leonard DM, Leonard JL. 2006. Identification of the key residues responsible for the assembly of selenodeiodinases. The Journal of biological chemistry 281(21):14615-14621.

Snyder PJ, Utiger RD. 1972. Inhibition of thyrotropin response to thyrotropin-releasing hormone by small quantities of thyroid hormones. The Journal of clinical investigation 51(8):2077-2084.

Song S, Adachi K, Katsuyama M, Sorimachi K, Oka T. 2000. Isolation and characterization of the 5'-upstream and untranslated regions of the mouse type II iodothyronine deiodinase gene. Molecular and cellular endocrinology 165(1-2):189-198.

St Germain DL, Galton VA. 1997. The deiodinase family of selenoproteins. Thyroid : official journal of the American Thyroid Association 7(4):655-668.

Steinsapir J, Bianco AC, Buettner C, Harney J, Larsen PR. 2000. Substrate-induced down-regulation of human type 2 deiodinase (hD2) is mediated through proteasomal degradation and requires interaction with the enzyme's active center. Endocrinology 141(3):1127-1135.

Streckfuß F, Hamann I, Schomburg L, Michaelis M, Sapin R, Klein MO, Köhrle J, Schweizer U. 2005. Hepatic deiodinase activity is dispensable for the maintenance of normal circulating thyroid hormone levels in mice. Biochemical and Biophysical Research Communications 337(2):739-745.

Sugiyama D, Kusuhara H, Taniguchi H, Ishikawa S, Nozaki Y, Aburatani H, Sugiyama Y. 2003. Functional characterization of rat brain-specific organic anion transporter (Oatp14) at the blood-brain barrier: high affinity transporter for thyroxine. The Journal of biological chemistry 278(44):43489-43495.

Sugrue ML, Vella KR, Morales C, Lopez ME, Hollenberg AN. 2010. The thyrotropin-releasing hormone gene is regulated by thyroid hormone at the level of transcription in vivo. Endocrinology 151(2):793-801.

Szentágothai J. 1968. Hypothalamic control of the anterior pituitary: an experimental-morphological study: Akadémiai Kiadó.

Taylor T, Gyves P, Burgunder JM. 1990. Thyroid hormone regulation of TRH mRNA levels in rat paraventricular nucleus of the hypothalamus changes during ontogeny. Neuroendocrinology 52(3):262-267.

Thommes RC, Caliendo J, Woods JE. 1985. Hypothalamo-adenohypophyseal-thyroid interrelationships in the developing chick embryo. VII. Immunocytochemical demonstration of thyrotrophin-releasing hormone. General and comparative endocrinology 57(1):1-9.

Thommes RC, Martens JB, Hopkins WE, Caliendo J, Sorrentino MJ, Woods JE. 1983. Hypothalamo-adenohypophyseal-thyroid interrelationships in the chick embryo. IV. Immunocytochemical demonstration of TSH in the hypophyseal pars distalis. General and comparative endocrinology 51(3):434-443.

Thommes RC, Williams DJ, Woods JE. 1984. Hypothalamo-adenohypophyseal-thyroid interrelationships in the chick embryo. VI. Midgestational adenohypophyseal sensitivity to thyrotrophin-releasing hormone. General and comparative endocrinology 55(2):275-279.

Tohyama K, Kusuhara H, Sugiyama Y. 2004. Involvement of multispecific organic anion transporter, Oatp14 (Slc21a14), in the transport of thyroxine across the blood-brain barrier. Endocrinology 145(9):4384-4391.

Toyoda N, Zavacki AM, Maia AL, Harney JW, Larsen PR. 1995. A novel retinoid X receptor-independent thyroid hormone response element is present in the human type 1 deiodinase gene. Molecular and cellular biology 15(9):5100-5112.

Trajkovic M, Visser TJ, Mittag J, Horn S, Lukas J, Darras VM, Raivich G, Bauer K, Heuer H. 2007. Abnormal thyroid hormone metabolism in mice lacking the

monocarboxylate transporter 8. The Journal of clinical investigation 117(3):627-635.

Trentin AG. 2006. Thyroid hormone and astrocyte morphogenesis. The Journal of endocrinology 189(2):189-197.

Trentin AG, De Aguiar CB, Garcez RC, Alvarez-Silva M. 2003. Thyroid hormone modulates the extracellular matrix organization and expression in cerebellar astrocyte: effects on astrocyte adhesion. Glia 42(4):359-369.

Tu HM, Kim SW, Salvatore D, Bartha T, Legradi G, Larsen PR, Lechan RM. 1997. Regional distribution of type 2 thyroxine deiodinase messenger ribonucleic acid in rat hypothalamus and pituitary and its regulation by thyroid hormone. Endocrinology 138(8):3359-3368.

Tu HM, Legradi G, Bartha T, Salvatore D, Lechan RM, Larsen PR. 1999. Regional expression of the type 3 iodothyronine deiodinase messenger ribonucleic acid in the rat central nervous system and its regulation by thyroid hormone. Endocrinology 140(2):784-790.

Vagenakis AG, Rapoport B, Azizi F, Portnay GI, Braverman LE, Ingbar SH. Hyperresponse to Thyrotropin-Releasing Hormone Accompanying Small Decreases in Serum Thyroid Hormone Concentrations. The Journal of clinical investigation 54(4):913-918.

Van der Geyten S, Sanders JP, Kaptein E, Darras VM, Kuhn ER, Leonard JL, Visser TJ. 1997. Expression of chicken hepatic type I and type III iodothyronine deiodinases during embryonic development. Endocrinology 138(12):5144-5152.

Van Herck SL, Geysens S, Bald E, Chwatko G, Delezie E, Dianati E, Ahmed RG, Darras VM. 2013. Maternal transfer of methimazole and effects on thyroid hormone availability in embryonic tissues. The Journal of endocrinology 218(1):105-115.

Vandenborne K, Roelens SA, Darras VM, Kuhn ER, Van der Geyten S. 2005. Cloning and hypothalamic distribution of the chicken thyrotropin-releasing hormone precursor cDNA. The Journal of endocrinology 186(2):387-396.

Vandesande F, Dierickx K. 1975. Identification of the vasopressin producing and of the oxytocin producing neurons in the hypothalamic magnocellular neurosecretory system of the rat. Cell and Tissue Research 164(2):153-162.

Verhoelst CH, Vandenborne K, Severi T, Bakker O, Zandieh Doulabi B, Leonard JL, Kuhn ER, van der Geyten S, Darras VM. 2002. Specific detection of type III iodothyronine deiodinase protein in chicken cerebellar purkinje cells. Endocrinology 143(7):2700-2707.

Virtanen KA, Lidell ME, Orava J, Heglind M, Westergren R, Niemi T, Taittonen M, Laine J, Savisto N-J, Enerbäck S, Nuutila P. 2009. Functional Brown Adipose Tissue in Healthy Adults. New England Journal of Medicine 360(15):1518-1525.

Visser TJ. 2007. Thyroid hormone transporters. Horm Res 68 Suppl 5:28-30.

Visser TJ, Does-Tobe I, Docter R, Hennemann G. 1976. Subcellular localization of a rat liver enzyme converting thyroxine into tri-iodothyronine and possible involvement of essential thiol groups. The Biochemical journal 157(2):479-482.

Visser TJ, Leonard JL, Kaplan MM, Larsen PR. 1982. Kinetic evidence suggesting two mechanisms for iodothyronine 5'-deiodination in rat cerebral cortex. Proceedings of the National Academy of Sciences of the United States of America 79(16):5080-5084.

Visser WE, Friesema EC, Jansen J, Visser TJ. 2008. Thyroid hormone transport in and out of cells. Trends Endocrinol Metab 19(2):50-56.

Weiss RE, Forrest D, Pohlenz J, Cua K, Curran T, Refetoff S. 1997. Thyrotropin regulation by thyroid hormone in thyroid hormone receptor beta-deficient mice. Endocrinology 138(9):3624-3629.

Wiegand SJ, Price JL. 1980. Cells of origin of the afferent fibers to the median eminence in the rat. J Comp Neurol 192(1):1-19.

Williams GR. 2000. Cloning and characterization of two novel thyroid hormone receptor beta isoforms. Molecular and cellular biology 20(22):8329-8342.

Williams GR. 2008. Neurodevelopmental and neurophysiological actions of thyroid hormone. Journal of neuroendocrinology 20(6):784-794.

Wittmann G, Fuzesi T, Liposits Z, Lechan RM, Fekete C. 2009. Distribution and axonal projections of neurons coexpressing thyrotropin-releasing hormone and urocortin 3 in the rat brain. J Comp Neurol 517(6):825-840.

Wu SY, Green WL, Huang WS, Hays MT, Chopra IJ. 2005. Alternate pathways of thyroid hormone metabolism. Thyroid : official journal of the American Thyroid Association 15(8):943-958.

Yant SR, Wu X, Huang Y, Garrison B, Burgess SM, Kay MA. 2005. High-Resolution Genome-Wide Mapping of Transposon Integration in Mammals. Molecular and cellular biology 25(6):2085-2094.

Yasuo S, Watanabe M, Nakao N, Takagi T, Follett BK, Ebihara S, Yoshimura T. 2005. The reciprocal switching of two thyroid hormone-activating and -inactivating enzyme genes is involved in the photoperiodic gonadal response of Japanese quail. Endocrinology 146(6):2551-2554.

Yoshimura T. 2010. Neuroendocrine mechanism of seasonal reproduction in birds and mammals. Anim Sci J 81(4):403-410.

Yoshimura T, Yasuo S, Watanabe M, Iigo M, Yamamura T, Hirunagi K, Ebihara S. 2003. Light-induced hormone conversion of T4 to T3 regulates photoperiodic response of gonads in birds. Nature 426(6963):178-181.

Zavacki AM, Ying H, Christoffolete MA, Aerts G, So E, Harney JW, Cheng SY, Larsen PR, Bianco AC. 2005. Type 1 iodothyronine deiodinase is a sensitive marker of peripheral thyroid status in the mouse. Endocrinology 146(3):1568-1575.

Zeold A, Doleschall M, Haffner MC, Capelo LP, Menyhert J, Liposits Z, da Silva WS, Bianco AC, Kacskovics I, Fekete C, Gereben B. 2006a. Characterization of the nuclear factor-kappa B responsiveness of the human dio2 gene. Endocrinology 147(9):4419-4429.

Zeold A, Pormuller L, Dentice M, Harney JW, Curcio-Morelli C, Tente SM, Bianco AC, Gereben B. 2006b. Metabolic instability of type 2 deiodinase is transferable to stable proteins independently of subcellular localization. The Journal of biological chemistry 281(42):31538-31543.

Zevenbergen C, Meima ME, Lima de Souza EC, Peeters RP, Kinne A, Krause G, Visser WE, Visser TJ. 2015. Transport of Iodothyronines by Human L-Type Amino Acid Transporters. Endocrinology 156(11):4345-4355.

Zhang J, Lazar MA. 2000. The mechanism of action of thyroid hormones. Annual review of physiology 62:439-466.

12. List of publications

12.1 List of publications the thesis is based on

1. Mohácsik, P., Füzesi, T., Doleschall, M., Szabó, AS., Vancamp, P., Hadadi, É., Darras, VM., Fekete, C., Gereben, B. 2016. Increased thyroid hormone activation accompanies the formation of thyroid hormone dependent negative feedback in developing chicken hypothalamus. Endocrinology 157(3):1211-211.

2. Kalló, I*., Mohácsik, P*.,Vida, B., Zeöld, A., Bardóczi, Z., Zavacki, AM., Farkas, E., Kádár, A., Hrabovszky, E., Arrojo e Drigo, R., Dong, L., Barna, L., Palkovits, M., Borsay, B.A., Herczeg, L., Bianco, A.C., Liposits, Z., Fekete, C., Gereben, B. 2012. A novel pathway regulates thyroid hormone availability in rat and human hypothalamic neurosecretory neurons. PLoS One 7: (6) Paper e37860. 16 p. *equally contributed

3. Mohácsik, P., Zeöld, A., Bianco, AC., Gereben, B. 2011. Thyroid hormone and the neuroglia: both source and target. Journal of Thyroid Research, Special issue: Thyroid Hormones and Their Receptors: From Development to Disease Article ID 215718, 16 pages doi:10.4061/2011/215718

4. Mohácsik, P, Erdélyi, F., Szabó, G., Fekete, Cs. and Gereben, B. (Inst. of. Exp Med., Hung. Academy of Sciences) 2016. Thyroid hormone action indicator transgenic mouse and recombinant DNA construct Hungarian Patent Claim #P1400563, International Patent Application No. PCT/HU2015/050020

12.2 Other publications

1. Wittmann, G., Szabon, J., Mohácsik, P., Nouriel, S., Gereben, B., Fekete, C., and Lechan, R. 2015. Parallel regulation of thyroid hormone transporters OATP1c1 and MCT8 during and after endotoxemia at the blood-brain barrier of male rodents. Endocrinology 156(4):1552–1564

2. McAninch, E., Jo, S., Preite, N., Farkas, E., Mohácsik, P., Fekete, C., Egri, P., Gereben, B., Li, Y., Deng, Y., Patti, M., Zevenbergen, C., Peeters, R., Mash, D., and Bianco, A. 2015. Prevalent polymorphism in thyroid hormone-activating enzyme leaves a genetic fingerprint that underlies associated clinical syndromes. The Journal of Clinical Endocrinology and Metabolism 100(3): 920-33

3. Wittmann, G., Mohácsik, P., Balkhi, MY., Gereben, B., Lechan, RM. 2015. Endotoxin-induced inflammation down-regulates L-type amino acid transporter 1 (LAT1) expression at the blood-brain barrier of male rats and mice. Fluids and Barriers of the CNS 12: p. 21.

4. Fonseca, TL., Fernandes, GW., McAninch, EA., Bocco, BM., Abdalla, SM., Ribeiro, MO., Mohácsik, P., Fekete, C., Li, D., Xing, X., Wang, T., Gereben, B., Bianco, AC. 2015. Perinatal deiodinase 2 expression in hepatocytes defines epigenetic susceptibility to liver steatosis and obesity. PROC NATL ACAD SCI USA 112(45):14018-23

5. Rafael Arrojo e Drigo, Fonseca, TL., Castillo, M., Salathe, M., Simovic, G., Mohácsik, P., Gereben, B., and Bianco, AC. 2011. Endoplasmic reticulum stress decreases intracellular thyroid hormone activation via an eIF2a-mediated decrease in type 2 deiodinase synthesis. Molecular Endocrinology 25(12): 2065-2075

13. Acknowledgements

First of all I would like to express my gratitude to my tutor, Dr. Balázs Gereben, who supported tirelessly my professional improvement in his laboratory, supervised my activity with his comprehensive knowledge and serene and calm attitude to life and science while at the same time providing me freedom in work.

I am also very grateful to Dr. Csaba Fekete for his help to extend my technical background and carry out experiments.

I wish to express my thanks to Professor Zsolt Liposits, Head of the Department of Endocrine Neurobiology for his support of my progress in scientific research.

I would like to express my deepest thank to Antonio C. Bianco (Chicago, USA), Veerle M. Darras (KU Leuven, Belgium) and their research groups for the successful collaboration.

I am very thankful to Andrea Juhász, Erzsébet Farkas, Anett Szilvásy-Szabó, Dr. Csilla Molnár, for friendly atmosphere and cooperation in work.

I also thank my colleagues in the Laboratory of Molecular Cell Metabolism for the scientific discussions: Péter Egri, Dr. Anikó Zeöld, Richárd Sinkó, Anna Kollár

I would like to thank to the members of the Lendület Laboratory of Integrative Neurobiology, and the Laboratory of Endocrine Neurobiology for supporting my research with productive cooperation: Dr. Andrea Kádár, Györgyi Zséli, Dr. Mónika Tóth, Dr. Edina Varga, Dr. Barbara Vida, Dr. Tamás Füzesi, Ágnes Simon Veronika Maruzs Dr. Erik Hrabovszky, Dr. Imre Farkas, Dr. Imre Kalló, Dr. Miklós Sárvári, Dr. Csaba Vastagh, Zsuzsanna Bardóczi, Flóra Bálint, Dr. Katalin Skrapits, Barna László, Márta Turek

Special thanks to László Barna from the Nikon Microscopy Center for his supporting and technical advices in different microscopic technics.

I would like to thank for the workers of the Medical Gene Technological Unit, especially Ferenc Erdélyi, Zsuzsanna Erdélyi, Mária Kaziné Szűcs, Rozália Szafner, who helped me to learn, how to work carefully and effectively with small animals.